

# Lawrence Berkeley National Laboratory

## Lawrence Berkeley National Laboratory

### Title

GEOCHEMISTRY AND ISOTOPE HYDROLOGY OF GROUNDWATERS IN THE STRIPA GRANITE RESULTS AND PRELIMINARY INTERPRETATION

### Permalink

<https://escholarship.org/uc/item/462170bq>

### Author

Fritz, P.

### Publication Date

1979-04-01

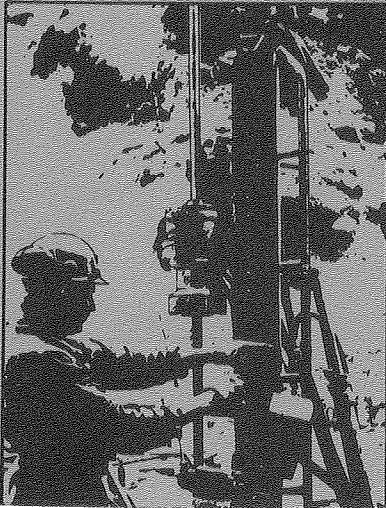
LBL-8285 *e.2*  
SAC-12  
UC-70

# SWEDISH-AMERICAN COOPERATIVE PROGRAM ON RADIOACTIVE WASTE STORAGE IN MINED CAVERNS IN CRYSTALLINE ROCK

RECEIVED  
LAWRENCE  
BERKELEY LABORATORY

JUN 14 1979

LIBRARY AND  
DOCUMENTS SECTION



Technical Information Report No. 12  
**GEOCHEMISTRY AND ISOTOPE  
HYDROLOGY OF  
GROUNDWATERS IN THE  
STRIPA GRANITE  
RESULTS AND  
PRELIMINARY INTERPRETATION**

P. Fritz, J. F. Barker, and J. E. Gale  
Department of Earth Sciences  
University of Waterloo  
Waterloo, Ontario, Canada

April 1979

TI  
wl  
Fc  
Te

copy  
no weeks.  
call

A Joint Project of

Swedish Nuclear Fuel Supply Co.  
Fack 10240 Stockholm, Sweden

Operated for the Swedish  
Nuclear Power Utility Industry

Lawrence Berkeley Laboratory  
Earth Sciences Division  
University of California  
Berkeley, California 94720, USA

Operated for the U.S. Department of  
Energy under Contract W-7405-ENG-48

*LBL-8285 e.2*



This report was prepared as an account of work sponsored by the United States Government and/or the Swedish Nuclear Fuel Supply Company. Neither the United States nor the U.S. Department of Energy, nor the Swedish Nuclear Fuel Supply Company, nor any of their employees, nor any of their contractors, subcontractors, or their employees, makes any warranty, express or implied legal liability or responsibility for completeness or usefulness of any information, product or process disclosed herein. It should not be construed to imply that the Government or the Swedish Nuclear Fuel Supply Company should not infringe upon any existing or future patent rights.

Available in the  
Aviation  
National Technical Information Service  
Department  
85 Port Roy  
Springfield, V  
Price Code:

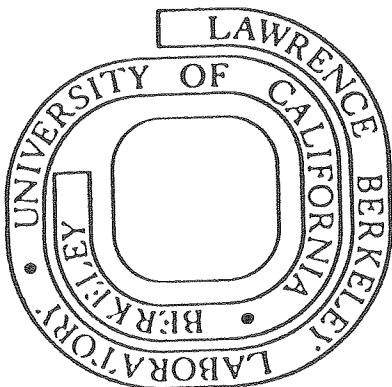
LBL-8285  
SAC-12  
UC-70

GEOCHEMISTRY AND ISOTOPE HYDROLOGY OF  
GROUNDWATERS IN THE STRIPA GRANITE

RESULTS AND PRELIMINARY INTERPRETATION

P. Fritz, J. F. Barker, and J. E. Gale  
Department of Earth Sciences  
University of Waterloo  
Waterloo, Ontario, Canada

April 1979





|

|

|

|

|

|

|

|

|

|

|

|

|

|

|

|

|

|

|

|

|

|

|

|

|

|

|

|

|

|

|

|

|

GEOCHEMISTRY AND ISOTOPE HYDROLOGY OF  
GROUNDWATERS IN THE STRIPA GRANITE

RESULTS AND PRELIMINARY INTERPRETATION

P. Fritz, J. F. Barker, and J. E. Gale  
Department of Earth Sciences  
University of Waterloo  
Waterloo, Ontario, Canada

April 1979

This report was prepared by Lawrence Berkeley Laboratory under the University of California contract W-7405-ENG-48 with the U. S. Department of Energy. The contract is administered by the Office of Nuclear Waste Isolation at Battelle Memorial Institute.





## PREFACE

This report is one of a series documenting the results of the Swedish-American cooperative research program in which the cooperating scientists explore the geological, geophysical, hydrological, geochemical, and structural effects anticipated from the use of a large crystalline rock mass as a geologic repository for nuclear waste. This program has been sponsored by the Swedish Nuclear Power Utilities through the Swedish Nuclear Fuel Supply Company (SKBF), and the U.S. Department of Energy (DOE) through the Lawrence Berkeley Laboratory (LBL).

The principal investigators are L. B. Nilsson and O. Degerman for SKBF, and N. G. W. Cook, P. A. Witherspoon, and J. E. Gale for LBL. Other participants will appear as authors of the individual reports.

Previous technical reports in this series are listed below.

1. Swedish-American Cooperative Program on Radioactive Waste Storage in Mined Caverns by P. A. Witherspoon and O. Degerman. (LBL-7049, SAC-01).
2. Large Scale Permeability Test of the Granite in the Stripa Mine and Thermal Conductivity Test by Lars Lundstrom and Haken Stille. (LBL-7052, SAC-02).
3. The Mechanical Properties of the Stripa Granite by Graham Swan. (LBL-7074, SAC-03).
4. Stress Measurements in the Stripa Granite by Hans Carlsson. (LBL-7078, SAC-04).
5. Borehole Drilling and Related Activities at the Stripa Mine by P. J. Kurfurst, T. Hugo-Persson, and G. Rudolph. (LBL-7080, SAC-05).
6. A Pilot Heater Test in the Stripa Granite by Hans Carlsson. (LBL-7086, SAC-06).
7. An Analysis of Measured Values for the State of Stress in the Earth's Crust by Dennis B. Jamison and Neville G. W. Cook. (LBL-7071, SAC-07).
8. Mining Methods Used in the Underground Tunnels and Test Rooms at Stripa by B. Andersson and P. A. Halen. (LBL-7081, SAC-08).
9. Theoretical Temperature Fields for the Stripa Heater Project by T. Chan, Neville G. W. Cook, and C. F. Tsang. (LBL-7082, SAC-09).



10. Mechanical and Thermal Design Considerations for Radioactive Waste Repositories in Hard Rock. Part I: An Appraisal of Hard Rock for Potential Underground Repositories of Radioactive Wastes by Neville G. W. Cook; Part II: In Situ Heating Experiments in Hard Rock: Their Objectives and Design by Neville G. W. Cook and P. A. Witherspoon. (LBL-7073, SAC-10).
11. Full-Scale and Time-Scale Heating Experiments at Stripa: Preliminary Results by Neville G.W. Cook and Michael Hood. (LBL-7072, SAC-II).

TABLE OF CONTENTS

	<u>Page</u>
LIST OF FIGURES. . . . .	vii
LIST OF TABLES . . . . .	ix
ABSTRACT . . . . .	1
1. INTRODUCTION . . . . .	3
2. SAMPLING AND ANALYSIS . . . . .	11
2.1 Field Methods . . . . .	12
Source of Samples . . . . .	12
Sampling Procedures . . . . .	12
Geochemical Measurements in the Field . . . . .	16
Groundwater Sample Collection . . . . .	19
Fracture Mineral Sampling . . . . .	22
2.2 Laboratory Methods . . . . .	23
Chemical Analyses of Groundwaters . . . . .	23
Dissolved Gas Analyses . . . . .	25
Isotope Analyses . . . . .	27
Deuterium . . . . .	27
Oxygen-18 . . . . .	27
Carbon-13 . . . . .	28
Tritium . . . . .	29
Carbon-14 . . . . .	29
Uranium-234 and Uranium-238 . . . . .	30
Helium-4 and other noble gases. . . . .	30
3. RESULTS AND DISCUSSION . . . . .	31
3.1 Groundwater Chemistry . . . . .	31
The Chemical Characteristics of Groundwaters . . . . .	31
Geochemical Processes and the Geochemical Evolution of Groundwaters . . . . .	35
3.2 Dissolved Gases. . . . .	43
Oxygen, Nitrogen, Methane. . . . .	43
Noble Gases . . . . .	45
3.3 Stable Isotopes. . . . .	49
Deuterium and Oxygen-18 in Groundwater . . . . .	49
Results . . . . .	53
Discussion. . . . .	56
Conclusions . . . . .	60
Carbon-13 and Oxygen-18 in Fracture Calcite and Dissolved Inorganic Carbon . . . . .	61
Results and Discussion . . . . .	62
Carbon-13 . . . . .	64
Oxygen-18 . . . . .	68



TABLE OF CONTENTS  
(continued)

	<u>Page</u>
3.4 Radioactive Isotopes (Groundwater Dating) . . . . .	70
Tritium . . . . .	70
Results and Discussion . . . . .	73
Carbon-14 . . . . .	75
Results and Discussion . . . . .	77
Shallow Groundwaters . . . . .	78
Deep Groundwaters . . . . .	83
Conclusions . . . . .	87
3.5 Elements of Uranium Decay Series . . . . .	87
Uranium-234/Uranium-238 Activity Ratios . . . . .	89
Helium-4 Dating. . . . .	94
Radiogenic Argon . . . . .	97
Radon. . . . .	98
Conclusions . . . . .	100
4. SUMMARY . . . . .	103
5. ACKNOWLEDGMENTS . . . . .	107
6. REFERENCES. . . . .	109
7. APPENDIX: Summary of Chemical and Isotopic Analyses . . . . .	113

LIST OF FIGURES

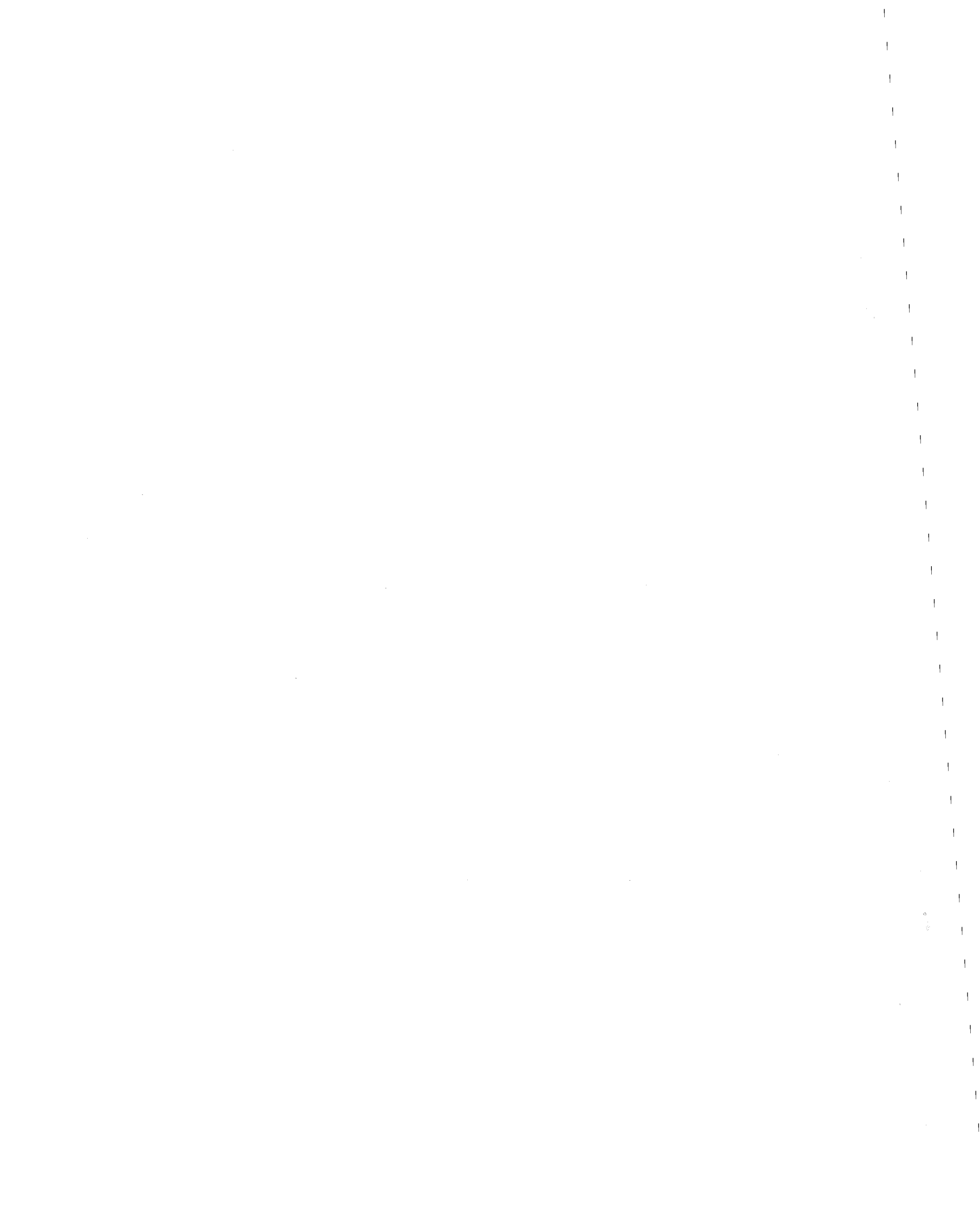
	<u>Page</u>
1. Surface geology and location of surface boreholes SBH-1 and SBH-2	6
2. Vertical profile showing the subsurface geology in the area of the test excavations along cross-section A-B in Fig. 1. . . . .	7
3. Underground excavations near the 330-m level showing the location of boreholes including M3 . . . . .	8
4. Location of private wells in the vicinity of the Stripa mine which were sampled for chemical and isotopic analyses . . . . .	14
5. Geochemical variation of groundwaters with depth . . . . .	33
6. Mineral stability diagram in terms of $\text{Na}^+$ , $\text{H}^+$ , and $\text{H}_4\text{SiO}_4$ activities in waters of the Stripa area . . . . .	40
7. Mineral stability diagram in terms of $\text{Mg}^{2++}$ , $\text{H}^+$ , and $\text{Na}^+$ activities in waters of the Stripa area . . . . .	41
8. Mineral stability diagram in terms of $\text{Ca}^{2+}$ , $\text{H}^+$ , and $\text{H}_4\text{SiO}_4$ activities in waters of the Stripa area . . . . .	42
9. The solubility of the noble gases in water at various temperatures	47
10. A generalized $\delta^{18}\text{O}$ versus $\delta^2\text{H}$ plot showing the Meteoric Water Line and processes commonly responsible for deviations from this line .	51
11. A plot of $\delta^{18}\text{O}$ versus $\delta^2\text{H}$ of waters from the Stripa area . . . . .	53
12. A plot of $\delta^{18}\text{O}$ versus chloride concentration for waters of the Stripa area . . . . .	60
13. The relationship between measured $\delta^{13}\text{C}$ of fracture calcites and $\delta^{18}\text{O}$ of the water from which they precipitated . . . . .	66
14. The weighted average monthly tritium concentration in rainfall in Ottawa, Canada, 1954-1975 . . . . .	71
15. Prediction of the present (1978) tritium content of groundwaters on the basis of radioactive decay since time of recharge . . . . .	72
16. Possible evolution of the TIC in Stripa 21 and Stripa 23 (A) and resulting dilution factors for these groundwaters (B) . . . . .	79



	<u>Page</u>
17. The relationship between the TIC concentration and degrees of saturation with respect to calcite for waters from the Stripa area. . . . .	81
18. The variation in corrected $^{14}\text{C}$ ages of groundwaters with various $^{14}\text{C}$ contents due to different assumed $\delta^{13}\text{C}$ values of rock carbonate . . . . .	82
19. The decrease in $\delta^{13}\text{C}$ of the precipitated phase as the reservoir is depleted in $^{13}\text{C}$ by equilibrium fractionation of carbon isotopes during continual precipitation. . . . .	85
20. The age difference between Stripa 16 and Stripa 29 groundwaters based on $^{234}\text{U}/^{238}\text{U}$ activity ratio evolution under closed system conditions . . . . .	92
21. The relationship of uranium content with TIC content and of excess $^{234}\text{U}$ with uranium content of Stripa groundwaters . . . . .	93
22. $^4\text{He}$ production in the uranium decay series ( $\alpha$ -decay) . . . . .	95

LIST OF TABLES

	<u>Page</u>
1. Origin of geochemical samples . . . . .	13
2. Analytical methods and estimated precision. . . . .	24
3. Rare gas content of groundwaters. . . . .	25
4. Dissolved gases and redox potential of groundwaters in the Stripa area . . . . .	26
5. A comparison of the ranges in chemical species in groundwaters from Stripa, Swedish granites, and gneisses from the Bohemian Massif . . . . .	34
6. Comparison of $pO_2$ and $pCH_4$ calculated from Eh with $pO_2$ and $pCH_4$ measured in groundwaters from Stripa area . . . . .	44
7. $^{18}O$ and $^2H$ analyses on water samples from Stripa . . . . .	54
8. $^{18}O$ in groundwaters . . . . .	55
9. Carbon and oxygen isotopic compositions of fracture calcites and of the water from which they precipitated . . . . .	63
10. Carbon isotope analyses on water samples . . . . .	64
11. Tritium analyses for Stripa project . . . . .	74
12. $pCO_2$ , TIC, and calcite saturation index for Stripa waters . . . . .	84
13. Uranium isotopic data . . . . .	88
14. $^{222}Rn$ and $^{226}Ra$ contents of groundwaters . . . . .	88



## ABSTRACT

This paper presents the results of geochemical and isotopic analyses on water samples from the granite at Stripa, Sweden. Groundwater samples collected from shallow, private wells; surface boreholes; and boreholes drilled from the 330 m and 410 m mine levels were analyzed for their major ion chemistry, dissolved gases, and environmental isotope contents.

The principal change in the chemical load with depth is typified by chloride concentration, which increases from less than 5 mg/liter to about 300 mg/liter. There is a parallel increase in pH, which changes from about 6.5 to over 9.75. It is important to notice that calcite saturation is maintained and that, because of rising pH, dissolved inorganic carbon is lost. The total carbonate content thus decreases from about 70 mg/liter to less than 7 mg/liter.

The  $^{18}\text{O}$  and deuterium analyses demonstrate that different fracture systems contain different water masses, whose age increases with depth. Groundwater age determinations with  $^{14}\text{C}$  and isotopes of the uranium decay series strongly indicate that water ages exceed 25,000 years. The  $^{13}\text{C}$  contents of the aqueous carbonate in these groundwaters indicate groundwater recharge through vegetated soil--presumably during an interglacial period.

The  $^{13}\text{C}$  and  $^{18}\text{O}$  determinations show that most fracture calcites have formed in a wide variety of depositional environments, and not in the waters circulating today.





## 1. INTRODUCTION

The ideal solution to the problem of disposal of nuclear wastes would be to find an impermeable, dry rock mass able to withstand major interferences such as mining and heat stress to such a degree that no water or gas could enter or leave the repository. Such a rock is unlikely to exist, and would be difficult to recognize. Thus the selection and preparation of any rock mass considered suitable for a repository which can contain high-level nuclear wastes for many thousands of years will have to involve extensive physical testing as well as investigation of the geochemistry and hydrogeology of the rock mass.

In general we have great experience in mining different geologic materials, but very little is known about the origin, age, movement, and geochemistry of groundwaters in largely impermeable rocks and no studies have integrated such information with structural geologic data.

If one could guarantee that no water could enter or leave a deep disposal site, the need for hydrogeochemical and hydrogeologic investigations would be minimal. Such assurances cannot be given, however, without detailed studies at all potential sites. These studies must:

- define potential and actual water movements before, during, and after the activities associated with any disposal operation;
- describe the geochemistry of the aqueous system, and the mineralogy and geochemistry of fracture minerals encountered during the various phases of repository preparation;
- predict the release and movement of radionuclides in an environment

in which the first containment barrier is an engineered system (whose design will depend on the hydrology and geochemistry of the virgin site), and in which the subsequent barrier is the rock mass.

An assessment of the fracture hydrology therefore requires information about the composition, origin, and age of groundwaters within the rock mass. The data obtained from our investigations of the granitic rock mass at Stripa, Sweden should provide the basic framework for geochemical studies needed in projects predicting containment movements from disposal sites in similar rock masses.

Major ion analyses and field determinations of pH and other less important parameters describe the chemical characteristics of groundwaters which arrive at the mine site and eventually fill any excavation. By sampling at different points, we attempt to understand the geochemical evolution of these groundwaters and to document which geochemical processes are dominant. An integral part of the discussion are analyses using the computer program WATEQ-F (Plummer, Jones, and Truesdell 1976), which gives the speciation of aqueous compounds in the system and defines mineral-water equilibria.

We use the stable isotopes  $^{18}\text{O}$  and  $^2\text{H}$  (deuterium) to obtain information on the origin of the groundwaters encountered. Both isotopes are a conservative property of the groundwaters, unless there has been large-scale isotope exchange at elevated temperatures with rock minerals, such as occurs in all major geothermal systems, and also in deep sedimentary basins. These isotope analyses thus indicate whether "normal" groundwater is discharging from the fracture system and under what environmental conditions it has been

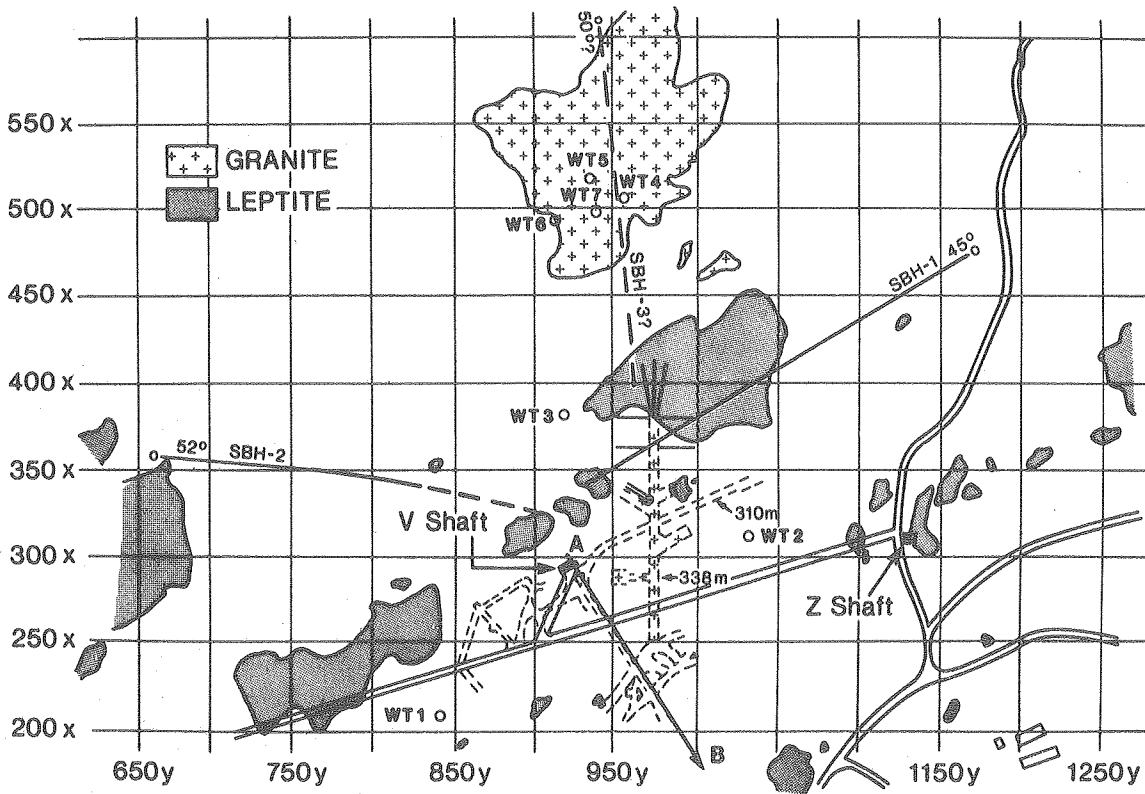
recharged, or whether deep circulation systems, metamorphic fluids, fossil seawater, etc., are present.

Indirect information on the environment of groundwater recharge is also obtained from rare gas analysis, done in conjunction with the analyses of isotopes of the uranium decay series in water and rocks. Since radioactive decay increases the helium concentrations of the groundwater, the abundance of helium reflects groundwater ages. Groundwater age dating was also attempted using tritium and  $^{14}\text{C}$ . Tritium concentrations are a function of input and decay only because the short half-life of tritium (12.35 years) removes this isotope from waters older than about 30 years. Interpretation of the data for  $^{14}\text{C}$  and uranium isotopes is more difficult because their concentrations very strongly depend on the geochemical processes that also affect the chemistry of the groundwaters. A thorough knowledge of these processes is necessary before rare gas analysis can be used to indicate water ages.

The geological framework and borehole locations of the geochemical work done at the Stripa mines are given in Figs. 1, 2, and 3. Figure 1 shows the distribution of surface outcrops of granite and leptite (metasedimentary rocks) in the area above the test excavations. In this area the contact between the two main rock types trends approximately east-west and plunges about  $45^\circ$  south (Fig. 2). The general outline of the test excavations (which are located in granite) is shown in Fig. 1 and, in more detail, in Fig. 3.

The surface boreholes consist of seven water wells, WT-1 through WT-7 (including a pump-test well, WT-7), and two long, inclined boreholes, SBH-1 and SBH-2. A third long borehole, SBH-3, is planned (Fig. 1). SBH-1 is an

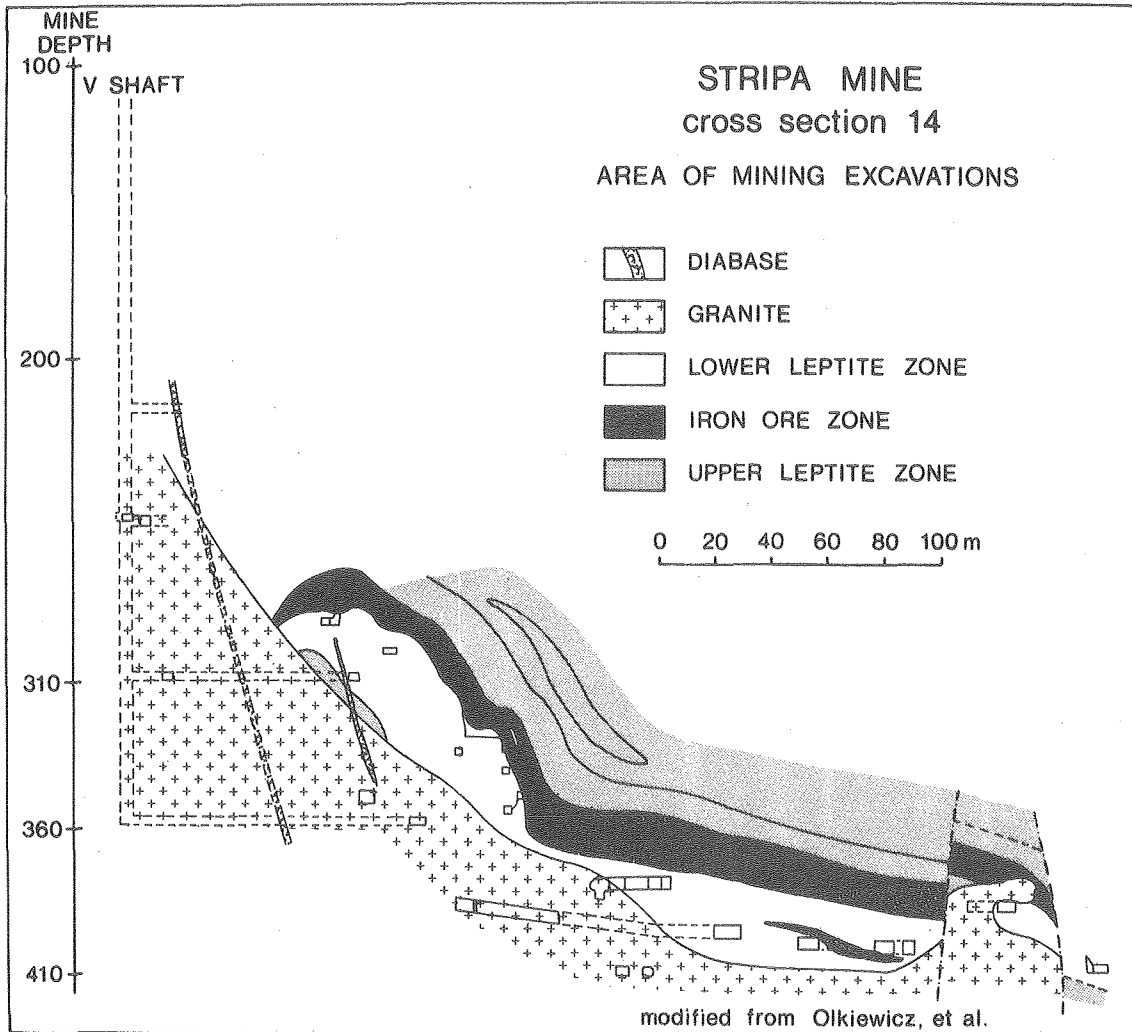
open, 76-mm diameter, diamond-cored borehole, 385 m long, that angles downward at 45°, passes over the test excavations, and terminates at approximately the 290-m level. SBH-2, also diamond cored, is drilled from the west toward the test excavations. This borehole is 365 m long, angled downward at 52° (from the horizontal), and terminates at approximately the 290-m level (Fig. 1). SBH-3 will be drilled from the north at an angle of approximately 50° from the horizontal, bearing south towards the underground test excavations. Collection of adequate water samples from this borehole will be critical to the geochemical program. It is planned to collect water samples at 100 m, 200 m, and ~350 m along SBH-3 as the drilling proceeds.



XBL 794-9484

Fig.1. Surface geology and location of surface boreholes SBH-1 and SBH-2. The location of test excavations at the 338-m level is shown as cross-hatched area enclosed by dashed lines.

Three subsurface boreholes have provided most of the water samples for the geochemical study: R-1 located near the north end of the ventilation drift (Fig. 3); M-3, located near the end of the time-scale room (Fig. 3); and a vertical 470-m borehole drilled by Sveriges Geologiska Undersöning (SGU) for Kärnbränslesäkerhet (KBS) from the 410-m mining level. All of the underground boreholes have pressure gradients directed into the excavations. All



XBL 794-9485

Fig. 2. Vertical profile showing the subsurface geology in the area of the test excavations along cross section A-B in Fig. 1.



three of the boreholes have reasonable flow rates: R-1, 30 m in length, flows at approximately 0.5 liters/min; M-3, 14 m in length, flows at approximately 0.15 liters/min; and the 410-m-level vertical borehole, 470 m in length, flows at approximately 0.1 liters/min.

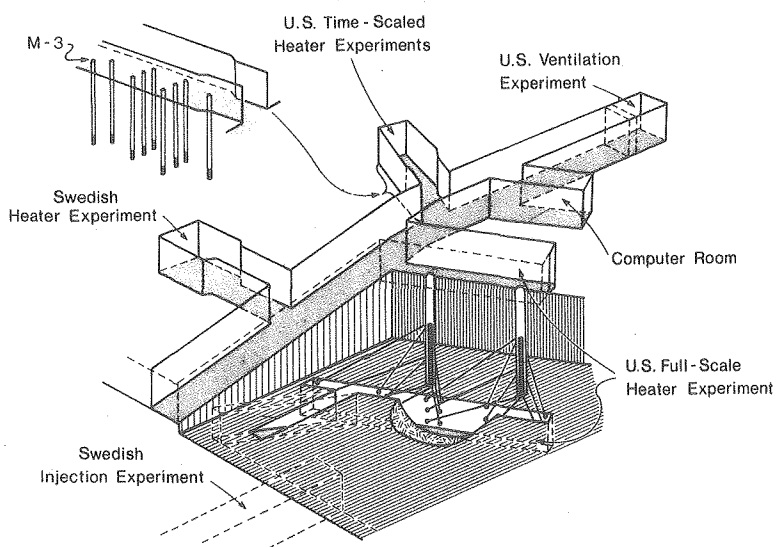


Fig. 3.

Underground excavations near the 330-m level showing the location of boreholes including M-3 (after Witherspoon, Cook, and Gale 1977; Witherspoon and Degerman 1978).

XBL 794-9486

The Stripa granite is in contact with the north limb of a plunging syncline (Fig. 2) of metasedimentary rocks. The iron ore beds within the metasedimentary rock sequence, excavated down to 410 m, have been mined for about 400 years, ending in 1977. This long period of mining activity must have greatly perturbed the local flow system, through the formation of a 410-m sink of considerable areal extent. Local enrichments in uranium minerals (O. Brotzen, pers. comm.) could significantly influence the geochemistry of the Stripa granite waters, specifically the abundance and isotopic composition of uranium and its daughter products.

This report is the first summary of hydrogeochemical and hydrogeologic investigations at the Stripa mines during FY 1978, and deals exclusively with observations relevant to the hydrology of the Stripa project. Some additional samples will be collected during FY 1979 and possibly FY 1980.

Future detailed reports will deal with:

- carbon-14 dating;
- dating with uranium isotopes and their daughter products;
- fracture mineralogy and geochemistry.



## 2. SAMPLING AND ANALYSES

Sampling points for which data are presented in this report are listed in Table 1; data are presented in the appendix. The analyses include:

- field measurements of alkalinity, Eh, pH, conductance, temperature, and dissolved oxygen;
- complete major ion analyses on samples from all groundwater types;
- determination of composition of dissolved gases on a selected number of samples, with special emphasis on noble gas analyses;
- deuterium and oxygen-18 analyses on water samples from all sampling points;
- carbon-13 and oxygen-18 analyses of fracture calcites; and
- analysis of carbon-13 in dissolved aqueous carbon from the different water types.

In addition, attempts were made to determine groundwater ages through analyses of tritium, carbon-14, uranium isotopes, and uranium daughter products.

Several laboratories participated in these analytical tasks:

University of Waterloo, Canada (Dr. P. Fritz and J. Barker)	Oxygen-18, deuterium, tritium, carbon-13, and carbon-14 analyses; and gas analyses
Section for Isotope Hydrology International Atomic Energy Agency Vienna, Austria (Dr. B. R. Payne)	Carbon-13 and carbon-14 analyses; enriched tritium determinations; chemical analyses
University of Uppsala, Sweden (Dr. E. Eriksson)	Tritium determinations
Florida State University, U.S.A. (Dr. K. Osmond)	Uranium isotope analyses
University of Bath, Great Britain (Dr. J. N. Andrews)	Uranium isotope analyses noble gas determinations

AB Atomenergi, Studsvik, Sweden	Radon analyses
Hydroconsult AB, Bromma, Sweden (H. Bormma)	Chemical analyses

Section 2.1 discusses field analytical methods and sampling procedures; Section 2.2 discusses laboratory procedures, information concerning the equipment used, and the final data.

## 2.1 Field Methods

### Source of Samples

Groundwater samples were obtained from four private wells, twelve boreholes, and three drips in the mine working (Table 1). The approximate locations of the private wells are shown in Fig. 4; locations of the various mine-working areas are shown in Figs. 2 and 3.

### Sampling Procedures

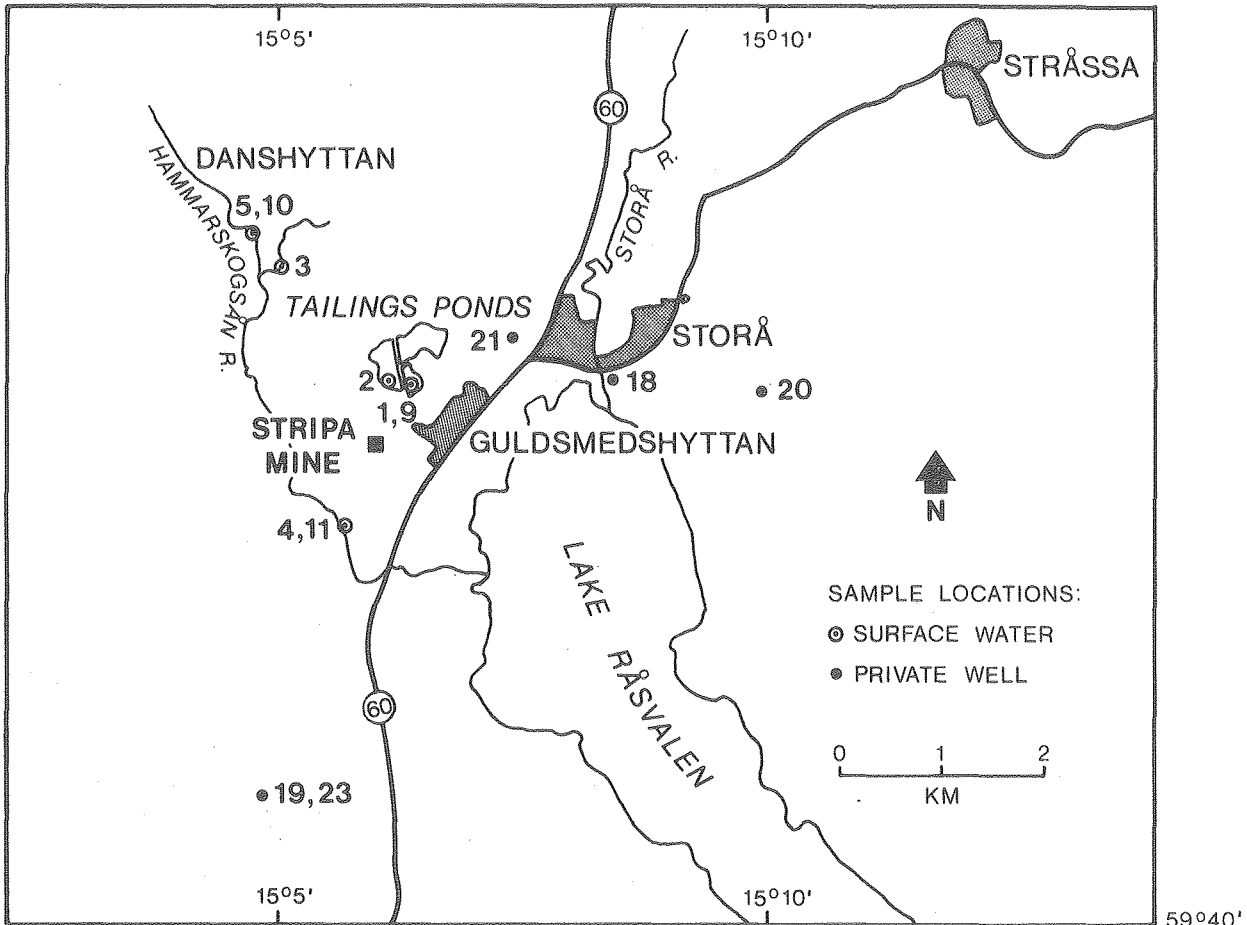
All private wells were equipped with commercial pumps (jet or suction), which provided adequate water, but enhanced groundwater degassing and allowed some groundwater-atmosphere contact. The three drip samples (Stripa 8, 26, and 27), as well as the boreholes sampled by bailing (Stripa 12, 30, 31, 47, and 48) were exposed to the mine atmosphere. Samples obtained from the dewatering system of borehole heaters (Stripa 38, 39, and 40) were subject to degassing by the vacuum pump and were stored in aluminum barrels for at least 16 hours before being collected.

Fortunately, a few boreholes (M-3, R-1, and the borehole drilled from the 410-m level) flowed, and thus required no pumping; here, specific intervals



Table 1. Origin of geochemical samples.

Stripa sample	Origin	Sampling date
1	Tailings pond 3 next to SBH-2	7 Sep 77
2	Aqueduct to pond 3 (from mine)	7 Sep 77
3	Stream (Korslund to Danshuttan)	7 Sep 77
4	Stream (Herrgård sauna)	7 Sep 77
5	Stream (Danshuttegård bridge)	7 Sep 77
6	410-hole, below 152.3 m	8-14 Sep 77
7	410-hole, above 152.3 m	8 Sep 77
8	Dripwater between 410- and 360-m level	8 Sep 77
9	Tailings pond 3 next to SBH-2	12 Sep 77
10	Stream (Danshuttegård bridge)	12 Sep 77
11	Stream (Herrgård sauna)	12 Sep 77
12	H-2 in time-scale room	13 Sep 77
13	M-3 in time-scale room	13 Sep 77
14	Drilling fluid in time-scale room	13 Sep 77
15	410-hole, below 285 m	14-20 Sep 77
16	M-3 in time-scale room	9-21 Sep 77
17	410-hole, 6.3 - 50 m	9-20 Sep 77
18	Private well 1, granite	27 Sep 77
19	Private well 2	28 Sep 77
20	Private well 3	9 Oct 77
21	Private well 5, granite	4-13 Oct 77
22	Drill water time-scale room	12 Oct 77
23	Private well 2	24-26 Oct 77
24	410-entire hole	10 Nov 77
25	Extension drift, drill water	
26	Dripwater, between 360 and 340 m	16-18 Nov 77
27	Dripwater, between 410 and 360 m	18 Nov 77
28	Horizontal borehole (SGU), 338-m level	6-7 Dec 77
29	410-hole, 471 to 376.5 m	Jan 78 - Mar 78
30	Borehole BH-E-5, time-scale room	3 Feb 78
31	Borehole BH-H-3, time-scale room	3 Feb 78
32	Drillwater, ventilation drift	3 Feb 78
33	410-hole, below 12 m	29 May 78
34	410-hole, below 129 m	May 78
35	Borehole M-3, time-scale room	30 May 78
36	Borehole R-1 flowing, ventilation drift	30 May 78
37	410-hole, below 387 m	30 May 78
38	Borehole H-2, time-scale room	31 May 78
39	Borehole H-3, time-scale room	31 May 78
40	Borehole H-4, time-scale room	31 May 78
41	Borehole H-5, time-scale room	31 May 78
42	Borehole M-3, time-scale room	31 May 78
43	410-hole, between 8 and 40 m	5-12 Jun 78
44	410-hole, below 235 m	12 Jun 78
45	410-hole, below 285 m	12-24 Jun 78
46	Borehole R-3, ventilation drift	16 Jun 78
47	Borehole HG-3, ventilation drift	16 Jun 78
48	Borehole HG-4, ventilation drift	16 Jun 78



XBL 794-9487

Fig. 4. Location of private wells in the vicinity of the Stripsa mine which were sampled for chemical and isotopic analyses.

were isolated by packers and the groundwater brought to the surface via nylon tubing. Contact of groundwater with the mine atmosphere was consequently reduced.

When drilling fluids are used, groundwater contamination can be expected for some time. To ensure that sampled groundwaters were free of significant contamination, (1) where possible, at least four borehole-volumes of water were removed from the borehole or well to remove contaminated groundwater before sampling, and (2) some or all of the following groundwater parameters were monitored at the site before and after sampling, with variations over the sampling period interpreted as related to various degrees of contamination:

- conductivity
- temperature
- pH
- dissolved O<sub>2</sub>
- alkalinity

Samples of drilling water, expected to be isotopically distinct from groundwater, were also collected for stable isotope analyses. When consistent isotopic concentrations were obtained before and after the following sampling sequence, the groundwater was considered to be uncontaminated by drilling fluid:

- (1) collect <sup>18</sup>O, deuterium, tritium sample
- (2) measure conductivity and temperature
- (3) measure dissolved oxygen
- (4) measure pH and Eh

- (5) collect field alkalinity sample
- (6) collect water chemistry samples
- (7) collect dissolved gas samples
- (8) collect uranium isotope samples
- (9) collect tritium (enriched) samples
- (10) collect water and  $^{13}\text{C}$  sample
- (11) collect water and  $^{14}\text{C}$  sample
- (12) repeat steps 1-7 in reverse order

For flowing boreholes, steps were omitted or performed out of sequence, and the degree of contamination, if any, was ascertained by the consistency of stable isotope contents ( $^{18}\text{O}$ ,  $^2\text{H}$ ).

The sampling and field geochemical procedures briefly described in this section are those currently used at Stripa--not the final, definitive procedures. Improved procedures essential for more advanced geochemical studies are being developed.

#### Geochemical Measurements in the Field

Conductivity and temperature measurements were made with the Yellow Springs Instrument battery-operated YS133 conductivity meter and probe following the manufacturer's instructions. Water was collected in a clean beaker or in a flow-cell, and the measurements repeated on different aliquots of sample until constant values ( $\pm 5 \mu\text{mhos}$ ) were obtained.

Dissolved oxygen (DO) was measured with the YSI64BP dissolved oxygen meter using a probe fitted with a high sensitivity membrane, following the methods outlined in the instruction manual. As considerable time was required

to obtain a stable reading, measurements were made on water flowing through a flow-cell to minimize groundwater-air contact. Temperature and DO readings were made until stable values were obtained. Previous experience with these meters suggested readings below 0.1 to 0.2 ppm dissolved O<sub>2</sub> were unreliable-- in fact, such readings could be obtained for waters with less than 0.01 ppm dissolved O<sub>2</sub>.

Buffer solutions of known pH were purchased or prepared as suggested by Langmuir (1970). A two-buffer standardization of the Corning model 610 pH meter and Corning combination electrode (#476051) was performed according to the manufacturer's instructions before (and checked after) each pH measurement, and near ( $\pm 2^{\circ}\text{C}$ ) the temperature of the water to be tested. Because of the high pH values encountered, standard buffers near pH 7 and near pH 9 were used for standardization. Standardization was considered satisfactory if the pH ~7 buffer redetermination was within 0.04 pH units. If the standardization made after the pH measurement indicated a change of the pH ~7 buffer value of more than 0.05 pH units, the standardization-measurement procedure was repeated.

Some pH measurements were made on water samples collected in a plastic beaker. After standardization, the pH of the sample was measured, then another aliquot of sample transferred to the beaker and the pH measured. This was repeated until a stable pH value was reached.

Eh standardization is not possible, but the measuring system can be evaluated on its ability to reproduce the Eh of a solution of known Eh--the Zobell solution. Therefore, the Zobell solution was made according to Langmuir (1970) and its potential measured with the Corning pH meter using the combination pH

electrode as a reference electrode and a Corning #476060, platinum disc, inert electrode, following the manufacturer's suggested method. The system was considered to be operating correctly if the measured potential was within  $\pm 5$  mV of the known potential of the Zobell solution at the temperature of measurement.

Most pH and Eh measurements were made using a simple flow cell. The purpose of this cell was to minimize temperature changes and to eliminate air contact for groundwaters which were flowing or pumped. The simple flow cell consisted of a 400 cm<sup>3</sup>, amber glass bottle fitted with a 4-holed rubber stopper. Two holes accept the electrodes; the other holes are fitted for water inflow and water outflow with thermometer. The cell was placed in a tray which retained the outflow of the cell and could be filled with ice. In this way the water in the cell was held within 2°C of the temperature of the groundwater discharging from the borehole or well. Water flow was interrupted during pH or Eh measurements and recommenced between measurements. The pH and Eh values were recorded until stable values were obtained.

Although pH and Eh measurements are expected to be within  $\pm 0.05$  pH units and  $\pm 5$  mV, respectively, of the actual values of the water in the flow cell, the uncertainty with respect to actual groundwater in situ cannot be evaluated. The effects of degassing due to pressure release during sampling is expected to be the major problem. The field-measured pH and Eh values are listed in Appendix A. Only two significant figures are recorded for pH measurements which were not made in the flow cell, or which were not considered adequately accurate due to technical problems.



Alkalinity determinations were made on samples collected in new 0.25- to 0.5-liter plastic bottles, which were thoroughly rinsed and filled by overflowing for several minutes with the water to be sampled. The samples were kept cool and returned to the field laboratory for alkalinity determination as soon as possible (usually within 4 hours). Two aliquots of unfiltered and/or filtered sample were titrated with acid. Initially, the titration was carried out to a pH of 4.3, but the procedure was modified to take the inflection point near pH 4.3 to 4.7 in a "pH versus volume of acid added" plot as a measure of alkalinity. Most field alkalinity determinations have precision of only 5 percent because of the very low alkalinities encountered. However, the charge balances of most analyses do not indicate such a large discrepancy. Although filtered and unfiltered samples were analyzed, the field alkalinities reported in Appendix A are for unfiltered samples.

#### Groundwater Sample Collection

A number of samples were collected for analyses of gases dissolved in groundwaters. Gases coming out of solution as water from boreholes came to the surface were collected by water displacement for  $^{222}\text{Rn}$  analysis by AB Atomenergi, Studsvik, Sweden. The small amount of air contamination encountered could be corrected for after analysis. Samples for helium, neon, argon, krypton, and xenon analysis were collected in small glass tubes, supplied by the analyst, J. N. Andrews, University of Bath, Great Britain. Groundwater was passed through the sampling tube for several minutes and then the sample was isolated by closing two stopcocks. For  $^{222}\text{Rn}$  analysis, 5-liter sample bottles, also supplied by the analysts, were filled by overflowing, and care was taken to avoid air contamination.

For a few samples, an attempt was made to determine the concentration of dissolved gases:  $O_2$ ,  $N_2$ , and  $CH_4$ . For methane analysis, 50  $cm^3$  plastic syringes with 18-gauge needles were first rinsed with the water to be sampled. The needle was placed into the end of the tubing delivering the groundwater and the plunger withdrawn until about 22  $cm^3$  of groundwater was drawn into the syringe. For most samples, water flow forced the plunger back and a snug fit of the needle hub into the tubing allowed any degassed methane to be included in the sample. The syringe needle was changed quickly to a 23-gauge needle, with water being expelled until 20  $cm^3$  remained. The needle was then stoppered quickly with a rubber stopper and the sample kept cool until it was returned to the laboratory for analysis.

For  $O_2/N_2$  analyses, greater care was taken to exclude atmospheric contamination of samples by using glass, 50  $cm^3$  syringes. The syringes and needles were flushed about 12 times, filled with prepurified helium, and then stoppered. The needle was unstoppered and quickly put into the groundwater flow of the delivery tubing, ensuring that helium was continuously expelled. About 25  $cm^3$  of water was drawn into the syringe and the 18-gauge needle replaced by a 27-gauge needle while water was expelled to a volume of 20  $cm^3$ . The needle was capped and the sample returned to the laboratory for analyses. Duplicate or triplicate samples were collected for  $CH_4$  and  $O_2/N_2$  analysis.

Groundwater samples for chemical analysis were collected in two 1-liter plastic bottles. The new bottles were rinsed with the water to be sampled and then filled by overflowing. About 2 ml concentrated  $H_2SO_4$  was added to one bottle, and both bottles were securely capped and returned to the field

laboratory for filtering. Samples were kept cool until they were filtered through 0.45  $\mu$  paper; two small aliquots were used to rinse the paper and receiving flask.

For  $^{234}\text{U}/^{238}\text{U}$  and  $^{226}\text{Ra}$  isotope analysis, twenty 1-liter plastic bottles were rinsed and filled with groundwater, and then each sample acidified to pH less than 2 with about 2  $\text{cm}^3$  of reagent grade HCl.

New 0.2-liter plastic bottles were used to collect samples for stable oxygen and hydrogen isotope analysis and normal tritium analysis. One-liter plastic bottles were used to collect samples for tritium analysis, by the enrichment procedure. All bottles were rinsed with water to be sampled, filled by overflowing to minimize air entrapment, capped, and sealed with household wax before shipment to the appropriate laboratory.

A precipitation technique was employed to collect samples for  $^{13}\text{C}$  and  $^{14}\text{C}$  analysis. For  $^{13}\text{C}$  samples, this involved adding about 5 ml of  $\text{CO}_3$ -free NaOH to a 2- to 4-liter sample, to raise the pH above 12. About 25 g of  $\text{BaCl}_2 \cdot 5\text{H}_2\text{O}$  was then added, and  $\text{BaCO}_3$  and  $\text{BaSO}_4$  quantitatively precipitated. After inverting the bottle, most of this precipitate settled into a scintillation vial fitted into the cap of the bottle. The scintillation vial was then removed, quickly capped, and returned to the analyzing laboratory. A similar precipitation was carried out in 60-liter plastic carboys, which had been filled by overflowing with groundwater. After the  $\text{BaCO}_3$ - $\text{BaSO}_4$  precipitate had settled to the bottom of the carboy, all but about one liter of water was drained via the stopcock and replaced by carbon dioxide-free air (air entered the carboy

through an Ascarite-Drierite trap). A 1-liter plastic bottle was attached through a one-hole rubber stopper to the carboy, the carboy inverted, and the precipitate collected in the 1-liter bottle.

At least 1 g and preferably 3 g of inorganic carbon is required for  $^{14}\text{C}$  analysis, so up to 3000 liters of water in some cases were processed in this way. The possibility of significant uptake of atmospheric carbon dioxide, containing  $^{14}\text{C}$ , when groundwater was added to the carboy increased when such large water volumes were collected. Consequently, a new technique for the collection of groundwater for such studies was developed, and is now in operation. Results and technical details will be described in a forthcoming report on  $^{14}\text{C}$  dating at Stripa.

#### Fracture Mineral Sampling

To assess the processes involving water-rock interaction, samples of minerals present along fractures were collected from various cores taken at the Stripa site. Initial sampling has concentrated on carbonate minerals (calcite) present on many fracture faces. In the future, a more complete range of samples for mineralogical/geochemical analyses will be collected. Personnel logging the cores collected calcite samples routinely. Milligram samples were usually obtained, although one fracture face in the mine workings yielded enough calcite for a  $^{14}\text{C}$  determination. Samples were sent to the University of Waterloo, Canada, for analysis of  $^{18}\text{O}$  and  $^{13}\text{C}$  content.

## 2.2 Laboratory Methods

### Chemical Analyses of Groundwaters

The determination of field pH, Eh, and alkalinity have been described on page 16, and results are included in the appendix. Those field pH values which were not considered to be the best possible measurements are reported to only two significant figures.

The analytical methods and expected precision for analyses by the IAEA and the University of Waterloo are listed in Table 2. The procedures used by Hydroconsult are not known, but they are assumed to be similar, with similar precision. It must be noted that analyses by the IAEA were done on samples collected for enriched tritium analysis (no field filtering or acidification). However, agreement between IAEA and Hydroconsult analyses of samples from the same location is excellent. For example, samples 15-26A and 15-27, 16-23A and 16-24, 17-32 and 17-32A, and 20-3 and 20-4 should be compared.

The reliability of the total chemical analyses can be estimated by calculating the charge balance for the analyses. If an analysis is essentially complete and accurate, such charge balances (as cation equivalents and anion equivalents) should show little excess of cations or anions. Analyses with charge imbalance of less than 10 percent were considered reliable. In general, the best analyses, judged on the basis of minimum charge imbalance, were Hydroconsult, IAEA, and Waterloo laboratory values combined with field alkalinities. Field pH was always accepted as more accurate than laboratory pH; the latter was usually lower than the former, possibly because of carbon dioxide uptake by these highly alkaline samples before laboratory measurements.

Table 2. Analytical methods and estimated precision.

Determination	IAEA <sup>a</sup>		UW <sup>b</sup>	
	Method	Precision (%) <sup>c</sup>	Method	Precision(%) <sup>c</sup>
Calcium	Atomic absorption	3	Atomic absorption	3
Magnesium	Atomic absorption	3	Atomic absorption	5
Sodium	Atomic absorption	2	Atomic absorption	2
Potassium	Atomic absorption	5	Atomic absorption	5
Chloride	Photometric	4	Photometric	4
Sulphate	Photometric and atomic absorption			
Alkalinity	Titrimetric	5	Titrimetric	1
SiO <sub>2</sub>	Photometric		Photometric	
Iron			Atomic absorption	10
Nitrate	Photometric	10		
pH	Electrometric	±0.05		

a. International Atomic Energy Agency, Section for Isotope Hydrology, Vienna Austria.

b. Department of Earth Sciences, University of Waterloo, Canada.

c. Precision expected for the reported range of concentrations for Stripa samples. Reported as (standard deviation/determined concentration)x100%.

Charge balance calculations indicated cation excess was more common than anion excess. Perhaps the omission of F<sup>-</sup> contributed to this, although its inclusion in analyses of samples 29-34-A and 20-61 did not provide a decrease in charge imbalance, especially since these samples already had a slight anion excess.

Rather than averaging analyses for samples from the same location, one analysis was selected as representative for the purpose of chemical discussions. A good charge balance was the prime factor in this selection. IAEA analyses were not selected because of the poor procedures employed in their collection, although these analyses agree well with other better-collected, sample analyses. This choice is arbitrary and does not introduce a significant uncertainty in the discussions which follow.

Dissolved Gas Analyses

The noble gases, He, Ne, Kr, and Ar, were determined using mass spectrometric procedures similar to those described by Mazor (1972). Analyses were performed by Dr. J. N. Andrews, University of Bath, Great Britain. Results are listed in Table 3.

Table 3. Rare gas content of groundwaters (cm<sup>3</sup> gas/cm<sup>3</sup> H<sub>2</sub>O)

Rare gas	Saturation at 5°C (a)	Stripa 16-41 (b) (14Feb78)	Stripa 16-42 (29Mar78)	Stripa 29-18 (b) (14Feb78)	Stripa 29-81 (29Mar78)
Helium	4.9x10 <sup>-8</sup>				
measured		36, 250x10 <sup>-8</sup>	30, 500x10 <sup>-8</sup>	142,000x10 <sup>-8</sup>	86,000x10 <sup>-8</sup>
corrected (c)		N.A.	N.A.	N.A.	N.A.
Neon	2.2x10 <sup>-7</sup>				
measured		3.91x10 <sup>-7</sup>	3.38x10 <sup>-7</sup>	6.2x10 <sup>-7</sup>	6.2x10 <sup>-7</sup>
corrected (c)		2.2 x10 <sup>-7</sup> 5°C	2.2 x10 <sup>-7</sup> 5°C	2.2x10 <sup>-7</sup> 5°C	2.2x10 <sup>-7</sup> 5°C
Argon	4.2x10 <sup>-4</sup>				
measured		6.39x10 <sup>-4</sup>	6.19x10 <sup>-4</sup>	9.65x10 <sup>-4</sup>	9.12x10 <sup>-4</sup>
corrected (c)		5.3 x10 <sup>-4</sup> <0°C	5.4 x10 <sup>-4</sup> <0°C	7.1 x10 <sup>-4</sup> <0°C	7.8 x10 <sup>-4</sup> <0°C
Krypton	1.05x10 <sup>-7</sup>				
measured		1.21x10 <sup>-7</sup>	1.20x10 <sup>-7</sup>	1.48x10 <sup>-7</sup>	1.5x10 <sup>-7</sup>
corrected (c)		1.1 x10 <sup>-7</sup> 8°C	1.1 x10 <sup>-7</sup> 4°C	1.1 x10 <sup>-7</sup> 4°C	1.3x10 <sup>-7</sup> 0°C
Xenon	1.6x10 <sup>-7</sup>				
measured		1.57x10 <sup>-8</sup>	1.50x10 <sup>-8</sup>	1.76x10 <sup>-8</sup>	1.86x10 <sup>-8</sup>
corrected (c)		1.43x10 <sup>-8</sup> 5°C	1.40x10 <sup>-8</sup> <9°C	1.4 x10 <sup>-8</sup> 9°C	1.7 x10 <sup>-8</sup> 2°C
Possible re-charge temperatures from Ne, Kr, Xe contents (d)		5-8°C	4-9°C	4-9°C	0-5°C

- (a) Equilibrium with atmospheric air is assumed.  
 (b) Average of two measurements.  
 (c) Corrected for air contamination using neon saturation at 5°C (Mazor 1976).  
 (d) Groundwater recharge temperatures estimated from rare gas concentrations after correction for air contamination.

Preliminary determinations of dissolved O<sub>2</sub>, N<sub>2</sub>, and CH<sub>4</sub> were made using a gas chromatographic technique based on the procedure by Stainton (1973). The syringe used to collect the water sample was used as a reaction chamber to establish a static equilibrium of dissolved gas between the liquid and helium. The helium was injected via a sample loop into a Fisher Hamilton Model 29 Gas Partitioner, the individual gases separated on dual columns, and the concentrations determined from signals produced by the thermal conductivity detector. Standards prepared by saturating deionized water with either CH<sub>4</sub> or air were also processed in this manner, and the gas concentrations calculated from a linear peak-height versus concentration plot. These analyses are reported, along with field dissolved oxygen and field Eh measurements, in Table 4.

Table 4. Dissolved gases and redox potential of groundwaters in the Stripa area.

Stripa sample	Dissolved gases ( $\mu$ moles/l) gas partitioner			Field measurements	
	CH <sub>4</sub>	N <sub>2</sub>	O <sub>2</sub>	DO meter	Eh, mV
6	10	580	104 <sup>a</sup>	< 2.5	+ 72
7	15	610	78 <sup>a</sup>		
13, 16, 35, 42	14	1410	40	< 30	+ 74
14	< 0.2	460	>300 <sup>a</sup>		
15	9	510	105 <sup>a</sup>	< 3	- 7
17				< 3	- 8
18				67	
19, 23				< 95	+257
21				133	+ 98
24				6	+ 38
29				3	
43	27	1380 <sup>b</sup>	18		- 87
45	14	1590 <sup>b</sup>	40		+ 23

a. Analyzed after storage with probable air contamination.

b. N<sub>2</sub> used to inflate packers could be contaminating the samples.

DO = dissolved oxygen



### Isotope Analyses

The following paragraphs provide a description of analytical techniques used for isotope analyses and discuss data presentation and reference standards used.

Deuterium. The deuterium content in groundwaters was determined on a specially designed, double-collecting mass spectrometer with semiautomatic inlet and recording system (Thurston 1971). It consists of a vapor-sampling device directly connected to a mass spectrometer via a uranium reduction furnace. Repeat analyses were done on a 602D Micromass mass-spectrometer. The  $^2\text{H}/^1\text{H}$  ratio of the hydrogen gas produced is determined by comparing the sample to reference standards. The results reported here are expressed in the  $\delta$  per mil notation with respect to the Standard Mean Ocean Water (SMOW), where

$$\delta^2\text{H} = \frac{R_x - R_s}{R_s} \times 1000$$

and  $R_x$  and  $R_s$  represent the  $^2\text{H}/^1\text{H}$  ratios of sample and standard, respectively. A  $\delta^2\text{H} = -10$  ‰ signifies that the sample has 10 ‰ less deuterium than the standard. Analytical precision is close to  $\pm 1$  ‰.

Oxygen-18. The  $^{18}\text{O}$  analysis of water is indirectly determined mass spectrometrically with a Micromass Ms 602D instrument by measuring the  $^{18}\text{O}/^{16}\text{O}$  ratios in carbon dioxide equilibrated at  $25^\circ\text{C}$  ( $\pm 0.1^\circ\text{C}$ ) with the water sample. The isotope exchange reaction,  $\text{H}_2^{18}\text{O} + \text{C}^{16}\text{O}_2 \rightleftharpoons \text{H}_2^{16}\text{O} + \text{C}^{16}\text{O}^{18}\text{O}$  is thermodynamically controlled and produces a constant isotope partitioning between the two compounds if equilibration is done at constant temperature. Samples and standards are prepared in the same manner and, if the data are expressed in ‰.

differences, the numerical value of the fractionation effect is of no importance. The  $\delta$ -definition is identical to the one described for deuterium, with  $R_x$  and  $R_s$  being the  $^{18}\text{O}/^{16}\text{O}$  ratios of sample and standard, respectively. All data are reported versus SMOW and a  $\delta^{18}\text{O} = +5 \text{ ‰}$  signifies that the sample has 5 ‰ more  $^{18}\text{O}$  than the standard.

During preparation of samples, a reference water sample was prepared for every nine test water samples. The overall analytical precision derived from these data is better than  $\pm 0.15 \text{ ‰}$ .

Carbon-13. The carbon-13 contents of the aqueous carbonate in water samples was determined on barium carbonate or strontium carbonate precipitated from 1/2-gal water samples with reagent-grade  $\text{BaCl}_2 \cdot 2\text{H}_2\text{O}$  in an alkaline medium.

This carbonate was reacted in the laboratory with 100 percent  $\text{H}_3\text{PO}_4$ , and the resulting  $\text{CO}_2$  was analyzed for its  $^{13}\text{C}/^{12}\text{C}$  ratios with an MS 602D mass spectrometer.

A similar procedure was followed for the fracture carbonates, but for these samples the reaction was carried out at  $25 \pm 0.1^\circ\text{C}$  in order to utilize the resulting  $\text{CO}_2$  for  $^{18}\text{O}$  analyses. During the  $\text{H}_3\text{PO}_4$  reaction, ( $\text{CaCO}_3 + 2\text{H}^+ \rightarrow \text{Ca}^{++} + \text{H}_2\text{O} + \text{CO}_2$ ), one oxygen from the carbonate remains in the resulting  $\text{H}_2\text{O}$  and an isotope effect occurs. This is constant if the samples are reacted at constant temperature; because the standards are treated in the same manner, the numerical value of the isotope fractionation factor cancels from the  $\delta$ -value, which is again used for the presentation of data. Reference

standard for both  $^{18}\text{O}$  and  $^{13}\text{C}$  analyses is PDB, a belemnoid rostrum from the Pee Dee Formation of North Carolina. This standard has been used to calibrate universally available secondary standards.

The overall analytical precision for both  $^{18}\text{O}$  and  $^{13}\text{C}$  analyses of solid carbonates such as the fracture minerals is close to  $\pm 0.15$  ‰, but approaches  $\pm 0.4$  ‰ for aqueous carbonates precipitated in the field. A complete set of water samples will be analyzed in the future, at which time the  $\text{CO}_2$  will be acid-stripped from water samples shipped to the laboratory. It is expected that in this case, the analytical precision will also be close to  $\pm 0.15$  ‰ for the  $^{13}\text{C}$  analyses.

Tritium. Tritium content was measured in enriched and nonenriched samples. Electrolytic procedures were used to concentrate tritium, and both gas counting (on methane produced from the enriched water) and liquid scintillation counting of  $^3\text{H}$  disintegration events were done. For the liquid scintillation counting, a liquid scintillator within a gelling agent (INSTAGEL) was mixed with the water (the proportion differs for different laboratory setups) and counted directly. The latter procedure was used exclusively for nonenriched samples. The analytical error is determined for each sample from counting statistics and comparisons with reference samples, and is quoted in the tables where tritium data are presented. The data are expressed in tritium units (TU) where  $1\text{TU} = ^3\text{H}/10^{18} \text{ }^1\text{H}$ .

Carbon-14. The extremely small amounts of  $^{14}\text{C}$  in natural carbon ( $\sim 10^{-10}$  ‰) require that the counting be done in the most efficient manner. Both gas and liquid scintillation techniques have been developed and were used. The gas

counting was done on methane and the liquid scintillation counting on benzene. Both preparation procedures require special catalysts, and details of the preparation vary somewhat from laboratory to laboratory. Analytical precision is quoted for each sample and is based on counting statistics. The results are expressed as percent modern carbon (pmC) which was determined as 95 percent of the activity of an Oxalic Acid Standard distributed by the National Bureau of Standards in Washington. The 95 percent activity of this standard represents the activity of wood grown during 1850 in an uncontaminated environment.

Uranium-234 and Uranium-238. Most commonly, the alpha activity ratio of  $^{234}\text{U}/^{238}\text{U}$  is measured directly rather than measuring the atomic  $^{234}\text{U}/^{238}\text{U}$  ratio itself, which requires expensive and time-consuming mass spectrometry. At least one microgram of  $^{232}\text{U}$ -spiked uranium is deposited on a counting planchet and counted for 3 to 4 days in an alpha counter to determine the relative abundance (relative alpha peak heights) of the individual isotopes. Uncertainty limits are about  $\pm 3$  percent on individual isotope count rates, and about 4 to 5 percent in isotope abundance and isotope ratio determinations.

Helium-4 and Other Noble Gases. Helium-4 analyses are usually done by mass spectrometry on gas samples extracted from small volumes of water collected in special vessels to minimize air contamination. Analytical error following complicated extraction and analytical procedures is not more than a few percent.

Radon analyses are given as direct counts in curies/sample size, in this case as  $\mu\text{Ci}/\text{sample bottle}$  (microcurie =  $10^{-6}\text{Ci}$ ) whereby the sample bottles had a volume of 1.16 liters. In the following discussion these results are presented as  $\mu\text{Ci}/\text{liter}$ .

### 3. RESULTS AND DISCUSSION

#### 3.1 Groundwater Chemistry

Chemical analysis of groundwaters in the Stripa area were performed to provide:

- a description of the chemical nature of groundwaters in a granitic rock mass;
- a database for evaluating the geochemical processes affecting groundwaters (water/rock interaction, especially) in such a terrain;
- data necessary for the application of chemical models to transform measured carbon-14 activities into groundwater ages.

It became evident that the geochemical processes controlling groundwater chemistry could be adequately treated only after detailed chemical and mineralogical studies of the rock mass, and especially of the fracture minerals, were completed. Since these studies have not yet been carried out, the groundwater chemistry can be treated in only a very qualitative manner. A more comprehensive interpretation will be provided once the fracture mineral data are available.

#### The Chemical Characteristics of Groundwaters

The surface waters sampled in the Stripa area are very dilute, with total dissolved solids (TDS) of less than 35 mg/liter. On a molal basis, the dominant species are:  $\text{Ca} (\approx \text{HCO}_3) > \text{Cl} \approx \text{Na} \approx \text{SO}_4 > \text{SiO}_2 (> \text{HCO}_3) > \text{K} > \text{Fe}$ . The pH is 6.5 to 6.8, nitrate is about 0.5 ppm, dissolved organic carbon is high (5 ppm), and the waters are undersaturated with respect to calcite. Shallow groundwaters (from less than 100-m depth) obtained from private wells contain TDS of 120 to 325 mg/liter. These groundwaters are dominantly calcium carbonate

waters with



The pH is 6.8 to 7.9, nitrate is very variable (0 to 2.5 ppm), and organic carbon concentrations are much lower than in surface waters - generally about 0.6 to 0.8 ppm carbon. These shallow groundwaters are, with few exceptions (Stripa 18), undersaturated with respect to calcite.

Deeper groundwaters from the 330-m level and from the upper part of the 410-m-level borehole are sodium chloride-bicarbonate waters with TDS of about 200 to 230 mg/liter, and molal concentrations decreasing in the order



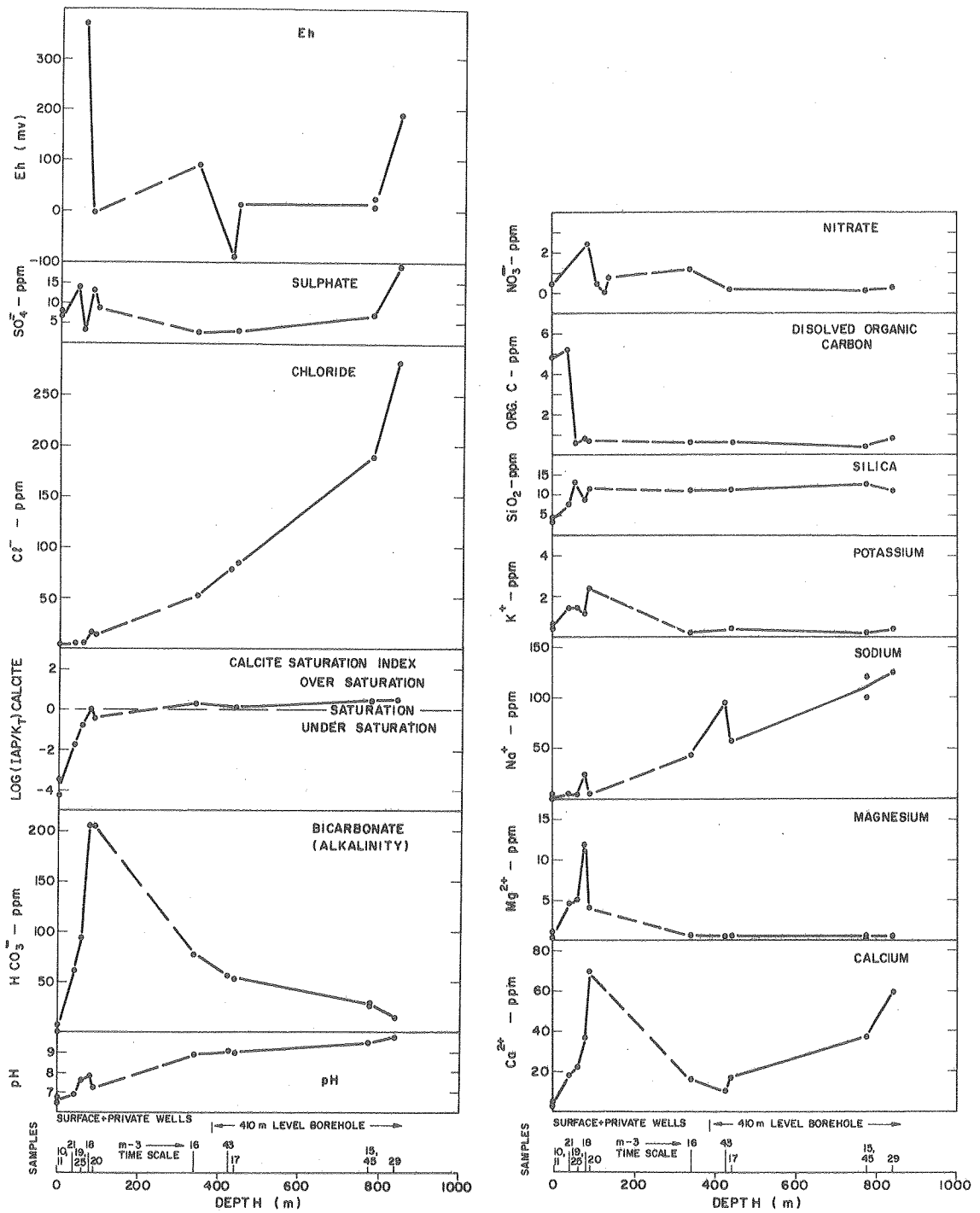
The pH is 8.8 to 9.05, nitrate is 0 to 1.2 ppm, and organic carbon is low (0.6 ppm carbon). Calcite saturation is slightly exceeded.

The deepest samples (Stripa 29, 37, 44, and 45), from below 700 m (from the borehole at the 410-m level) have the highest TDS (375 to > 510 mg/liter) and are sodium-calcium chloride groundwaters with



These waters have high pH (9.5 to 9.8), low nitrate (< 0.3 ppm), and low organic carbon content (< 0.8 ppm). Calcite saturation is exceeded in all samples. No sampling problems were encountered in samples collected from boreholes at the 330-m and 410-m levels.

Geochemical variations in groundwaters from Stripa are illustrated in Fig. 5, where the change in some geochemical parameters with depth can be seen. Depths of samples are from the surface and are only approximate in most cases,



XBL 794-9488

Fig. 5. Geochemical variation of groundwaters with depth.

especially where a sample was obtained over a depth interval. "Drip" samples were not included in Fig. 5; they are generally discounted because of exposure to mine air and probable contamination. The unusually high organic carbon, nitrate, and sulphate values for these samples (Stripa 26, 27) from the mine workings suggests contamination occurred. This is supported by stable isotope measurements.

Table 5. A comparison of the ranges in chemical species in groundwaters from Stripa, Swedish granites, and gneisses from the Bohemian Massif.

Species	Range of concentrations (mg/l)		
	Stripa	Sweden	Bohemian Massif
Ca	10 to 59	~10 to > 40	8.0 to 62.5
Mg	0.5	~ 5 to ~ 15	trace to 20.7
Na	43 to 125	~10 to > 40	2.5 to 10.5
K	0.2 to 5.4	~ 3 to ~ 5	trace to 4.5
Cl	52 to 283	~ 3 to >5000 <sup>a</sup>	1.8 to 7.8
SO <sub>4</sub>	2.7 to 19	~ 3 to ~ 50	18.5 to 235
HCO <sub>3</sub>	15.4 to 78.7	~60 to ~ 300	3.7 to 18.3
SiO <sub>2</sub>	11.0 to 12.8	~10 to ~ 60 <sup>b</sup>	5.5 to 18.0
Fe	0.02 to 0.24		trace to 1.9
pH	8.85 to 9.75	~ 6 to ~ 9	4.4 to 5.96

a Fossil seawater contamination assumed.

b No actual analyses given but general quote of literature data.

Table 5 presents a comparison of the ranges in chemical species found in groundwaters from the Stripa mine (excluding private wells), from granites and gneisses in Sweden (Jacks 1978), and from granite of the Bohemian Massif reported by Pačes (1972). The differences are important: much higher concentrations of Na, Cl, and HCO<sub>3</sub>, much higher pH values, but lower concentrations of Mg, SO<sub>4</sub>, and Fe were encountered at Stripa and other



Swedish sites than in the Bohemian Massif. The differences might be explained on the basis of:

- different atmospheric input; different geochemical conditions affecting groundwater in the unsaturated zone or in other rock-types before the groundwater enters granite;
- mineralogical variation in granites;
- control of geochemistry by fracture mineralogy which would be variable for different granites;
- different degrees of water/rock interaction due to different groundwater temperatures, duration of water/rock contact, physical fracture characteristics, etc.;
- presence of brines or seawater in the Stripa rocks.

#### Geochemical Processes and the Geochemical Evolution of Groundwater

In the qualitative discussion which follows, the Stripa groundwaters are considered to evolve from original recharged waters to the presently observed groundwaters. The major process causing geochemical change as waters flow in the subsurface is considered to be water/rock interaction. Other processes, such as microbial activity or mixing of different groundwaters, might be significant and are discussed briefly where appropriate. In view of the assumed increasing age of groundwaters with depth, the groundwater geochemical evolution is considered to parallel increasing depth, whereby deeper samples are thought to have undergone more geochemical evolution than shallow samples. The assumption is also made that modern shallow samples are similar to deeper samples as they existed at an earlier stage of evolution. Although this concept provides an apparently consistent framework for available groundwater ages,

stable isotope compositions, and geochemistry, it must be reevaluated on the basis of data from the ongoing hydrological/geochemical studies.

The increase in TDS from surface waters to shallow groundwaters is paralleled by increases in all dissolved species, except perhaps organic carbon. The shallow groundwaters have probably picked up and increased dissolved load from both the unsaturated and saturated zones, through mineral dissolution and hydrolysis of primary igneous and metamorphic minerals with the generation of clays and other minerals as well as ionic compounds. Marble has been identified in shallow bedrock cores (Stallsbergbogen borehole No. 2, for example) and its dissolution could account for some of the Ca, Mg, and  $\text{HCO}_3^-$  in these groundwaters, especially in Stripa 18. The latter is the only shallow groundwater found to be saturated with respect to calcite.

Compared to those for shallow groundwaters, the intermediate-depth groundwaters (from the 330-m and 410-m levels) have lower Mg, K, Ca, and  $\text{HCO}_3^-$ ; have gained Na and Cl; and have high pH. Calcite saturation and even some supersaturation is maintained, even with the decrease in Ca and  $\text{HCO}_3^-$ . Silica, organic carbon, sulphate, and nitrate are virtually constant. The observed evolution could be the result of any of the following processes:

- (1) Calcite precipitation
- (2) Incongruent dissolution of primary silicate minerals with clay mineral formation (thus maintaining constant aqueous  $\text{SiO}_2$  concentrations)
- (3) Cation exchange of  $\text{Ca}^{2+}$  and  $\text{Mg}^{2+}$  from solution for  $\text{Na}^+$  and  $\text{H}^+$  from clay mineral surfaces

- (4) Mixing of normal groundwaters with residual seawater (E. Eriksson, pers. comm.)
- (5) Release of brines from fluid inclusions.

The decrease in  $\text{Ca}^{++}$  and  $\text{HCO}_3^-$  is most simply explained by calcite precipitation, which is supported by the observation that calcite is a very common fracture mineral. The increase in  $\text{Cl}^-$  could be due to either (4) or (5) above, or to a much greater  $\text{Cl}^-$  concentration in these groundwaters during recharge at some past time. No chloride minerals are present in granitic rocks, but traces of  $\text{Cl}^-$  do occur in a variety of silicates. Changes in  $\text{Mg}^{2+}$ ,  $\text{Na}^+$ , and  $\text{K}^+$  concentrations are probably due to a combination of silicate dissolution and neoformation of clays, and to subsequent cation exchange.

Compared to the intermediate-depth groundwaters, the deepest groundwaters show increased concentrations of  $\text{Ca}^{2+}$ ,  $\text{Na}^+$ , and  $\text{Cl}^-$ ; decreased levels of  $\text{HCO}_3^-$ ; and about the same  $\text{NO}_3^-$ , organic carbon,  $\text{SO}_4^{=}$ ,  $\text{SiO}_2$ ,  $\text{K}^+$  and  $\text{Mg}^{2+}$  levels. The pH continues to increase slightly and slight calcite supersaturation is maintained. This geochemical evolution could be the result of:

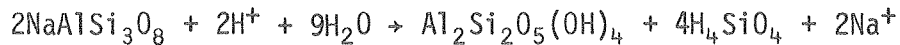
- continued calcite precipitation and (a) increased dissolution of  $\text{Ca}^{2+}$ -bearing primary minerals and/or (b) release of  $\text{Ca}^{2+}$  from calcium montmorillonite;
- minor exchange of  $\text{Ca}^{2+}$  and  $\text{Mg}^{2+}$  for  $\text{Na}^+$  from clays, especially the formation of Mg-chlorites;
- the pH is most probably controlled by the incongruent dissolution of silicates;

- mixing of normal groundwaters with NaCl brines, perhaps residual seawater.

Even though  $\text{HCO}_3^-$  decreases in the deeper groundwaters, the higher pH and  $\text{Ca}^{2+}$  concentrations permit calcite precipitation. The increased  $\text{Ca}^{2+}$  would be due to an excess of calcium-silicate-mineral dissolution over calcite precipitation. Too little is known about the respective reaction rates to make a quantitative discussion possible; nor have the observed evolutions been timed through groundwater age determinations. The impressive increase of  $\text{Cl}^-$  in the deepest groundwaters again is not yet explained, but could be due to mixing with fluid-inclusion water or fossil seawater. If fossil seawater plays a role, it should be possible to define at what time it might have penetrated and/or left the system--with important consequences for the age of the hydrologic regimes we observe today. The geochemical evolution described here would no longer concern only a single water mass but would reflect mixing of two different waters. An increasing chemical load would then not necessarily reflect increasing water ages or residence times.

Thus, groundwater chemistry is controlled by the water's interactions with the solid phases present in the flow system. In these fractured systems, the reactions are possibly restricted to a rather narrow area along fractures and dominated by the dissolution of primary minerals and precipitation of clays and carbonates. However, quantitative analysis based on reaction rates and thermodynamic constraints would demand a much deeper understanding of these processes. At present only a qualitative approach is possible, based on the assumption that although the dissolution of primary silicates is a nonequili-

brum process, the formation of clay minerals which occurs simultaneously is governed by the solution chemistry created in the local environments and follows thermodynamic constraints. General reactions, such as the incongruent dissolution of albite and the formation of kaolinite, where



can then be studied with thermodynamic data, and mineral stability diagrams based on ion activity ratios can be constructed. In the above case, the albite/kaolinite stability relationship could be presented on a diagram of activities of  $\text{Na}^+/\text{H}^+$  versus  $\text{H}_4\text{SiO}_4$ ; in other cases,  $\text{Ca}^{++}/\text{H}^+$  versus  $\text{Na}^+/\text{H}^+$ , or  $\text{Ca}^{++}/\text{H}^+$  versus  $\text{Mg}^{++}/\text{H}^+$  provide the most useful framework. Such diagrams have been constructed extensively for pure endmembers, and in this presentation the stability diagrams of Helgeson, Brown, and Leeper (1969) and Pačes (1972) are used. When quantitative mineralogical/geochemical data become available, the use of free energy data such as calculated by the method of Tardy and Garrels (1976) for constructing stability diagrams will make it possible to consider nonideal endmembers as well. Unfortunately, the lack of mineralogic data for Stripa necessitates the use of the pure endmember diagrams.

Figures 6, 7, and 8 present different mineral stability diagrams on which the groundwater data from Stripa have been plotted. In all cases a very clear evolutionary trend emerges--strong indication that all groundwaters sampled to date have followed similar evolutionary trends. This is important because in the following sections it will be shown that the origin of the water discharging from different fracture systems in the granite is not uniform.

In Fig. 6 mineral stabilities are defined with respect to  $\text{Na}^+$ ,  $\text{H}^+$ , and  $\text{H}_4\text{SiO}_4$  activities in the groundwater. The Stripa groundwaters have a rather constant  $\text{H}_4\text{SiO}_4$  concentration, perhaps controlled by the precipitation of some amorphous silica phase or clays. A geochemical-evolutionary trend of increasing  $\text{Na}^+$ /decreasing  $\text{H}^+$  can be seen for waters of increasing depth. In this system kaolinite is initially the stable clay mineral but in deep groundwater Na-montmorillonite tends to become a stable phase. Because albite appears to be almost stable in the deepest groundwater, it is possible that further albite dissolution is unlikely if the present  $\text{H}_4\text{SiO}_4$  concentration is maintained.

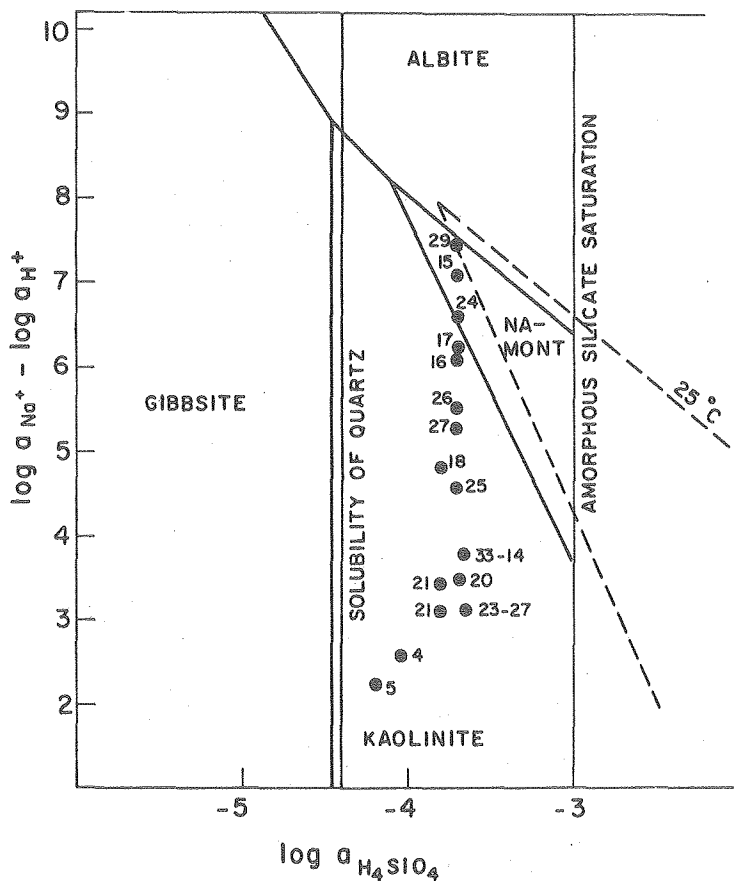


Fig. 6.

Mineral stability diagram in terms of  $\text{Na}^+$ ,  $\text{H}^+$ , and  $\text{H}_4\text{SiO}_4$  activities in waters of the Stripa area. Phase boundaries are after Helgeson, Brown, and Leeper (1969) for waters at  $0^\circ\text{C}$ , with boundaries for water at  $25^\circ\text{C}$  included as interrupted lines.

In Fig. 7 mineral stabilities are plotted with respect to  $Mg^{2+}$ ,  $H^+$ , and  $Na^+$  activities. Again a trend is observed for groundwaters which may describe a geochemical evolution with increasing depth. Waters initially in equilibrium with Mg-montmorillonite move into the stability field of low albite and then into the stability field of Mg-chlorite. The initial part of the trend seems to parallel the Mg-Na-montmorillonite boundary.

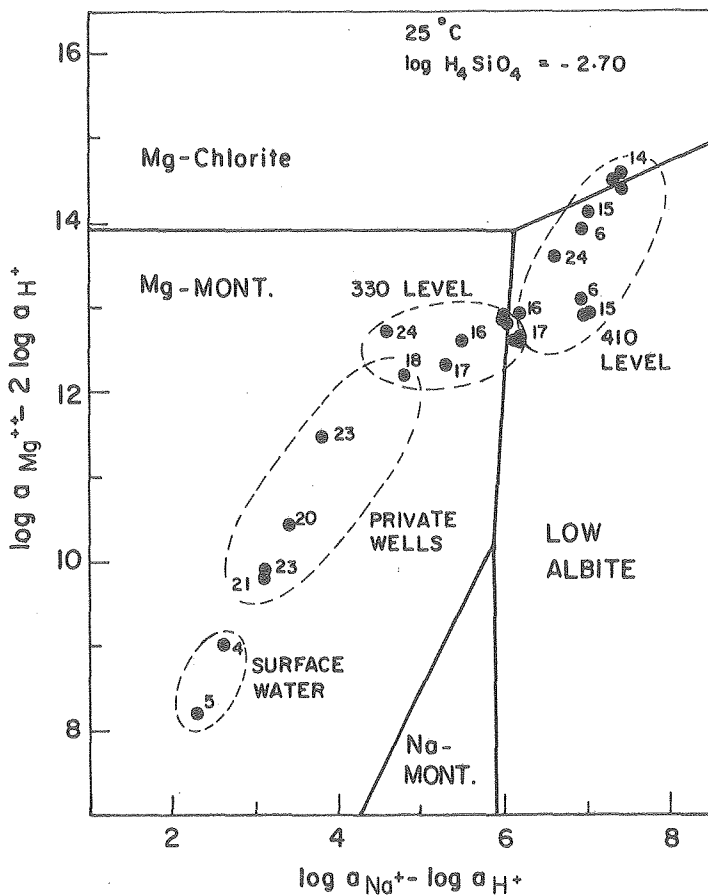


Fig. 7.

Mineral stability diagram in terms of  $Mg^{2+}$ ,  $H^+$ , and  $Na^+$  activities in waters of the Stripa area. Phase boundaries are after Helgeson, Brown, and Leeper (1969) for waters at 25°C with log  $H_4SiO_4$  fixed at amorphous silica saturation.

XBL 794-9490

Figure 8 describes mineral stabilities in terms of  $Ca^{2+}$ ,  $H^+$ , and  $H_4SiO_4$  activities. The evolutionary trends are again clear. The diagram suggests that in the surface waters kaolinite could form as a secondary clay mineral,

whereas in shallow and deeper groundwaters the more complex leonhardite could be stable. Assuming, also, equilibrium between  $\text{Ca}^{2+}$  and  $\text{H}^+$  aqueous and solid calcite, the  $\text{pCO}_2$  of these systems can be calculated and compared with the  $\text{pCO}_2$  at calcite saturation for various  $\text{Ca}^{2+}/\text{H}^+$  activity ratios. The  $\text{Ca}^{2+}/(\text{H}^+)^2$  activity ratios are shown in Fig. 8 and, as expected, they compare excellently with values determined by considering chemical equilibria in the groundwaters. This is because calcite saturation is maintained in all deeper groundwaters.

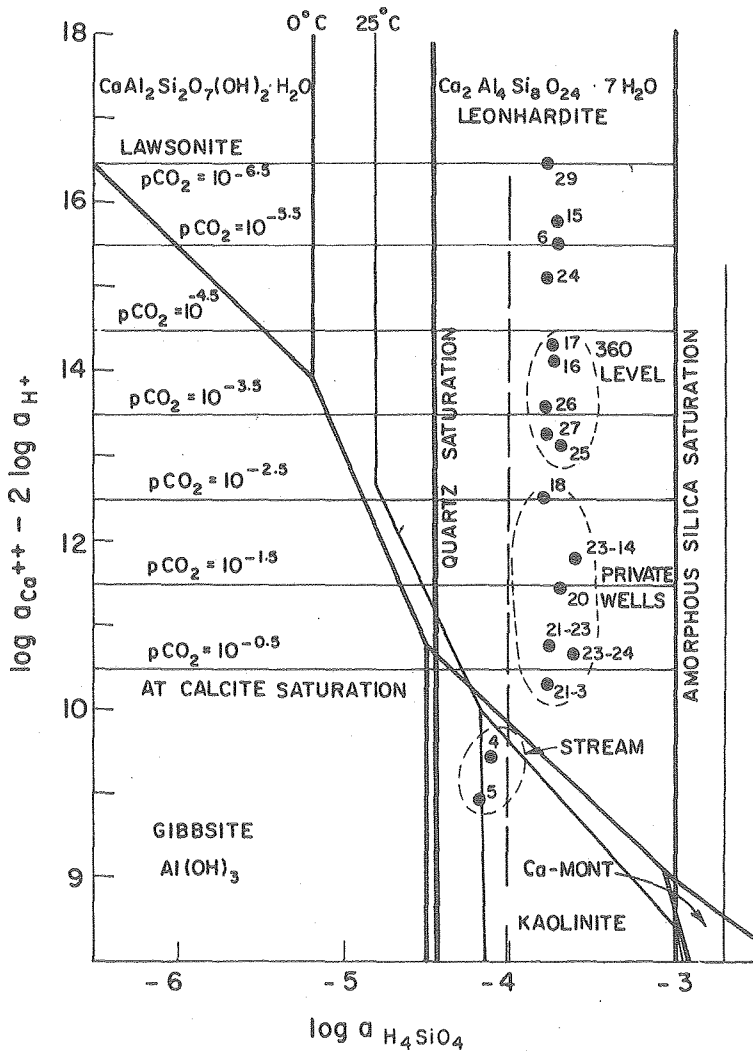


Fig. 8.

Mineral stability diagram in terms of  $\text{Ca}^{2+}$ ,  $\text{H}^+$ , and  $\text{H}_4\text{SiO}_4$  activities in waters of the Stripa area. Phase boundaries are for 0°C (heavy lines) and 25°C (light lines) and are from Helgeson, Brown, and Leeper (1969). Both quartz and amorphous silica saturation values of  $\log a_{\text{H}_4\text{SiO}_4}$  are shown.



### 3.2 Dissolved Gases

#### Oxygen, Nitrogen, Methane

These gases were analyzed mainly to determine the composition of gas bubbles observed in the flowing borehole M-3 in the time-scale room and in the flowing borehole drilled vertically downward from the 410-m level. Table 4 (p. 26) presents the dissolved gas analyses of waters from various points in the Stripa mine as well as from a reservoir of drilling water used in the time-scale room (Stripa 14).

The lack of agreement of DO meter and gas partitioner results for  $O_2$  indicated in Table 4 is probably due to slight contamination by air of the latter samples. Improved techniques have been developed and will be tested in the near future at Stripa. Contamination of samples by  $N_2$  when  $N_2$ -inflated packers were used is also possible, as indicated in Table 4.

Concentrations of  $O_2$  and  $CH_4$  were always lower than  $N_2$  concentrations. For comparison, water saturated with air at  $0^\circ C$  would contain about  $455 \mu M O_2$  and about  $850 \mu M N_2$ . Saturation of water with air at higher temperature would result in less  $O_2$  and  $N_2$  being dissolved. Thus, for samples from the M-3 borehole (Stripa 13, 16, 35, 42) and perhaps from the intervals 8 to 40 m and below 285 m in the borehole from the 410-m level,  $N_2$  must have been added to the groundwater after atmospheric exchange. Denitrification is an obvious source of  $N_2$  in groundwater. The presence of traces of  $CH_4$  suggests that conditions are anaerobic in these groundwaters, and so both denitrification and methanogenesis could have occurred microbially. Microbial utilization of  $O_2$  would explain the low concentrations of  $O_2$  in these waters.

We conclude that the observed gas bubbles in the M-3 borehole (time-scale room) and in the borehole drilled from the 410-m level are dominated by N<sub>2</sub> released from solution as the confining pressure on these anaerobic waters is released.

Table 6. Comparison of pO<sub>2</sub> and pCH<sub>4</sub> calculated from Eh with pO<sub>2</sub> and pCH<sub>4</sub> measured in groundwaters from Stripa area.

Stripa sample	Eh, mV	pO <sub>2</sub>		pCH <sub>4</sub>	
		Calculated	Measured	Calculated	Measured
6	+122	3.5x10 <sup>-43</sup>	<1.2x10 <sup>-3</sup>	7.5x10 <sup>-73</sup>	4.9x10 <sup>-3</sup>
29	+169	5.9x10 <sup>-39</sup>	1.5x10 <sup>-3</sup>		
16, 42	+ 92	6.4x10 <sup>-47</sup>	2.0x10 <sup>-2</sup>	1.5x10 <sup>-63</sup>	6.9x10 <sup>-3</sup>

It is possible to calculate the equilibrium partial pressure of both CH<sub>4</sub> and O<sub>2</sub> in groundwaters from measured Eh values. These calculated values can then be compared to measured partial pressures or concentrations to evaluate the state of equilibrium of the groundwater in terms of redox potential. The results of these calculations are shown in Table 6. The partial pressure of O<sub>2</sub> (pO<sub>2</sub>) was calculated by the method of Sato (1960). The partial pressure of CH<sub>4</sub> (pCH<sub>4</sub>) was calculated using Eh, pH, and HCO<sub>3</sub><sup>-</sup> content data as described by Thorstenson (1970) and Stumm and Morgan (1970). Henry's Law was used to calculate the actual groundwater pO<sub>2</sub> and pCH<sub>4</sub> from the dissolved O<sub>2</sub> and CH<sub>4</sub> values listed in Table 4. This calculation was done using WATEQF (Plummer, Jones and Truesdale 1976). DO meter results in Table 4 were used to calculate pO<sub>2</sub>. As seen in Table 6, actual (measured) pO<sub>2</sub> and pCH<sub>4</sub> values are invariably

too high by many orders of magnitude to be at equilibrium in groundwaters with the measured Eh values. This discrepancy could be due to any or a combination of the following:

- poor field measurements of Eh;
- thermodynamic limitations of the platinum electrode in these waters;
- poor Eh-poising in these waters, i.e., a lack of sufficient redox reactants (such as  $\text{Fe}^{2+}/\text{Fe}^{3+}$ ) to produce sufficient current in the Eh-measuring system;
- lack of equilibrium in systems involving  $\text{O}_2$  and  $\text{CH}_4$ . A much more detailed investigation, perhaps including measurement of concentrations of various redox couples ( $\text{Fe}^{2+}/\text{Fe}^{3+}$ ,  $\text{CH}_4/\text{HCO}_3^-$ , or  $\text{As}^{3+}/\text{As}^{5+}$ , for example) would be required to define the redox potential of these groundwaters.

#### Noble Gases

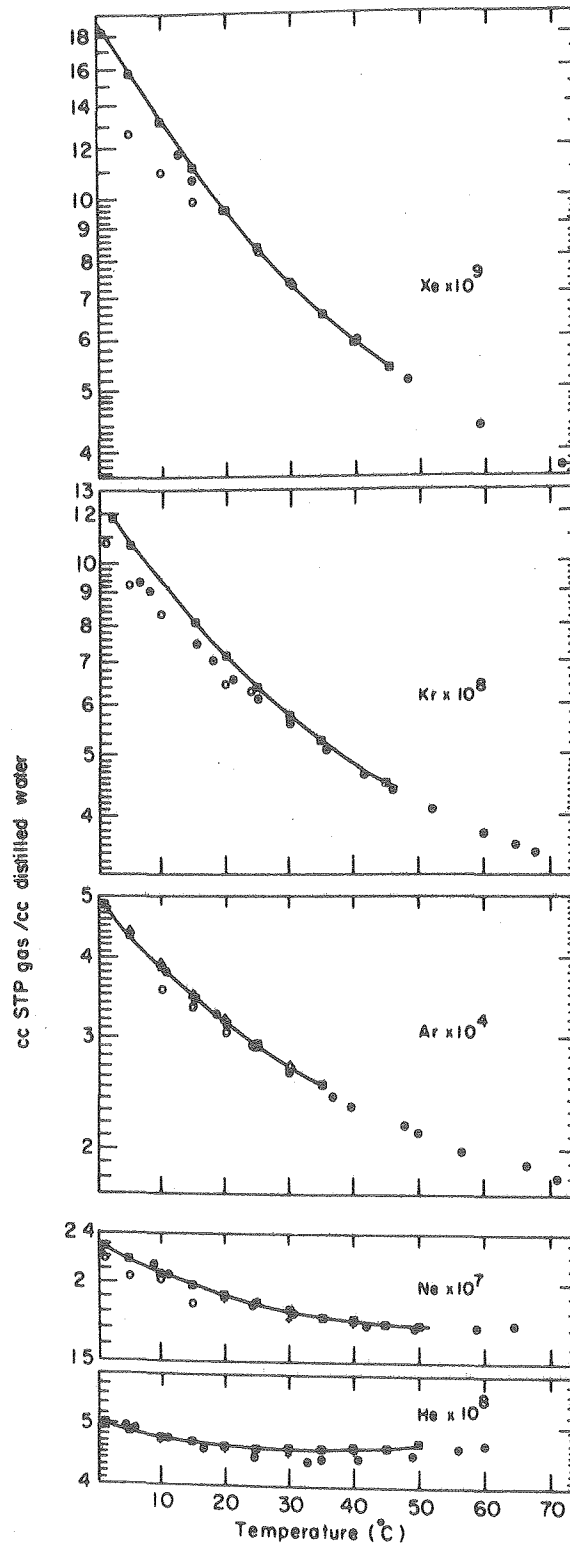
The noble gases, helium, neon, argon, krypton, and xenon, are present in the atmosphere in known but variable amounts. Infiltrating groundwater is usually saturated with these gases, and the ratio of noble gas in air to that in water (by volume at 20°C) is He:110, Ne:100, Ar:40, Kr:25, and Xe:15 (Mazor 1972). Because they are chemically inert and little or not sorbed in porous media, they lend themselves for a variety of tracer studies, including the possibility of using the concentrations of these gases in groundwaters as indicators of paleotemperatures of groundwater recharge.

The amount of noble gases that can be dissolved in water at saturation levels is relatively little temperature-dependent for He and Ne, but strongly temperature-dependent for Ar, Kr, and Xe. If a groundwater system remained

closed and neither lost nor gained gases, its dissolved gas content would reflect "paleotemperatures of recharge." This has been extensively documented by Mazor (1972, 1976). The temperature dependence of noble gas dissolution in water is shown graphically in Fig. 9.

In many subsurface environments, however, the requirements for a closed system are not met. Additions of radiogenic helium and sometimes argon can alter the noble gas ratios, notably in geothermal areas. If the production rate of these two gases in a given system is known, residence times can be determined from their concentrations--assuming again that no loss has occurred. The neon, krypton, and xenon contents should not be affected by this and, for example, in a geothermal system, their relative abundance could be used to detect magmatic in meteoric waters.

The most serious difficulty in collecting samples for noble gas analyses is the possibility of air contamination. Although care was taken, air bubbles sticking to collection vessel walls, or bubbles introduced into the wells and boreholes with pumping and/or sampling equipment could easily have introduced small amounts of air. According to Mazor (1972), a contamination of  $0.001 \text{ cm}^3$  of air in  $1 \text{ cm}^3$  of water (i.e., 0.1 percent by volume) adds about 10 percent Ne to a groundwater which had been in equilibrium with air at normal surface temperatures. At  $10^\circ\text{C}$  the saturation levels for Ne are  $2.1 \times 10^{-7} \text{ cm}^3 \text{ STP/cm}^2$   $\text{H}_2$  and, taking into account analytical uncertainties (Mazor 1972), concentrations above  $2.3 \times 10^{-7} \text{ cm}^3 \text{ STP/cm}^2 \text{ H}_2\text{O}$  indicate that such air contamination has occurred. However, solution under greater pressures and lower temperatures could increase Ne concentrations above these levels. We believe that the presently discharging groundwaters were recharged through vegetated soils (see  $^{13}\text{C}$



XBL 794-9492

Fig. 9. The solubility of the noble gases in water at various temperatures (from Mazor 1976).

data) and, therefore, exclude below 0°C temperatures from the discussion. The high neon content would then most logically be explained by air contamination.

Because the solubility of neon is not strongly temperature-dependent it can be used as "reference" and approximate corrections for any air contamination can be attempted. The results of such an exercise (Table 3, p. 25) show that the helium concentrations in these waters are very much higher than normal atmospheric saturation levels. This is certainly due to production of this gas during radioactive decay of uranium, thorium, and their daughter products. An enrichment above atmospheric concentrations is also evident for argon, especially in Stripa 29, the deepest sample collected from the 410-m well. There the concentration is about double the value expected for air saturation at 5°C. This could be caused by the accumulation of radiogenic argon produced during the decay of  $^{40}\text{K}$ .

Both the helium and argon enrichments could indicate that the water discharging from the deepest fractures intersected by the 410-m well must have been in a closed system for a considerable time. This should be especially true for the argon enrichment, which probably has to be explained by diffusion from the rock matrix into the water. The half-life of  $^{40}\text{K}$  is  $1.28 \times 10^9$  years, and the potassium concentrations in the rock plus the difficulties in getting the argon from its place of production within the rock matrix to the water in fractures would tend to make this accumulation a very slow process.

The helium and argon enrichment in the water discharging in the M-3 hole in the time-scale room at the 330-m level (Stripa 16) is much lower than the enrichment in the deeper waters. This might reflect different residence times

and will be discussed further in Section 3.4. Since the atmospheric helium and argon concentrations in these waters at the time of recharge could be recalculated only with a detailed knowledge of the production rate of these gases within the rocks, their abundances do not reflect paleotemperatures. Only the neon, krypton, and xenon contents of these waters can give hints about the temperature which existed at the time of infiltration. Furthermore, Stripa 29-18 has a very high neon concentration, indicating significant air contamination. The result of attempted corrections is doubtful.

The two sets of data from Stripa 16 (M-3) and the set from Stripa 29 (410-m hole) indicate that recharge temperatures for the waters presently discharging in the flowing well (M-3) in the time-scale room were between 4° and 9°C, whereas the deep waters in the 410-m hole infiltrated when ground temperatures were between 0° and 5°C (see Table 3). These are very crude estimates that might be refined once the reason for the high neon and argon contents is better understood.

In the following section we will discuss the stable isotope data obtained from these waters and show that they, too, indicate somewhat lower recharge temperatures for the deeper waters. See also the discussion of the  $^{13}\text{C}$  contents of the dissolved inorganic carbon (p. 61). Radon analyses are discussed in Section 3.4.

### 3.3 Stable Isotopes

#### Deuterium and $^{18}\text{O}$ in Groundwater

Mass and vibrational energy differences of different isotopes from the same element are responsible for the fractionation of isotopes between dif-

ferent compounds or phases. This is also true for the isotopes of oxygen and hydrogen, of which  $^{16}\text{O}$ ,  $^{18}\text{O}$ ,  $^1\text{H}$ , and  $^2\text{H}$  are the most important stable isotopes. They are incorporated into water molecules; among all isotopic species of water only three are of practical interest:  $^1\text{H}_2^{16}\text{O}$ ,  $^1\text{H}^2\text{H}^{16}\text{O}$ , and  $^1\text{H}_2^{18}\text{O}$ . The average  $\text{H}_2^{18}\text{O}$  content in terrestrial water is close to 2000 ppm, whereas  $^1\text{H}^2\text{H}^{16}\text{O}$  concentrations are close to 320 ppm.

The isotopic composition of the SMOW is very close to the average isotopic compositions of the oceans. Most vapor masses that carry water to the continents originate from the oceans and, because of isotopic fractionation during evaporation from the ocean, these vapor masses are considerably depleted in both  $^{18}\text{O}$  and  $^2\text{H}$  compared to ocean water. Subsequent condensation within cloud masses tends to reverse this depletion, but because evaporation from oceans involves kinetic effects (nonequilibrium conditions) which are larger than the equilibrium fractionations which occur during condensation in a vapor-saturated cloud, the heavy isotope contents of most precipitations are lower than those of the oceans (negative  $\delta$ -values). Condensation thus preferentially removes heavy isotopes from a vapor reservoir, and continuous cooling and condensation continuously deplete  $^{18}\text{O}$  and  $^2\text{H}$ . This, in turn, is reflected in the isotopic compositions of precipitations, and relationships between ground temperatures and  $^{18}\text{O}$  or  $^2\text{H}$  contents in precipitations are recognized. On a global basis, Dansgaard (1964) found that

$$\delta^{18}\text{O} \approx (0.7 t_a - 13.6) \text{ ‰}$$

and

$$\delta^2\text{H} \approx (5.6 t_a - 100) \text{ ‰}$$

where  $t_a$  = average annual ground temperature. Those relationships may differ from place to place in their slopes and intercepts, but they express the fact



that the  $^{18}\text{O}$  and  $^2\text{H}$  contents of precipitation are lower in a cooler climate than in warmer environments.

Another relationship of great importance connects the  $\delta^{18}\text{O}$  and  $\delta^2\text{H}$  values in precipitation. It has been found that on a global basis,

$$\delta^2\text{H} = (8\delta^{18}\text{O} + 10) \text{‰} \quad (\text{Craig } 1961).$$

On a  $\delta^2\text{H}$  vs  $\delta^{18}\text{O}$  plot (Fig. 10), this straight line is called the Meteoric Water Line (MWL). The position of this line may vary locally to some degree; for example, its  $\delta^2\text{H}$  intercept can range from about 0 ‰ to +25 ‰. The slope  $\delta^2\text{H}/\delta^{18}\text{O}$  of this line may also change to a minor degree, but is always

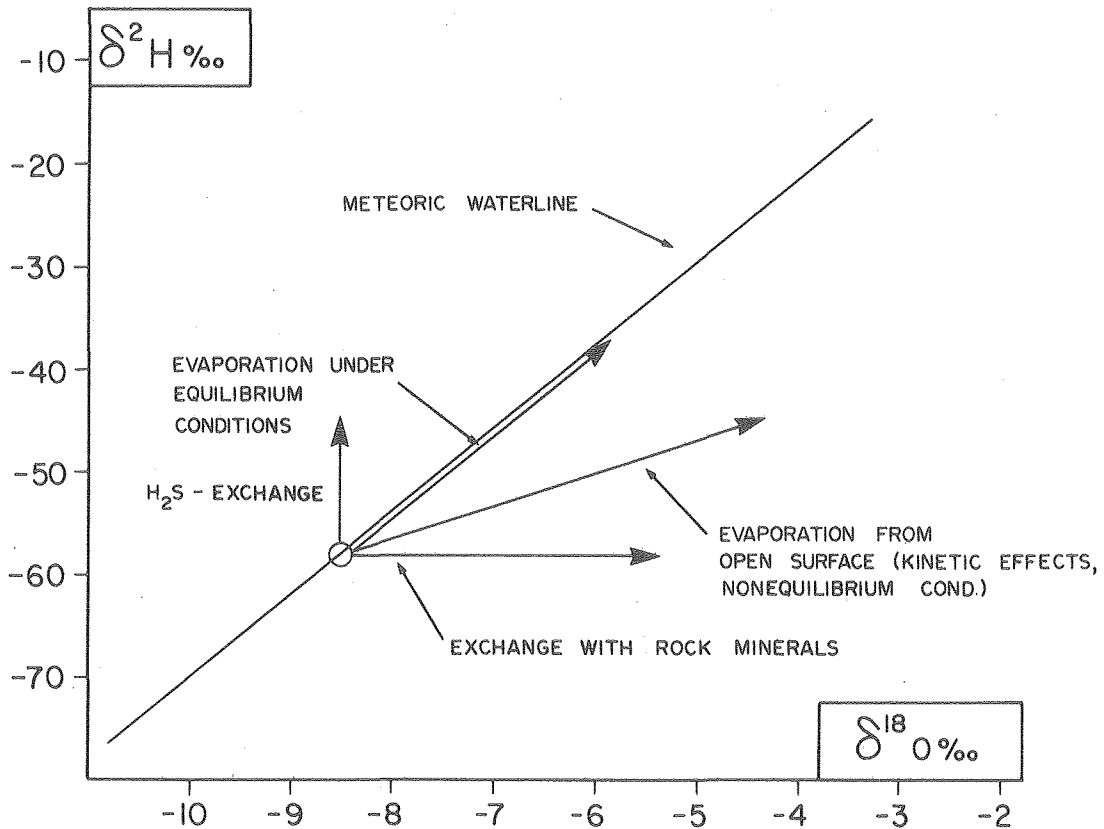
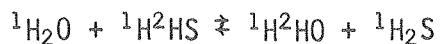


Fig. 10. A generalized  $\delta^{18}\text{O}$  versus  $\delta^2\text{H}$  plot showing the Meteoric Water Line and processes commonly responsible for deviations from this line.

XBL 794-9493

between 7 and 8, and usually close to 8. These variations depend on the origin of the vapor masses releasing local precipitation. Within a given region, such as continental central Sweden, however, these parameters are constant and variations usually do not exceed  $\pm 2$  ‰ for the intercept and  $\pm 0.2$  ‰ for the slope. Any deviation from this line is an indication that secondary processes, such as evaporation or rock-water interactions at elevated temperatures, have affected the isotopic composition of the groundwaters. Evaporation from a water with  $\delta^{18}\text{O}$  and  $\delta^2\text{H}$  values on the MWL can be recognized on a  $\delta^{18}\text{O}$  vs  $\delta^2\text{H}$  plot by a line with slope 3 to 6 originating at the MWL. Exchange with rock minerals affects only the  $^{18}\text{O}$  contents, and causes an  $^{18}\text{O}$  shift.

In strongly reducing environments,  $\text{H}_2\text{S}$  may become an important component of geochemical systems. Because there are extremely large isotope effects between  $\text{H}_2\text{S}$  and  $\text{H}_2\text{O}$ , and because the exchange



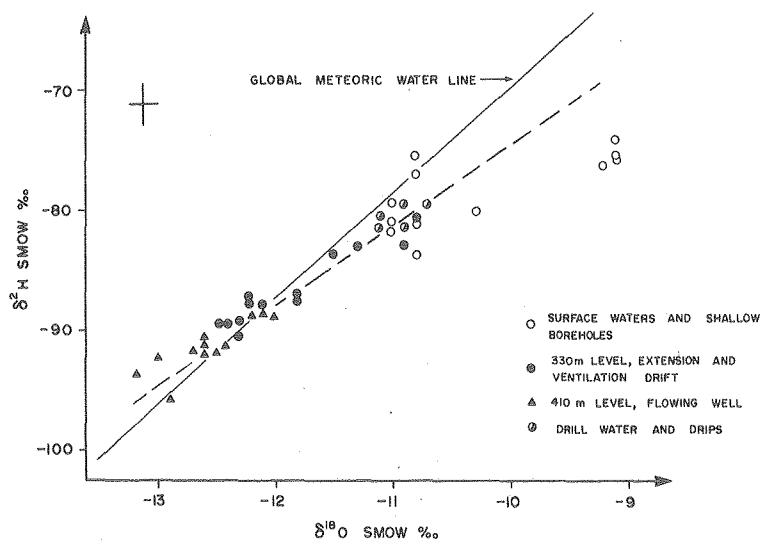
takes place rather easily, it is possible to obtain some  $^2\text{H}$  enrichment in the water.

Normal groundwater is not affected by these processes, and experience shows that the isotopic composition of most groundwaters very closely ( $\pm 2$  ‰ for  $^{18}\text{O}$ ) reflects the weighted average annual isotopic composition of precipitations. Minor shifts could be due to seasonally selective recharge if, for example, isotopically heavy summer rains are consumed by vegetation and only isotopically lighter fall-to-spring rains recharge groundwater reservoirs.

Furthermore, in normal groundwater aquifers with temperatures below  $50^\circ\text{C}$  or so, these isotopes are a conservative property of a given water mass. Exchange within rock minerals or with gases is then not important. The only

process which might have an influence is diffusive exchange of water migrating on fractures through clay deposits with water held by clay minerals. Therefore in most hydrogeologic situations the  $^{18}\text{O}$  and  $^2\text{H}$  contents of a groundwater reflect the recharge environment. One might expect, for example, isotopic differences between a groundwater recharged in a cool mountain area and one recharged through the alluvial fills at the foot of the mountain. Similarly, groundwaters formed in mid latitudes immediately following the retreat of the last glaciation are lower in heavy isotopes than groundwaters forming there today. Although it is not possible to use stable isotopes for groundwater dating, the isotopic composition of a water may well give some indication of the origin and time and/or season of infiltration.

Results. All  $^{18}\text{O}$  and  $^2\text{H}$  analyses done on surface and groundwaters are listed in Table 7 and graphically shown in Fig. 11. To facilitate discussion, Table 8 lists all groundwater samples by origin.



XBL 794-9494

Fig. 11. A plot of  $\delta^{18}\text{O}$  versus  $\delta^2\text{H}$  of waters from the Stripa area. The dashed line is a best fit through all groundwater points.

Table 7.  $^{18}\text{O}$  and  $^2\text{H}$  analyses on water samples from Stripa.

Stripa sample	$\delta^{18}\text{O}$ SMOW ‰	$\delta^2\text{H}$ SMOW ‰	Stripa sample	$\delta^{18}\text{O}$ SMOW ‰	$\delta^2\text{H}$ SMOW ‰
1-1	-9.2	-76.3	21-15	-11.4	
1-2	-10.8	-78.0	21-20	-10.8	
2	-9.1	-74.6	21-22	-10.9, -11.1	-81.7
4	-9.1	-73.4	23-3	-11.0	-81.0
5	-9.1	-73.4	23-5	-11.0	
6-1	-12.6		23-26	-10.8	
6-2	-12.5	-91.9	23-28	-11.0	-79.1
6-16	-12.4		24-1	-12.5	-91.8
6-19	-12.4		24-10	-12.8	
6-29	-12.4	-91.2	25-2		-81.4
7-1	-11.9		25-9	-10.9	
8-1	-10.8		26-4	-10.9	-79.4
13-1		-87.2	26-5	-10.8	
13-2	-12.2		27-3	-10.8	-79.4
14-1	-11.1	-81.2	28-1	-11.9	
15-1	-13.0, -12.7	-91.7	28-2	-12.1	-88.0
15-2	-12.8, -12.6	-91.2	29-1	-13.2	-93.7
15-24	-12.6	-91.2	29-65	-12.9	-95.9
16-1	-11.8	-86.9	30-1	-10.9	-82.1, -83.2,
16-2	-11.8				-83.8
16-3			31-1	-10.8	-80.6
16-22	-11.8	-87.7	32-1	-11.0, -11.0	-80.5
16-37	-11.9, -11.9		32-2	-12.4	
16-38	-11.9		35	-12.2	-86.4, -87.9
16-39	-11.9, -11.9		36	-12.1	-87.9
16-41	-12.0, -11.9		37-1		-93.8
17-1	-12.0		38-3	-12.4	-89.4
17-4	-11.9, -12.2	-88.8	40-2	-11.3	-82.1
17-31	-12.0	-89.0	40-3	-11.5	
17-38	-12.3		40-4	-11.5	83.1, 83.8
18-3	-10.8	-81.3	43-2	-12.6	-90.7
19-1	-11.0		45-2	-12.6	-90.7
20-1	-10.6		46-1	-12.3	-90.6
20-2	-10.9	-76.3	48-1	-12.3	88.7
21-2	-10.9		48-1	-12.2	87.7
21-6	-11.3				
21-7	-10.8	-83.7			

Note: Some repeats were done as a check on reproducibility and both values are included.

Table 8.  $^{18}\text{O}$  in groundwaters.

Origin	Stripa sample	$\delta^{18}\text{O}$ ‰ SMOW
<u>Private wells:</u>		
PW-1	18	-10.8
PW-2	19, 23	-11.0, -11.0, -11.0, -10.8, -11.0
PW-3	20	-10.6, -10.9
PW-5	21	-11.4, -10.8
<u>330-m level</u>		
Time-scale room:		
H-2	12, 38	-12.4
M-3	13, 16, 35	-12.2, -11.8, -11.8, -11.8, -11.9, -11.9, -11.9, -11.9, -12.0, -12.2, -11.9
BH-E-5	30	-10.9
BH-H-3	31	-10.8
BH-H-4	40	-11.3, -11.5, -11.5
Horizontal BH	28	-11.9, -12.1
Ventilation drift:		
BH-R-1	36	-12.1
BH-R-3	46	-12.3
BH-HG-3	47	-12.3
BH-HG-4	48	-12.2
<u>410-m level</u>		
Entire hole:	24	-12.5, -12.8
6.3 - 50 m	17	-12.1, -11.9, -12.2, -12.0, -12.3
8 - 40 m	43	-12.6
Above 152.3 m	7	-11.9
Below 152.3 m	6	-12.6, -12.5, -12.4, -12.4, -12.4
Below 285 m	15, 45	-13.0, -12.7, -12.8, -12.6, -12.6
Below 387 m	37	
376.5-471 m	29	-13.2, -12.9

A superficial analysis of the dates shows marked and significant isotopic differences between the different groups of water. Most enriched are the surface waters, and their position to the right of the MWL indicates that they were subject to surface evaporation. These effects are seasonal, and are less pronounced or absent during winter runoff.

For the groundwaters, the following grouping appears possible:

	$\delta^{18}\text{O}$ SMOW ‰	
	range	average
Private wells (max. ~100 m depth)	-10.8 to -11.4	-10.9
330-m level, all wells except Stripa 30, 31, and 40	-11.9 to -12.2	-12.0
410-m flowing well, 0-50 m	-11.9 to -12.6	-12.2
410-m flowing well, below 285 m	-12.6 to - 13.2	-12.9

The samples collected to date from BH-E-5 (Stripa 30), BH-H-3 (Stripa 31), and BH-H-4 (Stripa 40) were not included in these averages because chemical and isotope data indicate that these samples were still polluted, possibly with drilling fluid.

Discussion. The isotopic differences between the different waters clearly indicate that the waters originated under different conditions. A comparison of  $^{18}\text{O}$  and  $^2\text{H}$  data demonstrates that none of the deep groundwaters had their isotopic compositions modified by exchange processes or evaporation. This also seems to be true for most private wells sampled, with the possible exception of PW-5 (Stripa 21), which is the shallowest. This hydrogeologic setting would have to be investigated before an explanation for its isotopic variability can be given.

As previously indicated, the  $^{18}\text{O}$  and  $^2\text{H}$  contents in precipitations can be plotted for each region on a locally characteristic Meteoric Water Line (MWL). The slope and intercept of this line is primarily dependent on the origin of the vapor masses; the spread of data along the line is dependent on the magnitude of the seasonal temperature variations. The larger the temperature dif-

ference between summer and winter, the larger the spread.

In Fig. 11, the question arises whether the water samples from all levels lie on one line with a slope of about 7 (dashed line), or whether one has to draw two lines with slopes close to 8--the first passing through the shallow groundwater data and having an intercept of about 8, the second passing through the deep groundwaters with an intercept of about 11.

Since modern precipitation data from central Sweden which would tell us what slope to expect are not available, both possibilities must be discussed.

1) If all points fall on one MWL, all waters sampled condensed at different stages from the same vapor reservoir. Those with high heavy isotope contents (shallow groundwaters) would have resulted from precipitations falling in a warmer environment than those giving rise to the deeper groundwaters. The isotopic differences observed between waters in private wells, the 330-m-level hole, and the 410-m-level hole would then, in this region which is dominated by the same meteorologic regimes, most likely reflect differences in the climatic regime during recharge.

Although a slope of 7 for a MWL is very unusual, it could be produced under special circumstances by a combination of seasonally different meteorological patterns. Furthermore, since in many sedimentary basins, shallow groundwaters have a local origin, whereas deep groundwaters are the result of regional flow systems, the respective recharge areas can have quite different characteristics. The lower  $^{18}\text{O}$  and  $^2\text{H}$  contents of the deep system could be explained by its origin in higher altitudes, where lower condensation temperatures result in lower  $^{18}\text{O}$  and  $^2\text{H}$  contents in precipitations. These "altitude

effects" amount to 2 to 3 ‰ decrease in  $^{18}\text{O}$  for a 1,000-m rise in altitude. In our case, the recharge area of the deeper groundwater would have to be 400 m to 600 m higher than that of the shallow system.

Although regional systems could flow in crystalline rocks, the physiographic setting appears to exclude this explanation of the isotopic differences observed. For this reason, we favor at present the second explanation.

2) If waters in shallow and deep wells originated under different climatic conditions, their respective MWLs are slightly different: the former has an intercept of about 11, the latter of about 8, assuming that the slope is close to 8 in both cases. Meteorological patterns were then probably different during the respective recharge periods.

In this explanation, the deep waters must be considerably older than the modern waters found in private wells. The recharge temperatures were lower (as indicated by the lower  $^{18}\text{O}$  ( $^2\text{H}$ ) contents) because of the general climate of the region, not because the recharge area was at a higher elevation. Using Dansgaard's equation (p. 50), the isotope data would indicate that the deep waters were recharged at an average annual temperature  $1.5^\circ$  to  $2^\circ\text{C}$  lower than today's average annual ground temperature.

Such a simple application of this formula may not be justified, however, because meteorological conditions in the past may have been different from what they are now, and entering air masses may have been isotopically slightly different from current air masses. In this case, both slope and intercept of the  $\delta^{18}\text{O}$  ( $\delta^2\text{H}$ ) versus temperature relationship may have been somewhat different.



Despite this potential complication, it is fairly safe to assume that the climate was somewhat cooler during the infiltration of the deep waters than during that of the shallow waters.

The waters discharging at the 330-m level in borehole M-3 are intermediate in heavy isotope content between the shallow, private well waters and the deep groundwaters. This could be explained on the basis of the  $^{18}\text{O}$  data by assuming these waters are a 50/50 mixture of modern groundwaters and deeper, older waters. The  $^{14}\text{C}$  and uranium data presented below do not support this, however, at least not if modern groundwaters are involved.

Another argument against a simple mixing of shallow and deep groundwater comes from the chemical data. We have shown that the chemical load increases with depth. If the waters in the wells at the 330-m level were the result of a simple mixing, a straight mixing line should occur on a  $^{18}\text{O}$  versus  $\text{Cl}^-$  diagram. This is not the case, as shown in Fig. 12. This excludes the possibility that the M-3 waters formed by mixing of deeper, saline waters with shallower fresh waters. However, a mixing of the deep waters in the 410-m hole with the water of the 330-m-level type could explain both chemistry and isotope content of the "intermediate" samples from the 410-m hole. It is not yet clear whether this mixing occurs because different fracture systems discharge into the same borehole, or whether it is a "natural" phenomenon occurring within the fracture matrix of the rocks.

Isotope analyses do not permit the recognition of minor contributions of fossil sea water which would impart a higher salt content to the deeper water from the 410-m hole.

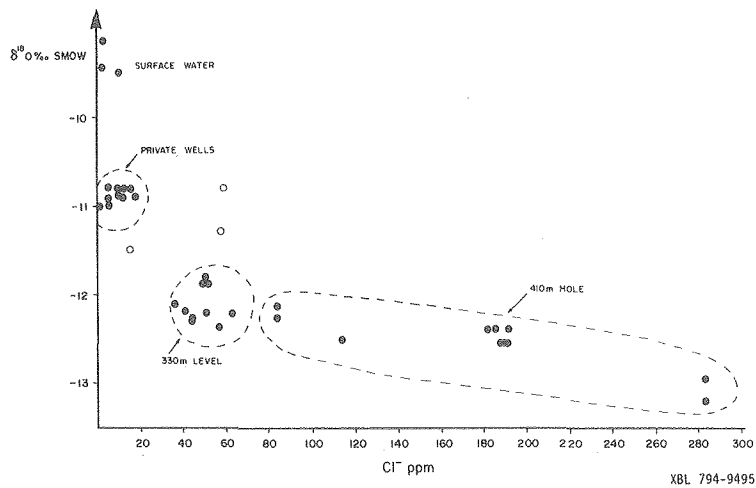


Fig. 12. A plot of  $\delta^{18}\text{O}$  versus chloride concentration for waters of the Stripa area. Samples of shallow (private wells), intermediate (330-m-level) and deeper (410-m-level) groundwaters are outlined.

The  $^{18}\text{O}$  contents of samples collected from boreholes in the time-scale room (Stripa 31 and 40), represented by three open circles in Fig. 12, are considerably higher than the  $^{18}\text{O}$  contents of other boreholes, and approach values known for the drilling fluids. We therefore suspect these samples were contaminated, and have excluded them from further discussion.

Conclusions. The  $^{18}\text{O}$  and  $^2\text{H}$  data show that different water masses circulate at different levels in this system: surface waters and shallow groundwaters are most enriched in both isotopes; waters discharging at the various mine levels are more depleted. This indicates that modern, shallow groundwaters presently do not penetrate to the depths sampled in boreholes at 330 m and 410 m.

The waters at the 330-m-level boreholes and the shallow part of the 410-m hole are isotopically different from the groundwaters that are discharging at about 900 m below ground surface from fracture systems intersected by the 410-m hole. The deepest waters have the lowest  $^{18}\text{O}$  and  $^2\text{H}$  contents encountered, and were probably recharged in a somewhat cooler environment than the shallower samples. Whether the recharge areas were cooler because they were at higher altitudes in the region or because the general climate was cooler is not clear, although the latter explanation is favored. In both cases we can assume that the water is fairly old, but recharge during cooler climates would make the deep water potentially very old.

It is important to notice again that isotope and chemical data clearly show that the fracture systems in this granite do not carry a more or less uniform watermass: at present, different fractures discharge different types of groundwater. We cannot predict how long this will be the case. Data collected by the authors in Canadian mines show that in a highly disturbed mining environment surface waters can be channeled very rapidly to great depth--waters younger than 25 years have been collected at depths exceeding 1,000 m (Fritz and Reardon 1978).

#### Carbon-13 and Oxygen-18 in Fracture Calcite and Dissolved Inorganic Carbon

The  $^{14}\text{C}$  contents of a groundwater depend strongly on the total carbon geochemistry of the system, and interpretation of  $^{14}\text{C}$  and other isotopic data requires some understanding of the processes which determine the chemistry of a water during recharge and during its subsurface history. Unfortunately, it is normally impossible to study directly chemical changes which occur during the

geochemical evolution of a groundwater. This is especially true for groundwater systems in crystalline rocks, where sampling density is very low. For this project we have analyzed modern, shallow groundwaters from the local area. Since modern recharge conditions are not necessarily comparable with those existing during the formation of the groundwaters presently discharging in the mine, models are used to compare the two environments.

Some indirect evidence on the geochemical history of older groundwaters may possibly also be derived from the study of fracture calcites. Many fractures encountered in SBH-1 and SBH-2 have secondary calcite coatings which have been sampled and analyzed for their  $^{13}\text{C}$  contents. Their isotopic compositions depend on those of the dissolved inorganic carbon (DIC) in the groundwater at the time of their formation, and thus reflect geochemical conditions which exist or may have existed in the fracture zones. This assumes that isotopic equilibrium has been maintained, which is the case in many if not most systems depositing calcite. The importance of the information derived from  $^{13}\text{C}$  data will have to be assessed in terms of the movement of contaminant ions from repositories. In addition, the isotope analyses of these calcites will yield data necessary for the "correction" of  $^{14}\text{C}$  water ages, since any secondary calcite dissolution affects these ages.

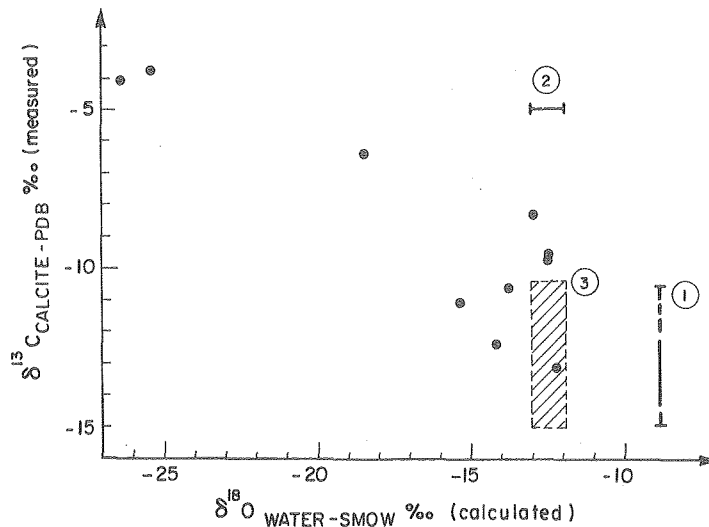
Results and Discussion. Results of  $^{18}\text{O}$  and  $^{13}\text{O}$  analyses on fracture calcites are shown in Table 9, and  $\delta^{13}\text{C}$  values obtained on aqueous carbonates are given in Table 10.

Table 9. Carbon and oxygen isotopic compositions of fracture calcites and of the water from which they precipitated.

Sample origin					
Calcite fracture filling		Fracture calcite		Water	
Borehole	Depth (m)	$\delta^{13}\text{C}$ PDB (‰)	$\delta^{18}\text{O}$ PDB (‰)	$\delta^{18}\text{O}$ SMOW (‰) <sup>a</sup>	
SBH -1	106.43	-10.7	-11.1	-13.8	
	107.85	- 7.0			
	124.03	- 4.5			
	132.31	- 9.0			
	152.90	-10.1			
		-12.4	-11.5	-14.2	
	174.67	- 6.8			
	178.35	-13.2	- 9.5	-12.2	
	189.95	-11.3			
	206.63	-11.6			
	237.02	LOST			
	247.11	- 8.3	-10.3	-13.0	
	278.40	- 4.1	-23.7	-26.4	
		- 3.9			
	305.7	-15.2			
306.20	- 3.8	-21.7	-24.4		
SBH-2	79.43	-13.5			
	92.43	- 6.5			
	99.43	-11.1	-12.7	-15.4	
	103.82	+15.3			
	104.27	+13.0			
OV2 BHH1	9.54	- 9.6	- 9.8	-12.5	
	BHH3	6.64	- 9.7	- 9.8	-12.5
	BHH6	1.64	- 6.4	-15.8	-18.5
Stahl SBH2	(Marble, upper 9.4m)	- 1.4			
Back wall of	time-scale room				
	<sup>14</sup> C: below				
	detection limit <sup>b</sup>				
		- 4.2			

a It is assumed that isotopic equilibrium between calcite and water was established at 5°C.

b This sample has been analyzed for <sup>14</sup>C and less than 0.3 pmC were detected.



XBL 794-9497

Fig. 13. The relationship between measured  $\delta^{13}\text{C}$  of fracture calcites and  $\delta^{18}\text{O}$  of the water from which they precipitated. The  $\delta^{18}\text{O}$  value was calculated from the measured  $\delta^{18}\text{O}$  of fracture calcites using fractionation factors given by Friedman and O'Neil (1977). Range 1 includes the expected  $\delta^{13}\text{C}_{\text{calcite}}$  values that would be precipitating from the present groundwaters. Range 2 covers the observed  $\delta^{18}\text{O}$  values of groundwaters at Stripa. Range 3 is the expected field of  $\delta^{13}\text{C}_{\text{calcite}}$  and  $\delta^{18}\text{O}_{\text{water}}$  for calcite precipitation from present groundwaters.

which existed within the fracture systems at the time of their deposition. The  $\delta^{13}\text{C}$ s vary by almost 30 ‰; this extremely large range was not expected.

Using isotope fractionation data summarized by Friedman and O'Neil (1977) one can calculate that the isotopic difference between bicarbonate (the dominant aqueous carbonate species in these waters) and fracture calcite should be close to 3 ‰, following the relationship,

$$1000 \ln \alpha_{\text{calcite} - \text{HCO}_3^-} = 2.99 \times 10^6 T^{-2} - 17.22 \times 10^3 T^{-1} + 26.56.$$

Thus, as shown in Fig. 13, the  $\delta^{13}\text{C}$  values expected for calcites precipitated

from waters discharging at present from the different fracture systems in the Stripa granite should be between -12 and -15 ‰. With few exceptions, such low values are not reached, which indicates that no, or only small amounts of calcite are deposited under present-day conditions in this rock mass--at least in the fractures sampled to date. We thus assume that most calcite found must have formed long ago and under different environmental conditions (see below). We know from the chemical data presented above that today calcite saturation is maintained in these waters; one might therefore expect to find more evidence of "active" calcite precipitation in the yet uncoupled deeper horizons.

We pointed out above that the low  $^{13}\text{C}$  contents in the presently discharging waters demonstrate that the dissolved inorganic carbon is dominated by a biogenic component, i.e., much of the aqueous carbon must have originated in a soil zone with active vegetation. This does not seem to be the case for the waters which deposited the calcites with  $\delta^{13}\text{C}$  values between -6.8 and -11.6 ‰. In inorganic systems such values are typical of a mixed origin, i.e., a mixture of soil gas and  $^{13}\text{C}$ -rich rock carbonate dissolved in the water. Such carbonate occurs in the vicinity of Stripa as marble in metamorphic sequences and has a  $\delta^{13}\text{C} \approx -1.4$  ‰. One could envisage that at the time of recharge of these calcite depositing waters, the carbonates existed over wider areas than at the time of infiltration of the deep groundwaters discharging today (glacial erosion). The  $\delta^{13}\text{C}$  values between -6.8 and 0 ‰, too, could be explained by dilution with carbon from this source, if one envisages more complex geochemical processes (additional proton donors) which would allow a greater contribution of marble carbon.

"Secondary" biologic processes have also influenced the carbon isotope composition of some of these calcites, specifically the deep samples of SBH-2 for which  $\delta^{13}\text{C}$  values of +13.0 and +15.2 ‰ have been measured. These values are typical for carbonates whose carbon originated in a  $\text{CO}_2$  produced by bacteria which usually exist under very reducing conditions. In such environments, the bacterial breakdown of organic matter generates  $\text{CO}_2$  and  $\text{CH}_4$  with very different isotope contents whereby the  $\text{CO}_2$  becomes strongly enriched in  $^{13}\text{C}$ . Such bacterial activities are not unusual even in crystalline shield environments (Fritz et al. 1978), but it is important that they be recognized because they can profoundly modify the carbon geochemistry of a groundwater. Enriched  $\text{CO}_2$  certainly went into the formation of the two deep samples from SBH-2, and possibly affected some of the other more positive samples, for which a marble contribution could also explain their carbon isotopic composition.

The  $\delta^{13}\text{C}$  data from discharging groundwaters indicate that the strongly reducing conditions which must have existed in the past in some parts of these fracture systems have not been encountered by the presently discharging deep groundwaters. This could indicate either that the reducing conditions no longer exist or that the actively discharging systems sampled do not flow through them.

Further comments on the  $^{13}\text{C}$  contents of the aqueous carbon species are made in the discussion on  $^{14}\text{C}$  dating of these groundwaters (page 75).

Oxygen-18. The  $^{18}\text{O}$  contents of some fracture calcites were determined (Table 9) to obtain additional information on the possibility of recent carbonate formation by the waters present in the granite fracture system. Assuming



that isotopic equilibrium prevailed during calcite precipitation, the relationship,

$$t = 16.9 - 4.3 (\delta_{\text{carb}} - \delta_{\text{wat}}) \quad (\text{Friedman and O'Neil 1977})$$

can be used to calculate approximate  $\delta^{18}\text{O}$  values for the water ( $\delta_{\text{wat}}$  ‰ SMOW) from the  $\delta^{18}\text{O}$  values ( $\delta_{\text{carb}}$  ‰ PDB) given in Table 9. The carbonate precipitation temperature ( $t$ , C) was assumed to lie between 5° and 10°C, but could have been slightly higher as we know that the deeper groundwaters reach temperatures between 15° and 20°C.

The results are plotted versus measured  $\delta^{13}\text{C}$  values in Fig. 13. There appears to be a negative correlation between  $\delta^{13}\text{C}_{\text{calcite}}$  and  $\delta^{18}\text{O}_{\text{H}_2\text{O}}$ , signifying that at a time when isotopically light waters (low  $\delta^{18}\text{O}$  values) entered the fracture system, only  $^{13}\text{C}$ -rich carbonate was available. The calculated  $\delta^{18}\text{O}$  values of -25 ‰ to -26 ‰ are typical for precipitations in arctic climates and could suggest that at one time subglacial recharge did occur. Under these conditions no soil carbon would be present and the  $\delta^{13}\text{C}$  values in the carbonates would be close to 0 ‰.

The calculated  $\delta^{18}\text{O}$  of the water which participated in the formation of most of the other calcites analyzed to date is similar to or slightly lower than what is sampled at present (Fig. 13, range 2). Only the comparison of  $\delta^{18}\text{O}$  with  $\delta^{13}\text{C}$  values shows that most of the calcites sampled to date from the shallower fracture systems in the Stripa granite must have formed earlier, from water whose aqueous carbonate had higher  $^{13}\text{C}$  contents.

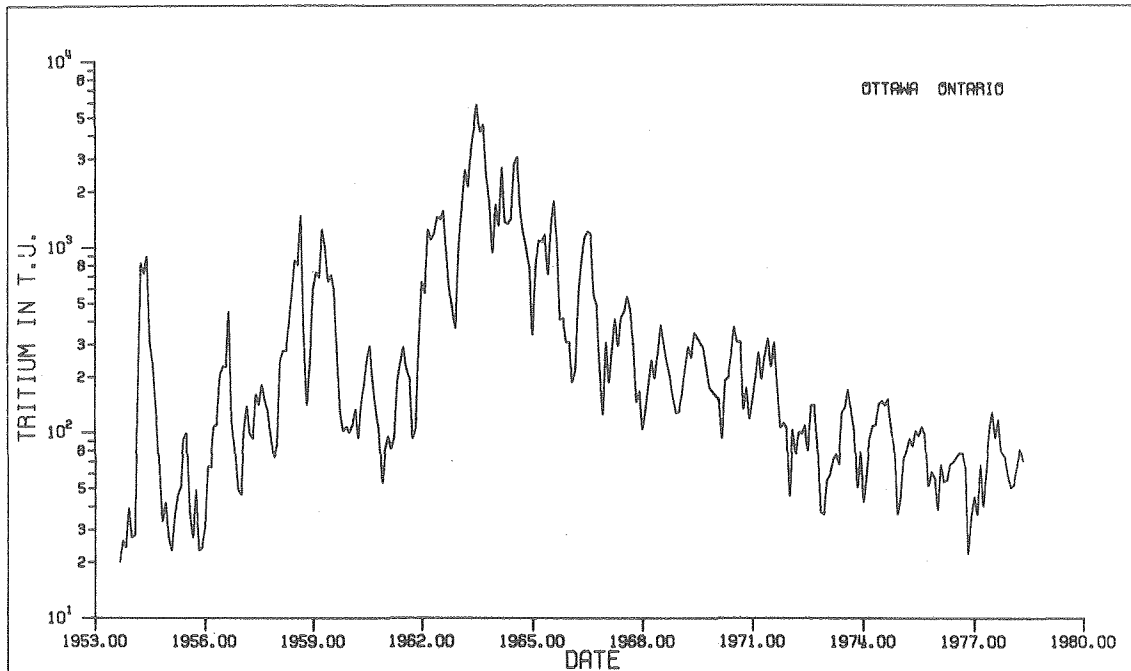
### 3.4 Radioactive Isotopes (groundwater dating)

#### Tritium

Tritium (T or  $^3\text{H}$ ), a radioactive isotope of hydrogen with a half life of 12.35 years, is probably the single most important environmental isotope for hydrogeological studies. Its natural abundance is usually expressed in Tritium Units ( $1 \text{ TU} = 1^3\text{H}/10^{18}$  hydrogen atoms) with detection limits varying between  $< 1$  and  $< 10$  TU depending on the analytical techniques used (see p. 29).

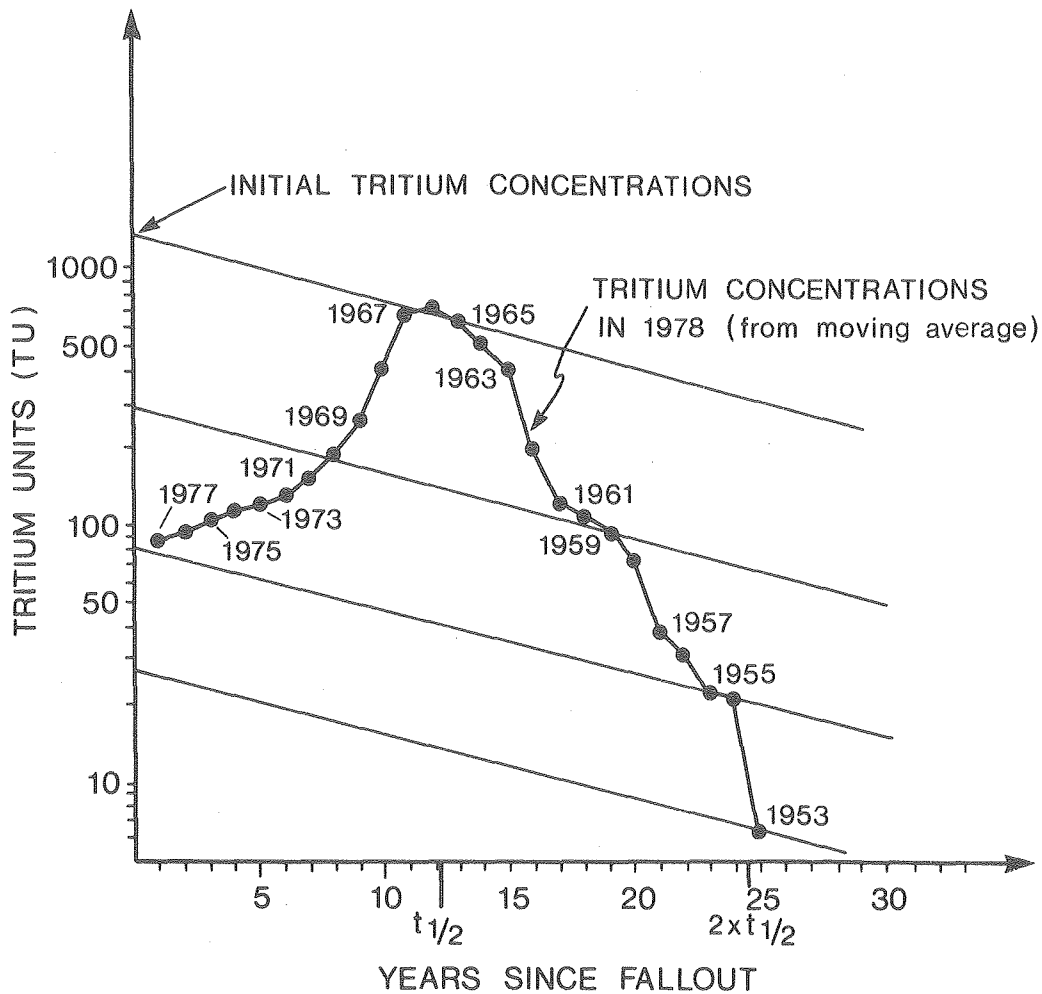
Before significant amounts of tritium were injected into the atmosphere through man's nuclear activities, precipitations over North America had a natural background level of 10 to 15 TU. Today atmospheric background levels in the Northern Hemisphere are between 50 and 100 TU, and during the early 1960s concentrations well above 1,000 TU were measured. This is graphically shown in Fig. 14 which depicts the weighted average annual tritium concentrations in precipitations in Ottawa. Equivalent data for central Sweden are not available.

It is thus, at present, virtually impossible to use tritium for very accurate groundwater dating. However, estimates are possible if some background information on tritium fallout and groundwater formation is available. For example, if one assumes that groundwater in recharge areas is always a mixture of several years' recharge before it moves away and is no longer subject to further additions, then a tritium decay curve can be constructed. This has been done in Fig. 15 for a 5-year moving average of groundwater mixing. The tritium contents expected in 1978 for groundwater formed at any period are indicated by the year of the last contribution made.



XBL 794-9496

Fig. 14. The weighted average monthly tritium concentration in rainfall in Ottawa, Canada, 1954-1975. Data from IAEA, Vienna.



XBL 794-9498

Fig. 15. Prediction of the present (1978) tritium content of groundwaters on the basis of radioactive decay since time of recharge. Recharge is assumed over a 5-year period identified by the last year of this period.

Like the stable isotopes  $^{18}O$  and  $^2H$ , tritium is an integral part of the water molecules. Thus, in groundwater it is not affected by physico-chemical and biological processes and--except for its decay--can be considered a conservative property of the groundwater.

Results and Discussion. Tritium determinations were done on all types of groundwater available at Stripa, and the results obtained at different laboratories are listed in Table 11. In general, very good agreement is observed for data from different laboratories on different samples from the same sampling points, although there are some unexplained differences for samples from Stripa 6 and 15. It is suggested that some contamination had occurred, although it is not clear where and when. Sampling procedures were tested in the mine and, to confirm that contamination with tritium present in the mine air is of no importance, sample Stripa 6-18 was left standing in the bottle without stopper for one week. It still contains less than 1 TU although there might be some tritium uptake.

All groundwaters from private wells have measurable amounts of tritium, indicating that at least a portion of their waters are younger than 25 years. More specifically, using the decay curve given in Fig. 15, one could estimate that the water from private wells 3 and 5 (Stripa 20 and 21) have a probable average age between 5 and 10 years. Other models, such as the exponential model, would give similar curves.

Not as clear is the situation for private wells 1 and 2 (Stripa 18 and 23), which have rather low tritium contents. If they do not discharge a mixture of young and old water, their ages would be close to 25 years (accepting the results of the enriched tritium counting as being the best).

The groundwaters from the 330-m and 410-m levels are essentially free of tritium although one recognizes some pollution in the first samples taken from M-3 well (Stripa 13) and the Stripa 15 series of the 410-m flowing well.

Table 11. Tritium analyses for Stripa project.

Stripa sample	UW <sup>a</sup> (direct L.S. counting)	IAEA <sup>b</sup> (direct L.S. counting and enriched gas counting)	UUC <sup>c</sup> (enriched L.S. counting)
6-2	8 ± 8		
6-3		0.4 ± 0.2	
6-7			(45 ± 6) <sup>e</sup>
6-18		0.8 ± 0.3 <sup>d</sup>	
6-27			(11 ± 6) <sup>e</sup>
6-28		0.3 ± 0.2	
6-29	-0.6 ± 8		
7-1	-8 ± 8		
12-1			
13-1	10 ± 9		
14-1	115 ± 10		
15-1	19 ± 8		
15-2	3 ± 9		
15-5		0.4 ± 0.2	
15-24	-1 ± 9, -6 ± 9		
15-26		0.5 ± 0.2	(65 ± 6) <sup>e</sup>
16-3	-2 ± 9		
16-4		0.7 ± 0.3	
16-23		0.5 ± 0.3	4 ± 6
17-2		1 ± 0.2	
17-4	9 ± 9		
17-31	12 ± 9		
17-33		0.6 ± 0.3	4 ± 6
18-2		12.6 ± 0.4	
18-3	0 ± 9		
20-2	103 ± 11		
20-4		109 ± 2	
21-4		86.2 ± 7.0	
21-6	122 ± 10		
21-7	99 ± 10		
21-14		98.3 ± 2.3	
21-22	108 ± 10		
21-27		92 ± 2.1	
22-1		103.4 ± 2.4	
22-3	100 ± 11		
23-2		6.8 ± 1.0	
23-26	38 ± 10		
23-30		6.8 ± 1.0	21 ± 6
25-3		95.7 ± 2.6	
29-1	2 ± 10		
36	-1 ± 8		

a University of Waterloo, Canada

b International Atomic Energy Agency, Section for Isotope Hydrology, Vienna Austria

c University of Uppsala, Sweden

d Open to air for one week at the 410-m level

e Result is doubtful.

These data thus clearly show that no modern surface waters reach the various mine levels. Whatever tritium is found must represent contamination with drill fluids which have tritium contents typical for shallower groundwaters (e.g., Stripa 25).

#### Carbon-14

Carbon-14 "age determinations" on the dissolved inorganic carbon in a groundwater do not yield direct water dates such as those obtained from tritium analyses. The basic concept underlying the carbon-14 dating method is that waters infiltrating through vegetated soils become charged with soil-CO<sub>2</sub> before they become part of a groundwater reservoir. Because this soil-CO<sub>2</sub> has a partial pressure up to two orders of magnitude higher than the partial pressure of atmospheric CO<sub>2</sub>, it dominates the carbon isotope content of infiltrating water. Its <sup>14</sup>C activity is very close to the <sup>14</sup>C activity of the atmosphere (Fritz et al. 1978). Therefore, if no other carbon were added to the water, and only decay altered the <sup>14</sup>C contents of the dissolved carbonate, this residual activity would be a function of time only, and reflect the water age

$$A_{\text{measured}} = A_{\text{initial}} \cdot e^{-\lambda t}$$

where A = <sup>14</sup>C activity in pmC and λ = decay constant.

Unfortunately most groundwaters get their aqueous carbonate not only from the soil reservoir, but also from the aquifer carbonates. The latter are normally free of <sup>14</sup>C and their carbon will therefore "dilute" the <sup>14</sup>C contents of the initial soil carbon. The measured ages then become too old.

Many attempts have been made to quantify this geochemical dilution and to establish correction factors which would permit recalculation of the water ages. Three approaches have been taken:

- a statistical approach, which defines an average correction factor on the basis of a large number of analyses;
- chemical analyses to assess the amount of rock carbonate dissolution and precipitation;
- $^{13}\text{C}$  is used as an indicator for dead carbon contributions from isotopically distinct sources.

In a forthcoming report on  $^{14}\text{C}$  dating in Stripa, we will discuss the various correction procedures in detail; here a brief summary will suffice.

The statistical approach does not attempt to understand the geochemical processes which control the carbon geochemistry of a groundwater. For crystalline terrains Geyh (1972) proposed "correction factors" which reduce the initial activity by 0 to 20 percent. The numerical value of such "q" factors thus varies between 1 and 0.8 and appears in the decay equation as

$$A_m = qA_0e^{-\lambda t}.$$

This approach is not very satisfactory primarily because the q-factors were developed only on data from water samples which contained tritium and, therefore, any further geochemical dilution occurring in waters older than 25 to 30 years could not be taken into account.

The  $^{14}\text{C}$  contents of the aqueous carbon of a groundwater is strongly dependent on the carbon geochemistry of the system, and various methods have been developed to quantify these processes. In systems where the geochemical evolu-



tion of groundwaters can be followed from recharge to discharge areas, the simplest correction factor is derived from a comparison of initial versus final carbonate content. Such comparison implies (1) no carbon loss through mineral precipitation and (2) that isotope exchange with the rock matrix was not important. Both processes do, however, take place, and more sophisticated models based on a total assessment of the geochemistry of a groundwater and its evolution have been developed. These combine geochemical considerations with observed  $^{13}\text{C}$  variations (Reardon and Fritz 1978; Wigley, Plummer, and Pearson 1978).

The final choice of how to transform  $^{14}\text{C}$  ages obtained on aqueous carbonate into water ages depends on the amount of information available. For this project, samples were collected from private wells in the area as well as from all flowing wells and boreholes in the underground working area, in an attempt to understand as completely as possible the geochemistry and isotopic evolution of the Stripa groundwaters.

This report presents a preliminary interpretation of incomplete findings. A new stripping technique should allow us to collect a reliable  $^{14}\text{C}$  sample from the deepest part of the flowing well at the 410-m level, and at that time we will present a more complete report on the  $^{14}\text{C}$  data.

Results and Discussion. All  $^{13}\text{C}$  and  $^{14}\text{C}$  results obtained on aqueous carbonates are listed in Table 10. Two of these samples come from shallow wells from farms in the vicinity of the mine (Stripa 21 and 23), and the remainder from the flowing well in the time-scale room (Stripa 16, 43), and from the flowing well at the 410-m level (Stripa 17, 24, and 25).

Similarly, the measured  $\delta^{13}\text{C}_{\text{DIC}} = -15.2 \text{ ‰}$  for Stripa 23 can be explained if:

- the pH of the water in the unsaturated zone was close to 5,
- the soil- $\text{CO}_2$   $^{14}\text{C}$  activity was about 100 pmC, and
- the water dissolved additional  $^{14}\text{C}$ -free carbonate with a  $\delta^{13}\text{C} \sim -6.5$  under closed system conditions. (The average  $\delta^{13}\text{C}$  value of fracture calcites measured in Stripa is close to this value.)

These assumptions are not unreasonable: The low pH implies a  $\text{pCO}_2 \geq 10^{-2}$  atm. which is normal for soils in these environments where, under moss covers,  $\text{pCO}_2$ 's can be even higher. Since these surface environments are usually free of carbonate, most dissolution must occur in closed systems within the fractures. This explains why a  $^{14}\text{C}$  dilution exists: if this dissolution took place in contact with the soil atmosphere the  $^{14}\text{C}$  activities of the aqueous carbonate would remain close to modern even if the carbonate were free of  $^{14}\text{C}$ . The calculation suggest that the  $\delta^{13}\text{C}$  values of this carbonate should be more negative than the  $-1.4 \text{ ‰}$  measured on a marble outcrop of Stripa (see Table 9), and we assume that fracture calcites deposited much earlier are now partially redissolved by infiltrating groundwaters. Such dissolution must have taken place wherever the shallow waters were in contact with carbonate, since all but one of the samples of shallow waters are undersaturated with respect to calcite (Fig. 17).

Figure 17 emphasizes that the inorganic carbon content of these waters increases until calcite saturation is reached--as, for example, in Stripa 18. The isotopic composition of the dissolving calcite can only be estimated, although the  $^{13}\text{C}$  content is very critical. If the  $\delta^{13}\text{C}$ -DIC is used as an

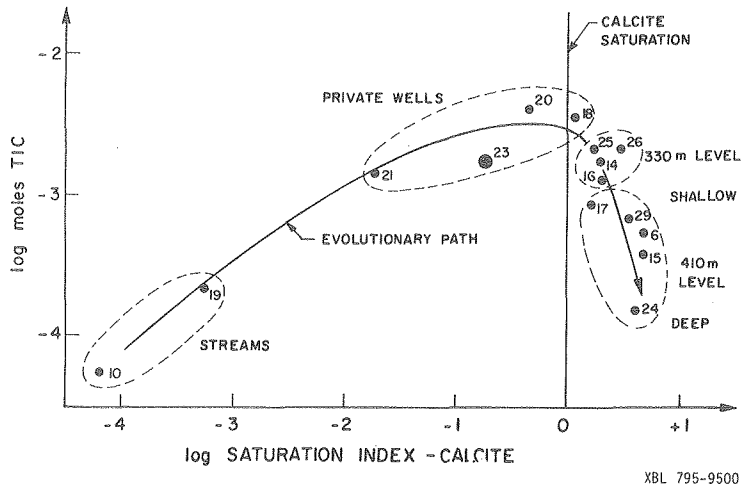


Fig. 17.

The relationship between the TIC concentration and degree of saturation with respect to calcite for waters from the Stripa area. The saturation index is defined as the ratio between Ion Activity Product (IAP) and equilibrium constant (K). For  $\log SI = 0$ ,  $IAP = K$ , and saturation is reached.

indication for the uptake of inorganic carbon, then a carbon isotope mass balance will lead to the following relationship to obtain an approximate correction factor q:

$$q = \frac{\delta^{13}\text{C-DIC} - \delta^{13}\text{C-carb}}{\delta^{13}\text{C-soil} - \delta^{13}\text{C-carb}}$$

$\delta^{13}\text{C-DIC}$  is the measured  $\delta^{13}\text{C}$  value of the sample,  $\delta^{13}\text{C-soil}$  describes the soil- $\text{CO}_2$  composition (-23 ‰) and  $\delta^{13}\text{C-carb}$  is the value for the dissolving rock carbonate (Pearson 1965). Figure 18 shows how the corrected  $^{14}\text{C}$  ages for samples with different measured  $^{14}\text{C}$  activities vary significantly with the choice of rock carbonate value. Because of the wide variation in  $\delta^{13}\text{C}$  of the deep fracture calcites (Table 9), it is imperative that we obtain much more information about the carbonates occurring on the near surface and very deep fractures of this granite.

The last finding, a 130 pmC and 100 pmC  $^{14}\text{C}$ -activity of the soil- $\text{CO}_2$ , is also very reasonable: the water from Stripa 21 is very young and the  $^{14}\text{C}$  activity of the atmosphere has increased parallel to the increase known for tritium

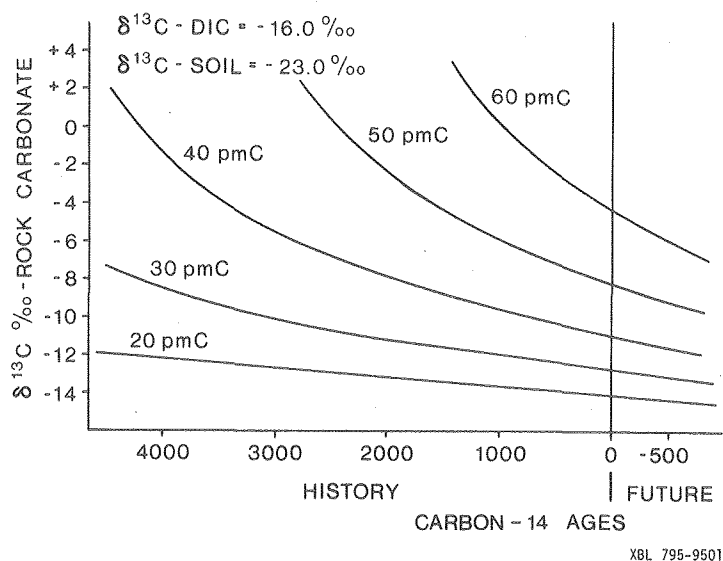


Fig. 18. The variation in corrected  $^{14}\text{C}$  ages of groundwaters with various  $^{14}\text{C}$  contents due to different assumed  $\delta^{13}\text{C}$  values of rock carbonate. The soil  $\text{CO}_2$  carbon is assumed to have  $\delta^{13}\text{C} = -23 \text{ ‰}$ , which is typical for most northern environments (Fritz et al. 1978). The measured  $\delta^{13}\text{C}_{\text{DIC}} = -16 \text{ ‰}$  is a value typical for the waters in the Stripa granite. The corrected  $^{14}\text{C}$  ages for a given  $^{14}\text{C}$  activity were calculated using Pearson's (1969) approach.

(also as a result of nuclear bomb tests). Tritium contents of the water of Stripa 23 show that it is older; thus, prebomb  $^{14}\text{C}$  concentration levels (100 pmC) had to be expected.

Since the dilution factors (q) derived for the two samples are 0.7 for Stripa 21 and 0.5 for Stripa 23, we must subtract up to one half-life (5730 years) from the measured ages. The ultimate correction for deeper waters could be even bigger, since neither Stripa 21 nor Stripa 23 have reached calcite saturation, and will continue to dissolve calcium carbonate.

Deep groundwaters. Total inorganic-carbonate concentrations are plotted versus the calcite saturation index (Table 12) in Fig. 17, which demonstrates that the total carbonate contents of the groundwaters decrease with depth. If our interpretation of the chemical data is correct, the "evolution" from shallow to deep groundwater involves calcite precipitation. This is possible because the pH of the waters increases and thus maintains calcite saturation. Hydrolysis by and dissolution of silicate minerals is probably responsible for this pH increase and also explain why the  $\text{Ca}^{2+}$  concentrations do not decrease. The carbonate decrease reduces the total carbonate contents of the deep water to about 10 percent of the contents of the shallower water.

If such removal of carbonate occurs under isotopic equilibrium conditions, then the difference in  $^{13}\text{C}$  between total aqueous carbonate and the solid precipitate will be between 2.5 and 3.0 ‰ at the pH levels typical for these groundwaters. Under those conditions (pH values close to 10), the  $^{13}\text{C}$  isotope fractionation factor between aqueous and solid carbonate will be close to  $\alpha = 1.0025$ . At much lower values (pH < 8), much higher  $\alpha$ 's can be expected with a maximum near  $\alpha = 1.01$ . The solid carbonate will be the enriched phase. Thus a continuous isotope depletion in the aqueous phase might be expected and can be approximated by a Rayleigh distillation where  $\Delta = 1000(f^{\alpha-1} - 1)$ . This is shown for  $\alpha = 1.0025$  in Fig. 19, which also shows the changes in  $\delta^{13}\text{C}$  one might expect in the residual aqueous carbon reservoir. For conditions typical for Stripa, the maximum decrease will be between 3 and 4 ‰.

The data listed in Table 10 show about 1 ‰ difference between the flowing well M-3 at the 330-m level (Stripa 16, 43) and the deep part of the well at the 410-m level (Stripa 15, 45). Between the two, the total dissolved

Table 12.  $p\text{CO}_2$ , TIC, and calcite saturation index for Stripa waters.

Stripa sample	$\log p\text{CO}_2^a$		Total dissolved <sup>b</sup> inorganic carbonate TIC (log moles/liter)	$\log \text{SI}_{\text{calcite}}^b$
	Field	Lab		
4-11	-2.86	-3.06	-3.66	-3.23
5-10	-2.77	-3.30	-3.73	-3.68
6-5	-5.02	-5.18	-3.27	0.70
6-28		-5.17		
6-30	-5.11	-5.21	-3.36	0.63
15-4	-5.30	-5.36	-3.42	0.65
15-27	-5.38	-5.36	-3.51	0.57
16-5	-4.03	-4.07	-2.88	0.31
16-23		-4.09		
16-24	-4.06	-4.07	-2.90	0.31
17-32	-4.28	-4.29	-3.07	0.19
17-33	-4.21	-4.23	-3.07	0.12
18-1	-2.62		-2.46	0.06
20-3	-2.00	-1.99	-2.42	-0.36
20-4	-2.00	-2.02	-2.42	-0.38
21-3	-2.01	-2.13	-2.71	-1.73
21-10	-2.15	-2.12	-2.82	-1.73
21-23	-2.24	-2.22	-2.79	-1.31
21-26	-2.24	-2.25	-2.78	-1.31
23-14	-2.72	-2.70	-2.78	-0.70
23-23	-2.68	-2.72	-0.71	
23-29	-2.8	-2.10	-2.67	-1.29
24-2	-4.76	-4.76	-3.71	0.56
25-1	-3.12	-3.07	-2.71	0.18
26-7	-3.34	-3.36	-2.68	0.47
27-4	-3.19	-3.22	-2.76	0.29
29-3	-6.03	-6.13	-3.81	0.61
29-34a	-6.22	-6.24	-4.00	0.40
29-39	-6.09	-6.00	-3.94	0.47
29-61	-6.02	-6.47	-3.86	0.55

a Field  $p\text{CO}_2$  values were calculated from field pH measurements and field alkalinity titrations. Laboratory  $p\text{CO}_2$ 's were determined from laboratory pH and alkalinity data.

b TIC and SI values are based on field measurements.

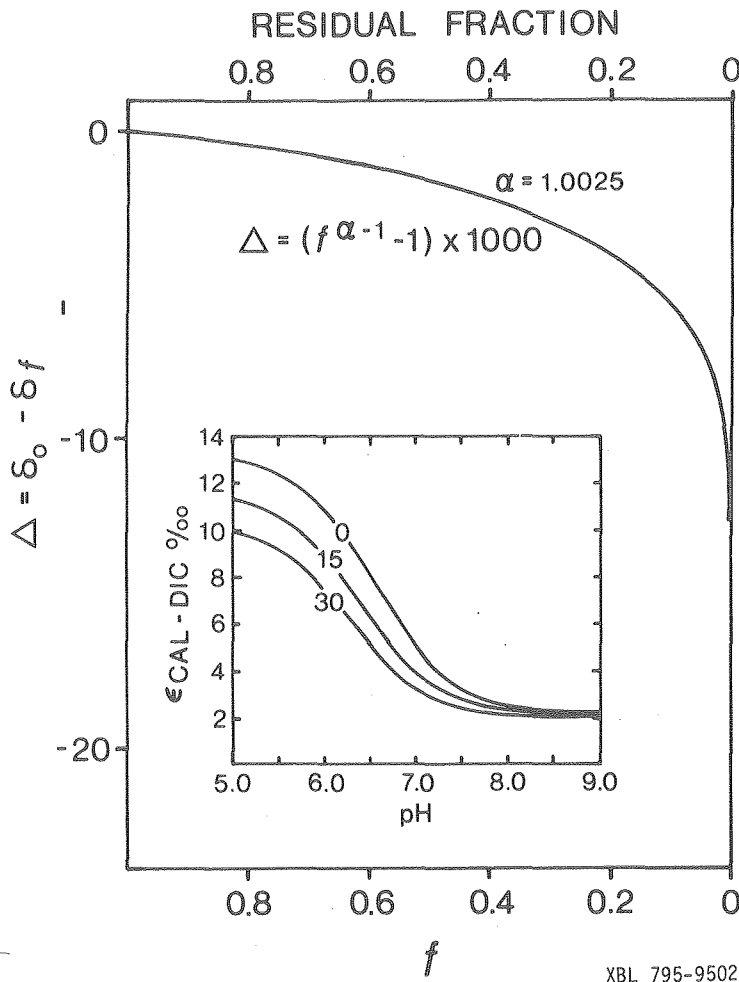


Fig. 19.

The decrease in  $\delta^{13}\text{C}$  of the precipitated phase as the reservoir is depleted in  $^{13}\text{C}$  by equilibrium fractionation of carbon isotopes during continual precipitation.  $\alpha_{\text{calcite-TIC}}$  was assumed to be 1.0025. This is the fractionation factor expected if calcite precipitation occurs above  $\text{pH} = 7.5$  and is shown in the inset. Note that  $\epsilon = (\alpha - 1) \times 1000$ . Isotope effects for 0, 15, and 30°C are shown.

carbonate decrease reaches between 60 and 80 percent; therefore, the isotopic differences tend to support the model proposed ( $\alpha \sim 1.0025$ ) and indicate that active calcite precipitation occurs.

The removal of calcium carbonate from solution has little effect on the  $^{14}\text{C}$  activities, because the  $^{14}\text{C}$  effects are only twice those known for  $^{13}\text{C}$ . Thus a 2 ‰ decrease in  $^{13}\text{C}$  corresponds to a 4 ‰ or 0.4 percent decrease in  $^{14}\text{C}$  activity. This change is within analytical error.

Thus, in correcting measured  $^{14}\text{C}$  ages, only dilution occurring during carbonate uptake until calcite saturation is reached (amounting to one half-life-- 5,730 years or more) has to be taken into account. These dilution factors-- which will be better defined when we have samples from the future, deeper borehole SBH-3--are probably the only corrections applicable for transforming measured  $^{14}\text{C}$  contents into water ages, provided only calcite precipitation but no dissolution occurs after saturation is reached. (The incongruent dissolution of Mg-carbonates is theoretically still possible, but no such minerals have been recognized as fracture coatings.) Applying this correction to the results presented in Table 10, the waters discharging at the 330-m level would have an age between 23,000 and 25,000 years. Samples from the shallow part of the deeper hole tend to be slightly younger.

This age discrepancy is of great concern to us and has to be resolved. Some contamination of the low carbonate waters from the 410-m well may have occurred. The sample size was extremely large and up to twenty-five 60-liter jugs had to be stripped. Because these bottles were full of air before water was added, we assumed that all  $\text{CO}_2$  in this air was adsorbed by the high-pH water, and a maximum contamination of 3 percent could occur. However, the sampling arrangement was such that water in contact with the air was discharged from the last bottle amongst three to five connected jugs before the carbonate was precipitated and no contamination with atmosphere  $\text{CO}_2$  should have occurred.

The possibility of  $^{14}\text{C}$  exchange between the fracture calcites and the aqueous carbon will have to be considered, because other studies have shown that it may be important--at least in systems where fine grained carbonate is



exposed to migrating groundwater (Wigley 1976). There, however, the aqueous carbon approaches isotopic equilibrium with the carbonate minerals. We have no indication that this is the case in Sweden. We hope to present a more complete discussion on the potential significance of exchange and diffusive loss using mathematical models now being developed in Waterloo and elsewhere.

Conclusions.  $^{14}\text{C}$  dating of the groundwaters discharging at the 330-m and 410-m levels from fracture zones within the granite strongly indicates that these waters are very old, possibly older than 20,000 years. For a final assessment it will be necessary to:

- better define the  $^{14}\text{C}$  dilution which occurs in the shallower parts of the groundwater systems (this should be possible once SBH-3 is drilled);
- sample the deepest part of the flowing well at the 410-m level (because the carbon contents of these waters are extremely low, we are developing new sampling techniques);
- assess potential  $^{14}\text{C}$  losses from the aqueous carbonate due to isotope exchange and diffusion.

### 3.5 Elements of the Uranium Decay Series

The analytical work and a preliminary interpretation of the data have been provided by Dr. J. K. Osmond, Florida State University, U.S.A., and Dr. J. N. Andrews, University of Bath, Great Britain. Their determinations of  $^{234}\text{U}/^{238}\text{U}$  activity ratios on water samples are listed in Table 13, which also gives the uranium contents of the samples. The  $^4\text{He}$  analyses done at the University of Bath are listed with the noble gas data in Table 3. Radon analyses (University of Bath and AB Atomenergi, Sweden) are summarized in Table 14.

Analysis of rock samples for uranium isotope contents has not been completed.

Table 13. Uranium isotopic data.

Stripa sample	Lab. sample	Total dissolved inorg. carb. (log moles/l)	Uranium ( $\mu\text{g}/\text{l}$ )	$^{234}\text{U}/^{238}\text{U}$ Activity ratio	$^{234}\text{U}$ excess <sup>a</sup> Ueq ( $\mu\text{g}/\text{l}$ )
Private wells					
21-7	FSU <sup>b</sup> 1354	-2.85	1.61	3.11	3.4
23-9	FSU 1352	-2.78	2.84	2.62	4.6
23	U of B <sup>c</sup>	(-2.78)	2.26	2.57	3.5
330-m level					
16-25	FSU 1355	-2.91	8.25	10.75	80.5
16-30	FSU 1358	(-2.91)	9.22	10.65	89.0
16	U of B	(-2.91)	8.33	10.70	80.8
410-m level					
17-30	FSU 1357	-3.07	10.43	5.55	47.6
24-5	FSU 1359	-3.17	6.24	5.87	30.4
6	FSU 1356	-3.44	4.56	3.87	13.1
15-3	FSU 1353	-3.42	4.12	4.08	12.7
29	U of B	-3.81	1.03	4.02	3.11

a This  $^{234}\text{U}$  excess is calculated with  $(A_i - 1) \cdot C_i$  where  $A_i$  = activity ratio of sample and  $C_i$  its uranium content in  $\mu\text{g}/\text{l}$ .

b Florida State University, U.S.A.

c University of Bath, Great Britain.

Table 14.  $^{222}\text{Rn}$  and  $^{226}\text{Ra}$  contents of groundwaters.

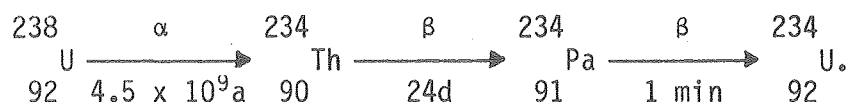
Stripa sample	Laboratory	$^{222}\text{Rn}$ ( $\mu\text{Ci}/\text{l}$ )	$^{226}\text{Ra}$ (pCi/l)
16	ATA <sup>a</sup>	1.9	n.d.
16	UB <sup>b</sup>	1.3	34
17	ATA <sup>a</sup>	0.48	n.d.
29	UB <sup>b</sup>	0.56	40

a AB Atomenergi, Sweden.

b University of Bath, Great Britain.

A more comprehensive report on groundwater dating in crystalline rocks with the uranium-decay series will be prepared after all analytical work has been completed. This will include analyses of additional samples from SBH-3 and the 410-m-level borehole.

$^{234}\text{U}/^{238}\text{U}$  Activity Ratios.  $^{238}\text{U}$  decays into  $^{234}\text{U}$  according to the following scheme:



One would expect that most natural systems containing uranium would be in a state of equilibrium with respect to the activities of the two uranium isotopes where the activity ratio  $A_{234}/A_{238} = 1$ . During the 1950s, however, Russian researchers discovered that most natural waters are enriched in  $^{234}\text{U}$ , and that a disequilibrium is maintained (Cherdyntsev, Chalov, and Khaidarov 1955).

The cause of disequilibrium has been the topic of many discussions, which were recently summarized in an article by Osmond and Cowart (1976). It has been proposed that the magnitude of the disequilibrium and its change within an aquifer could be used for groundwater dating purposes.

Kigoshi (1971) and Kronfeld et al. (1975) proposed that excess  $^{234}\text{U}$  builds up in confined groundwater bodies as a result of the continuous addition of  $^{234}\text{Th}$  injected from the rock matrix because of alpha recoil. The age of the water could be calculated if the initial activity ratio were known.

Kronfeld and Adams (1974), however, noted elsewhere that the activity ratio can also decrease within a well-defined groundwater flow system, and proposed to use this decay as indication of age. To complicate matters further, Cowart and Osmond (1974) present data showing that, as a result of geochemical processes causing precipitation and/or dissolution of dissolved uranium in groundwaters, activity within an aquifer can either increase or decrease. The uranium concentrations, in turn, influence the effectiveness of recoil enrichment, and thus the activity ratios.

The conclusion must be that, unless it is possible to study in detail the initial activity ratios in the aquifer rocks and the geochemical evolution of the groundwater, any age dating based on  $^{234}\text{U}/^{238}\text{U}$  activity ratio is at best speculative.

Despite these problems we will attempt age calculation based on various models as soon as we have reliable data on the activity ratios in the rocks. A complicating factor is that it is important to obtain samples of local uranium enrichments in fractures and/or the granite, because there may be significant variability both within the rock mass and among the different fracture systems.

The simplest model calculation assumes that a groundwater is moving into closed system conditions with a certain activity ratio which then changes as a function of time because of the decay of  $^{234}\text{U}$  and  $^{238}\text{U}$ . This assumption has been made by Barr and Carter (1978) who derive the following relationship for a system to which no new uranium is added by dissolution or recoil mechanisms:

$$t = \frac{\ln \frac{A_m - 1}{A_0 - 1}}{-\lambda_{234}}$$

$A_m$  and  $A_0$  are the  $^{234}\text{U}/^{238}\text{U}$  activity ratios of the sample analyzed and of the water at the time it moved into closed system condition, respectively. The  $\lambda_{234}$  is the decay constant of  $^{234}\text{U}$  ( $2.806 \times 10^{-6}\text{a}^{-1}$ ). If  $(A-1) \equiv X$  is defined as uranium excess the above equation describes the decay of the  $^{234}\text{U}$  excess with time and can be written as:

$$X = X_0 \exp - \lambda_{234} t$$

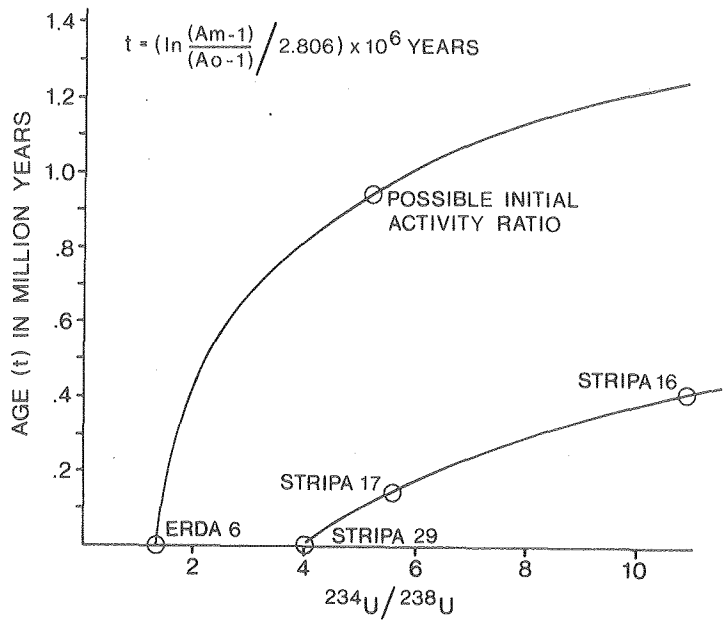
which is a normal decay equation. The decay of  $^{238}\text{U}$  is negligible during the time spans considered here.

For the purpose of this model, it is now assumed that the uranium in the Stripa waters was taken up outside the granitic mass and that it moves within a closed system in the granitic mass from the 330-m level to the depths reached by the 410-m-level borehole. The activity ratios of Stripa 16 would then correspond to  $A_0$ , and those of Stripa 29 to  $A_m$ . The calculated age difference between the two waters would be:

$$t = - \frac{\ln \frac{4.02 - 1}{10.7 - 1}}{2.806 \times 10^{-6}} = 4.16 \times 10^5 \text{a},$$

that is, Stripa 29 would be more than 400,000 years older than Stripa 16. This is graphically shown in Fig. 20. One can also deduce from Fig. 20 that if the evolution moved from a Stripa-17-type water (collected between 6.3 m and 50 m in the 410-m hole) to Stripa 29 water (collected between 376.5 m and 471 m in the 410-m hole), the age difference between the two would be about 140,000 years.

It is difficult to estimate how reasonable this type of model assumption is. In a comparison of  $^{232}\text{U}$  excess with uranium contents (Fig. 21--top), ura-

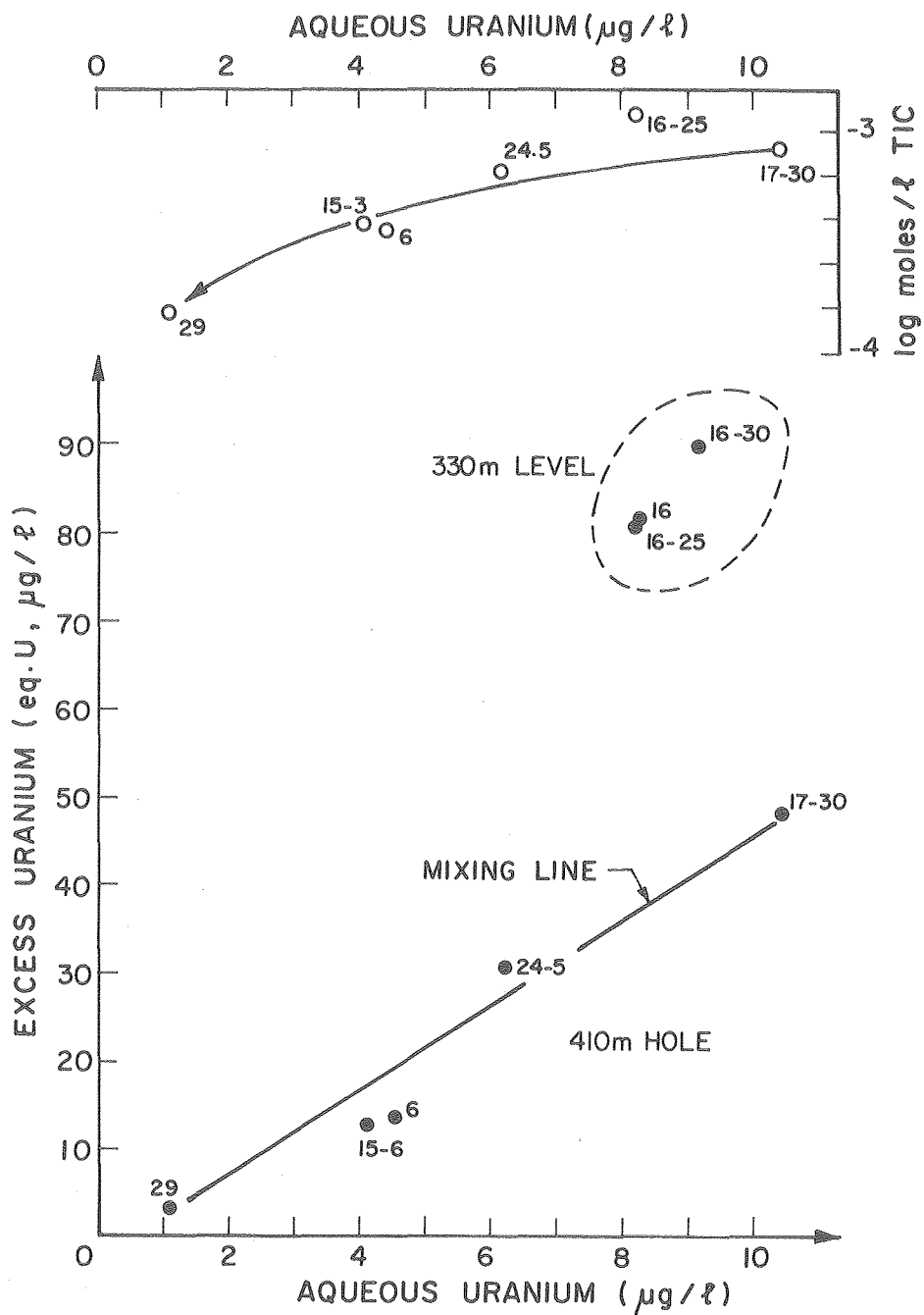


XBL 795-9503

Fig. 20. The age difference between Stripa 16 and Stripa 29 groundwaters based on  $^{234}\text{U}/^{238}\text{U}$  activity ratio evolution under closed system conditions.

nium and TIC concentrations decrease with depth; one could therefore conclude that uranium is precipitated but not dissolved. What effect this accumulation of uranium minerals on the fracture surface would have on the activity ratios of the water is difficult to estimate, but if anything, it could tend to augment the activity ratios because of recoil processes.

In a comparison of dissolved uranium contents with excess uranium concentrations (Fig. 21--bottom), all samples from the 410-m borehole lie close to a straight line, which is probably a mixing line between the endmembers Stripa 17 and 29. Note that the M-3 samples (Stripa 16) do not fall on this line, indicating that at least three different types of groundwater discharge from the granite fracture system.



XBL 795-9504

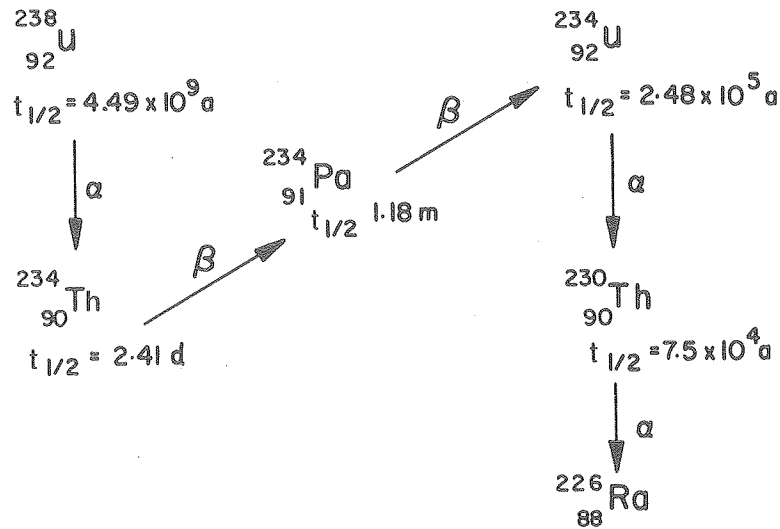
Fig. 21. The relationship of uranium content with TIC content and of excess  $^{234}\text{U}$  with uranium content of Stripa groundwaters.

The water samples from the 330-m and the top of the 410-m-level holes are very similar chemically and also in  $^2\text{H}$ ,  $^{18}\text{O}$ , and  $^{14}\text{C}$  contents. A similar age could thus be assumed for the samples Stripa 16 and 17. The differences in uranium geochemistry might then reflect flow paths for these waters along which isotopically different uranium was encountered. The model calculations presented above would then no longer be valid for these two samples and their different uranium activity ratios might be simply a reflection of the uranium input rather than age differences. This argument is not valid for Stripa 29 and Stripa 17, and it is possible that Stripa 29 evolved from a Stripa 17-type water during a 140,000-year history.

This reveals the complexity of these systems, despite their apparently simple geochemistry; it is impossible at present to define an acceptable model. Note, however, that the uranium data suggest rather high ages for all of these deep groundwaters.

Helium-4 Dating. The decay of  $^{238}\text{U}$  to  $^{206}\text{Pb}$  and of  $^{234}\text{U}$  to  $^{208}\text{Pb}$  is accompanied by the production of  $^4\text{He}$  (Fig. 22). The amount of helium present in a closed system is thus a function of time and amounts of radioactive elements. Therefore, from the quantity of helium collected in a water sample and the uranium and thorium contents of the host rock, the residence time of the water in the rock can be calculated. Among the assumptions to be made are that helium is not lost by diffusion (the ages would then be too young) and that no rapid gas release trapped in the rock mass had occurred as a consequence, for example, of pressure release after deglaciation and the following isostatic uplift. (This would lead to artificially high helium contents and the calculated ages would then be too old.)





XBL 795-9505

Fig. 22.  $^4\text{He}$  production in the uranium decay series ( $\alpha$ -decay).

Few attempts have been made to do direct helium dating based on the concentrations of this gas in water samples. Noteworthy is the study by Marine (1976) who attempted to evaluate by  $^4\text{He}$  methods the age of groundwater encountered in crystalline-metamorphic rocks underlying the Savannah River Plant. Making assumptions on uranium and thorium contents in the rocks, fracture spacing, porosity, and the  $^4\text{He}$  generation rate, Marine calculated water ages of up to 840,000 years. Although this number may be in error, it does indicate that, unless the uranium and thorium contents of the rocks were very high, waters containing this amount of helium are quite old.

The helium concentrations in the Stripa waters are even higher than those observed by Marine. Helium concentrations are transformed into water ages in a

relationship which considers  $^4\text{He}$  content, rock porosity, rock density, the concentrations of uranium and thorium in the aquifer rocks, and helium production from uranium and thorium:

$$t = \frac{{}^4\text{He} \cdot n}{(U \cdot p_U + \text{Th} \cdot p_{\text{Th}}) \cdot \xi}$$

where

$${}^4\text{He} = 3.5 \times 10^{-4} \text{ cm}^3/\text{cm}^3 \text{ H}_2\text{O} \text{ for Stripa 16}$$

$$1.4 \times 10^{-3} \text{ cm}^3/\text{cm}^3 \text{ H}_2\text{O} \text{ for Stripa 29}$$

$$n = 2 \times 10^{-3} \text{ gH}_2\text{O}/\text{cm}^3 \text{ rock (fracture + nonfracture porosity)}$$

$$\xi = 2.9 \text{ g}/\text{cm}^3 \text{ (rock density).}$$

Uranium and thorium are contents in g/g rock, where U:Th  $\sim$  1:4 in average crustal rocks. Helium production rates are  $p_U = 11 \times 10^{-8} \text{ cm}^3/\text{g U}\cdot\text{year}$  for uranium and  $p_{\text{Th}} = 3.1 \times 10^{-8} \text{ cm}^3/\text{g Th}\cdot\text{year}$  for thorium. Thus,

$$t = \frac{({}^4\text{He}) \cdot 2 \cdot 10^{-3}}{(U)(11 + 4 \cdot 3.1) \cdot 10^{-8} \cdot 2.9} \cdot$$

Thus if the rock contains 1 ppm uranium (close to average in granites), attaining the concentrations of  $^4\text{He}$  observed would have required close to 900,000 years in the water discharging at the 330-m level, and 3.6 million years in the Stripa 39 waters. These are clearly excessive ages and could reflect uranium enrichments which occur locally. If this enrichment were as high as a factor of 100, which is unlikely, then the age of Stripa 16 would be reduced to  $\sim$  9,000 years and the age of Stripa 29 to  $\sim$  36,000 years.

If the  $^{14}\text{C}$  dates discussed above were correct and Stripa 16 were about 25,000 years old, then Stripa 29 would be close to 100,000 years old, and the average uranium content in the rock mass in contact with these waters would be 34 ppm--still reflecting very significant enrichments.

The conclusion must be that the waters discharging from the fracture network in the granite were in contact with rocks significantly enriched in uranium and also that they took many thousands of years to acquire the observed  $^4\text{He}$  levels. The large age differences calculated for the different samples could signify that the uranium content and uranium activity ratios of the rocks differ along the flow path of the two systems. This would be supported by the arguments presented above on excess  $^{234}\text{U}$  and uranium contents in the water.

Radiogenic Argon. Dr. J. N. Andrews, R. L. F. Kay, and D. J. Lee contributed the following comments based on their analyses:

"Assuming that all the radiogenic  $^{40}\text{Ar}$  generated in a rock of fractional porosity,  $\phi$ , is dissolved in the interstitial water, the  $^{40}\text{Ar}$  dissolved in the interstitial water residence time  $t$  years can be shown to be given by

( $p$  - density;  $[K]$  = K content, %):

$$\begin{aligned} \frac{p}{\phi} [K] (^{40}\text{Ar production rate})t &= \frac{2.6}{0.3} \times 5 \times 3.975 \times 10^{-14} t \\ &= 1.72 \times 10^{-12} \text{cm}^3 \text{ STP Ar cm}^{-3} \text{ H}_2\text{O/year} \end{aligned}$$

or  $1.72 \times 10^{-6} \text{ cm}^3$  after  $10^6$  years, which is negligible compared with dissolved atmospheric argon.

"Radiogenic  $^{40}\text{Ar}$ , therefore, can only significantly add to dissolved atmospheric argon if it diffuses out of the rock matrix. Such an addition of  $^{40}\text{Ar}$  will increase the  $^{40}\text{Ar}/^{36}\text{Ar}$  ratio. These ratios are:

Atmospheric argon	295.5
Stripa 16, dissolved argon	302.8
Stripa 29, dissolved argon	315.6

Even for Stripa 29, this represents an addition of only about 7 percent of radiogenic  $^{40}\text{Ar}$ .

"Release of  $^{40}\text{Ar}$  by diffusion is time dependent and enhanced  $^{40}\text{Ar}/^{36}\text{Ar}$  ratios are observed only for old groundwaters. We have observed such enhancement for thermal waters and for 'connate' waters in the Lincolnshire Limestone but not for  $> 30,000$ -year-old waters from the Bunter Sandstone. The higher ratio for Stripa 29 is indicative of its greater age."

Radon. The naturally occurring radioactive element radon (Rn) occurs primarily in the form of its isotope  $^{222}\text{Rn}$ . This isotope, with a half life of 3.8 days, is the heaviest of the noble gases. It is produced within the decay series of  $^{238}\text{U} \rightarrow ^{206}\text{Pb}$  from  $^{226}\text{Ra}$ . The latter is similar in its geochemical behavior to the alkaline earths calcium, strontium, and barium, and undergoes similar processes of adsorption and coprecipitation; it is thus rather immobile (Tanner 1964a,b). The abundance of  $^{222}\text{Rn}$  in a groundwater is dependent on the amount of  $^{226}\text{Ra}$  (i.e.,  $^{238}\text{U}$ ) present in aquifer rocks and secondary minerals on fractures, etc., as well as on the time a given water mass has been removed from the radon-generating source. Of further importance in "stagnant" systems is migration by diffusion to the point of sampling which might be enhanced by stress release.

Magri and Tazioli (1970) document that higher groundwater flow velocities are characterized by higher radon contents. The concentration of radon in shallow groundwater is usually in the order of a few hundred pCi/liter ( $10^{-12}$  Ci/liter) but can be as high as  $10^{-10}$  Ci/liter in geothermal areas (Mazor 1976; Kruger, Stoker, and Umana 1977). A similar spread, with maximum values near  $3 \times 10^{-9}$  Ci/liter has been observed in groundwaters from quartzitic rocks in northern Finland (Ketula and Sarikkola 1973).

The radon concentration in the waters at Stripa is very much higher than is typical for any of the above-mentioned environments. This is shown in Table 14, (page 88) which also lists  $^{226}\text{Ra}$  contents as determined by different laboratories. These high  $^{222}\text{Rn}$  contents almost certainly are related to uranium enrichments in or adjacent to the granite. It may be noteworthy that the average granite releases only about 10 percent of the radon produced within its minerals--again indicating rather significant uranium enrichments.

The  $^{222}\text{Rn}$  activity can be related to the  $^{234}\text{U}$  excess if a number of assumptions are made. K. J. Osmond and J. B. Cowart provided the following comment on this topic:

"A semiquantitative estimate of age can be made by comparing the  $^{234}\text{U}$  excess values of Stripa 16 and 17 with their corresponding radon contents. If most of the radon accumulates as a recoil product, or if it is in equilibrium with radium which accumulates primarily as a recoil product, then the short-lived radon represents the 'steady-state' disequilibrium which would be expected eventually to be reached by the daughter  $^{234}\text{U}$ :

$$X_{234} = X_{222}(1 - e^{-\lambda t})$$

where  $X_{234}$  ( $= A_{234} - A_{238}$ ) is the observed  $^{234}\text{U}$  excess activity in water, and  $X_{222}$  is the corresponding excess of radon.  $\lambda$  is the decay constant of  $^{234}\text{U}$  (half life is 250,000 years) and  $t$  is the time that the water has been percolating through the rock.

"The age calculated for Stripa 16 by this model is 30,000 years, using a radon content of 0.5 microcuries per liter. If we use for the excess radon the sum of water and gas values, this figure is reduced to about 12,000 years.

The corresponding ages calculated for Stripa 17 are 35,000 and 10,000 years, respectively. The agreement between these two sample ages (16 and 17) seems reasonable; that their activity ratios are different is taken as a manifestation of different rock-water relationships, e.g., porosity along different percolation routes.

"These ages are based on a recoil model. If radon is leached preferentially with respect to radium, then the ages are too young (i.e., the 'steady state' excess estimate based on radon, daughter of radium, is too high, and the approach of  $^{234}\text{U}$  excess to this steady state is closer than originally calculated). The same is true if radon diffusion and accumulation has caused the radon values to be too high."

This recoil model can also be used to explain the  $^{226}\text{Ra}$  concentrations measured in Stripa 16 and 29. J. N. Andrews and coworkers point out that:

"The dissolved  $^{226}\text{Ra}/^{238}\text{U}$  activity ratios for the Stripa 16 and 29 waters are about 13/1 and 120/1, respectively, whereby  $^{226}\text{Ra}$  solution is largely controlled by the  $\text{Ca}^{++}$  and  $\text{Ba}^{++}$  chemistry, and uranium solution is redox controlled. Whereas for Stripa 29 the uranium content is much lower than that of Stripa 16, the  $^{226}\text{Ra}$  contents of the two samples are about the same. It seems possible that the  $^{226}\text{Ra}$  solution could be recoil controlled, a process that would result in a constant  $^{226}\text{Ra}$  content in solution for waters older than 8,000 years on the assumption that the granite composition is uniform."

Conclusions. The results from the analyses of  $^{238}\text{U}$  decay products very strongly suggest that the waters discharging from the fractures in this granite

are thousands of years old. However, it is impossible to present absolute ages because we do not yet know the distribution and abundance of uranium in this granite and its fracture minerals.





#### 4. SUMMARY

This report presents a first summary and interpretation of the chemical and isotope data obtained on groundwaters in the Stripa granite. Although much has been achieved within one year, we are still missing essential information before a more complete picture can be presented. We therefore propose to prepare, as data become available, a number of specific reports dealing with well-defined topics such as "uranium dating of groundwaters," " $^{14}\text{C}$  in Stripa groundwaters," and "fracture minerals and chemistry of groundwaters in the Stripa granite."

Despite this incompleteness we now feel fairly confident in stating that old groundwaters do discharge from different boreholes in the granite and that the geochemistry of these waters is dependent on dissolution and precipitation of silicates and calcium carbonate. More specifically we can state:

--The geochemical evolution of the groundwaters appears to follow a consistent trend with depth. This evolution is possibly related to silicate hydrolysis and the formation of specific secondary mineral assemblages. Future studies will have to be directed toward the determination of these assemblages because the knowledge of their composition will be essential for prediction.

--The total dissolved solids of all groundwaters analyzed to date is below ~500 mg/liter, with chemical characteristics which change from calcium bicarbonate waters in shallow groundwaters to sodium-calcium-chloride waters at depth.

--The pH of the deep waters exceeds 9.5, in contrast to groundwaters in other crystalline terrains where much lower pH values are measured. This discrepancy would have important implications on the design of containment systems.

--The groundwaters become saturated with respect to calcite fairly early during their geochemical evolution. This saturation is maintained by rising pH's and calcium addition, despite calcite precipitation in fracture surfaces. This leads to a loss in dissolved inorganic carbonate which is significant for  $^{14}\text{C}$  dating, and because many radionuclides form soluble carbonate complexes.

--Oxygen and deuterium document that the deep groundwaters recharged under different (cooler) climatic conditions than exist today. This is supported by noble gas analyses.

--Fracture systems intersected at the 330-m level have isotopically different water than those encountered at the bottom of the 410-m-level hole.

--Modern surface waters are not actively discharging from fracture systems encountered at the 330-m and 410-m levels.

-- $^{13}\text{C}$  contents of presently discharging groundwaters indicate that recharge has occurred through vegetated soils.

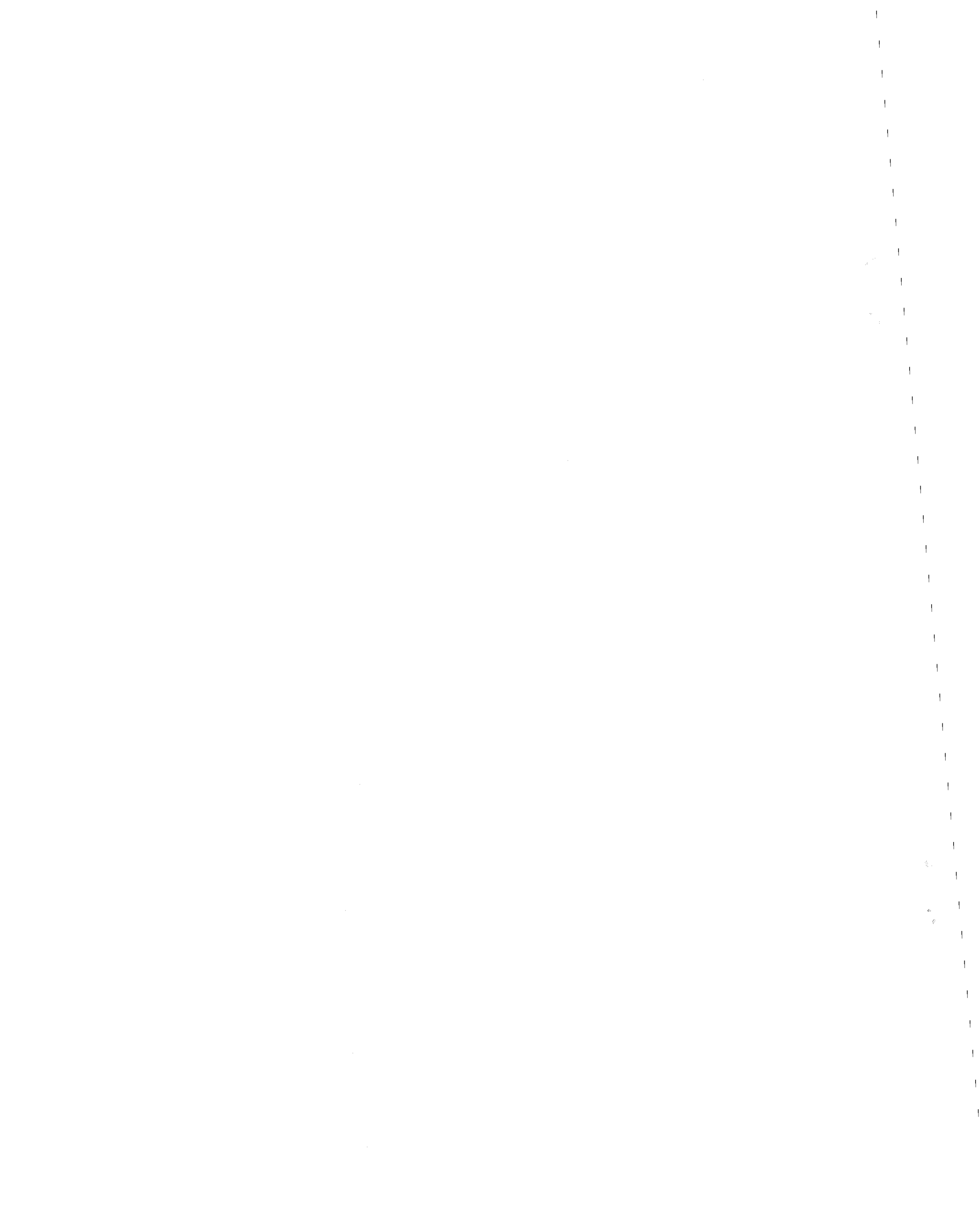
--There is good indication that some fracture calcites have been precipitated from subglacially recharged waters; others show evidence of strongly reducing conditions existing in the past on some fracture systems.

--No tritium was found in actively discharging groundwaters at the 330-m or 410-m level. However, tritiated waters have been introduced as drilling fluids, and tritium indicates contamination by drilling fluids in some "groundwaters."

--Preliminary  $^{14}\text{C}$  ages indicate that waters presently discharging at the 330-m and 410-m levels were recharged more than 20,000 years ago. However, the

final interpretation of the data will have to await the collection of a sample from the deepest part of the fracture systems encountered by the 410-m hole as well as intermediate samples from the future SBH-3 hole.

--Data obtained from the uranium decay series support the indication that very old groundwaters occur in these fracture systems. However, we lack the knowledge of uranium contents and their isotopic composition in the host rock that would permit a quantitative age estimate.



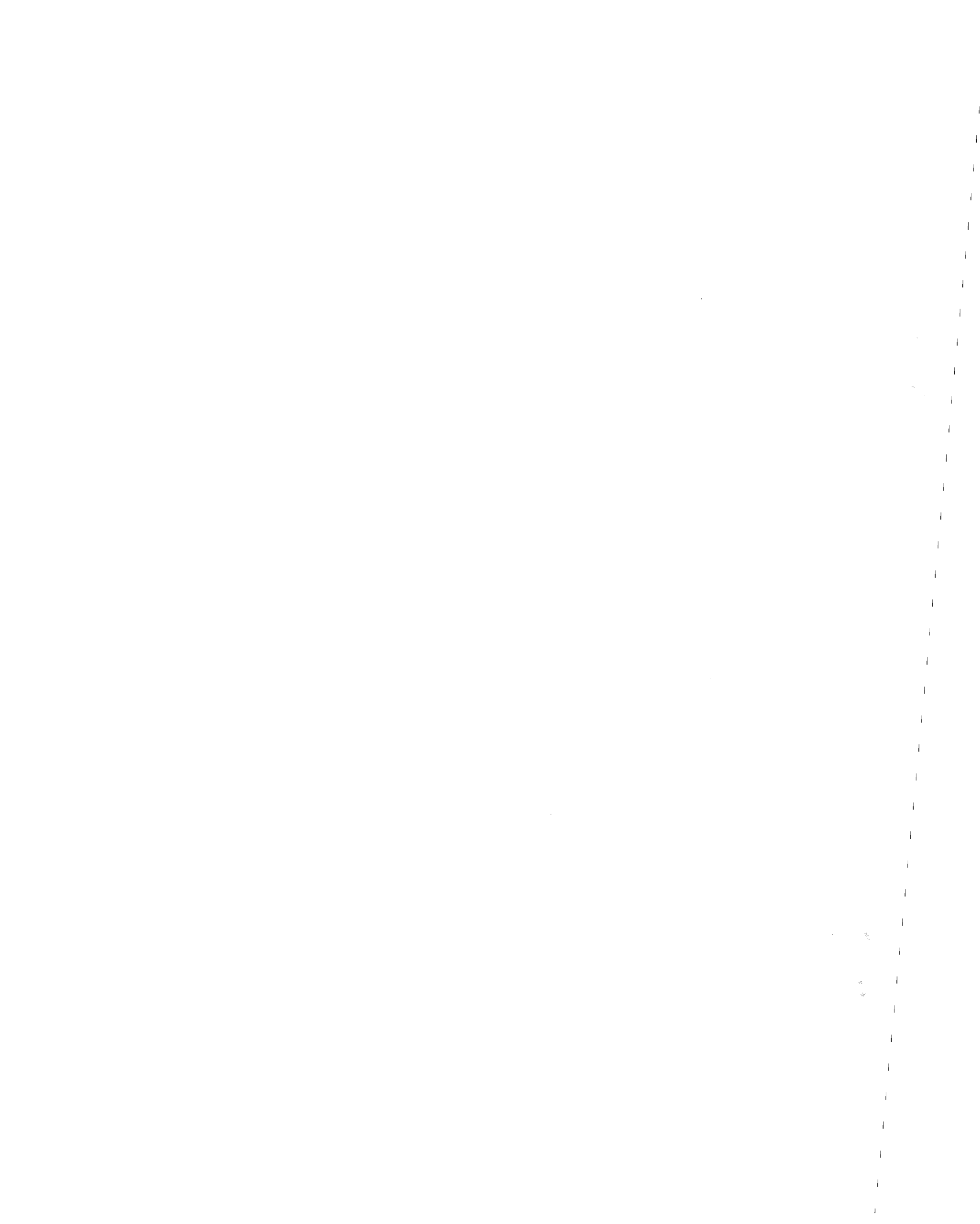
## 5. ACKNOWLEDGMENTS

The progress made so far in the geochemical program could not have been achieved without the help of the staff of the Lawrence Berkeley Laboratory (LBL), University of California, U.S.A.; Department of Earth Sciences, University of Waterloo, Canada; the International Atomic Energy Agency, Section for Isotope Hydrology, Vienna, Austria; and Kärnbränslesäkerhet (KBS) and Sveriges Geologiska Undersökning (SGU), both of Stockholm, Sweden; as well as the various laboratories providing analyses. The assistance of Ställbergsbologen personnel, particularly P-A. Halén and O. Hagström, is also gratefully acknowledged. The sampling program at Stripa was carried out with the particular assistance of T. Doe (LBL), C. Forster (University of Waterloo), and K-E Almén, P. Hammargren, K. Hansson, and L. Ekman, all of SGU. Preliminary interpretation of the results of the uranium series and noble gas analyses was provided by J. N. Andrews, University of Bath, Great Britain, and K. Osmond, Florida State University, U.S.A. The interpretations presented in this report, however, are the sole responsibility of the authors.

This work was supported by funds from the Lawrence Berkeley Laboratory under Purchase Order 478 3802 and through WRI contract 803-12.

- Kigoshi, K. 1971. Alpha recoil thorium-234: dissolution into water and the uranium-234/uranium-238 disequilibrium in nature. Science 173: 47-48.
- Kronfeld, Joel and Adams, A. S. 1974. Hydrologic investigations of the groundwaters of central Texas using U-234/U-238 disequilibrium. J. of Hydrol. 22 (1,2): 77-88.
- \_\_\_\_\_ ; Gradsztahn, E.; Muller, H. W.; Radin, J.; Yaniv, A.; and Zach, R. 1975. Excess  $^{234}\text{U}$ : an aging effect in confined waters. Earth Planet. Sci. Lett. 27: 342-345.
- Kruger, P.; Stoker, A.; and Umana, A. 1977. Radon in geothermal reservoir engineering. Geothermics 5: 13-20.
- Langmuir, D. 1970. Eh-pH determination. In Procedures in Sed. Petrology, ed. R. E. Carver, pp. 597-633.
- Magri, G. and Tazioli, G. S. 1970. Radon in groundwaters of dolomitic and calcareous aquifers in Apulia (S. Italy). In Isotope Hydrology, IAEA Symposium. Sm-129/53, 835-845. Vienna.
- Marine, I. W. 1976. Geochemistry of groundwater at the Savannah River Plant. Report to ERDA by DuPont de Nemours and Co. No. DP 1356. 102 pp. Aiken, South Carolina.
- Mazor, E. 1972. Paleotemperatures and other hydrological parameters deduced from noble gases dissolved in groundwaters; Jordan Rift Valley, Israel. Geochim. Cosmochim. Acta 36: 1321-1336.
- \_\_\_\_\_. 1976. Geothermal tracing with atmospheric and radiogenic noble gases. Geothermics 5: 21-36.
- Olkiewicz, A.; Gale, J. E.; Thorpe, R.; and Paulsson, B. (in progress). Geology and fracture system at Stripa. Lawrence Berkeley Laboratory Report.
- Osmond, J. K. and Cowart, J. B. 1976. The theory and uses of natural uranium isotopic variations in hydrology. At. Energy Rev. 14: 621-680.
- Pačes, T. 1972. Chemical characteristics and equilibrium in natural water - felsic rock -  $\text{CO}_2$  system. Geochim. Cosmochim. Acta 36: 217-240.
- Pearson, J. F. 1969. Use of  $^{13}\text{C}/^{12}\text{C}$  ratios to correct radiocarbon ages of materials initially diluted by limestone. Proc. Sixth Int. Conf. on Radiocarbon and Tritium Dating, Pullman, Washington (1969), 357 pp.
- Plummer, C. N.; Jones, B. F.; and Truesdell, A. H. 1976. WATEQ - A Fortran IV version of WATEQ, a computer programme for calculating chemical equilibrium of natural waters. U.S.G.S. Water Resource Investigations 76-13

- Reardon, E. J. and Fritz, P. 1978. Computer modeling of groundwater  $^{13}\text{C}$  and  $^{14}\text{C}$  isotope compositions. J. Hydrol. 36: 201-224.
- Sato, M. 1960. Oxidation of sulfide ore bodies. Econ. Geol. 55: 928-961.
- Stainton, M. P. 1973. A syringe gas-stripping procedure for gas-chromatographic determination of dissolved inorganic and organic carbon in fresh water and carbonates in sediments. J. Fish. Res. Board. Can. 30: 1441-1445.
- Stumm, W. and Morgan, J. J. 1970. Aquatic Chemistry. New York: Wiley-Interscience. 583 pp.
- Tanner, A. B. 1964a. Radon Migration in the Ground. A Review. In The Natural Radiation Environment, ed. J. A. S. Adams and W. M. Lowder, pp. 161-190. Chicago: Univ. of Chicago Press.
- \_\_\_\_\_. 1964b. Physical and chemical controls on distribution of radium-226 and radon-222 in groundwater near Great Salt Lake, Utah. In The Natural Radiation Environment, eds. J. A. S. Adams and W. M. Lowder, pp. 253-276. Chicago: Univ. of Chicago Press.
- Tardy, Y. and Garrels, R. M. 1976. Prediction of Gibbs' energies of formation - I. Relationships among Gibbs' energies of formation of hydroxides, oxides and aqueous ions. Geochim. Cosmochim. Acta 40: 1051-1056.
- Thorstenson, D. C. 1970. Equilibrium distribution of small organic molecules in natural waters. Geochim. Cosmochim. Acta 34: 745-770.
- Thurston, W. M. 1971. Steam film sampling of water for mass-spectrometric analyses of the deuterium content. Rev. Sci. Inst. 42: 700-703.
- Whitfield, M. 1974. Thermodynamic limitations on the use of the platinum electrode in Eh measurements. Limnol. Oceanogr. 19: 857-865.
- Wigley, T. M. L. 1976. Effect of mineral precipitation on isotopic composition and  $^{14}\text{C}$  dating of groundwater. Nature 263: 219-221.
- \_\_\_\_\_; Plummer, L. N.; and Pearson, F. J. 1978. Mass transfer and carbon isotope evolution in natural water systems. Geochim. Cosmochim. Acta 48: 1117-1140.
- Witherspoon, P. A.; Cook, N. G. W.; and Gale, J. E. 1977. Cooperative work program with Swedish Nuclear Fuel Supply company on radioactive waste storage in mined caverns. In Rept. Y/OWI-9, National Waste Terminal Storage Program Progress Report, Oct. 1, 1976 to Sept. 30, 1977, pp. 87-100. Oak Ridge, Tenn: OWI.
- \_\_\_\_\_. and Degerman, O. 1978. Swedish-American Cooperative Work Program on Radioactive Waste Storage in Mined Caverns. Lawrence Berkeley Laboratory report LBL-8049, SAC-01. Berkeley, California.



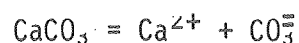


7. APPENDIX: SUMMARY OF CHEMICAL AND ISOTOPIC ANALYSES

Calcite Sat (calcite saturation,  $SI_{\text{calcite}}$ ) is reported as

$$\log[(Ca^{2+})(CO_3^{2-})/K_{\text{calcite}}]$$

where  $(Ca^{2+})$  and  $(CO_3^{2-})$  are the activities of these ions and  $K_{\text{calcite}}$  is the equilibrium constant for the dissolution of calcite as:



and is for the sampled water temperature. Negative values indicate undersaturation of water with respect to calcite and positive values indicate supersaturation.

Charge balance is calculated after corrections for ion pairs as:

$$\frac{\Sigma \text{ cations} - \Sigma \text{ anions}}{(\Sigma \text{ cations} + \sigma \text{ anions})/2} \times 100\%$$

where milliequivalents of the reported ions were used in the summations. Charge balances employing laboratory alkalinity determinations are bracketed.

Isotopic Results - Definitions

SMOW	Standard mean ocean water reference standard
TU	Tritium units where 1 TU = $^3\text{H}/10^{18} \text{ } ^1\text{H}$
PDB	Reference standard for stable carbon isotope ratio measurements: a belemnoid rostrum from the Pee Dee Formation in North Carolina, U.S.A.
pmC	Percent modern carbon.

STRIPA

SAMPLE NO	1-1	1-2		2		3		4		5
DATE	7.9.77	16.6.78		7.9.77		7.9.77		7.9.77		7.9.77
Temp. °C'										
Cond µS										
Field (Lab) pH										
Field Eh										
Field Alk.										
LABORATORY	UW	UW		UW				UW		UW
Ca <sup>++</sup> ppm										
Mg <sup>++</sup> ppm										
Na <sup>+</sup> ppm										
K <sup>+</sup> ppm										
Cl <sup>-</sup> ppm										
SO <sub>4</sub> <sup>=</sup> ppm										
HCO <sub>3</sub> <sup>-</sup> ppm										
SiO <sub>2</sub> ppm										
FeTOT ppm										
PO <sub>4</sub> ppm										
NO <sub>3</sub> <sup>-</sup> ppm										
Org. C ppm										
Calcite Sat.										
Charge Bal. (Lab Alk.)										
18O ‰ SMOW	-9.2	-10.8		-9.1						
2H ‰ SMOW	-76.3	-78.0		-74.6				-9.1		-9.1
3H T.U.								-73.4		-73.4
13C ‰ PDB										
14C pmC										

## STRIPA

SAMPLE NO	6-1	6-2	6-2-A	6-3	6-5	6-7	6-8/26	6-16	6-18	6-19
DATE	7.9.77	8.9.77	8.9.77	8.9.77	8.9.77	8.9.77	8-13.9.77	9.9.77	9.9.77	12.9.77
Temp. °C					9.3					
Cond µS					439					
Field (Lab) pH					9.38(8.7)					
Field Eh					+122					
Field Alk.					38.6					
LABORATORY	UW	UW	UW	IAEA	HYDRO	E	IAEA	UW	IAEA	UW
Ca <sup>++</sup> ppm					35					
Mg <sup>++</sup> ppm					0.5					
Na <sup>+</sup> ppm					96					
K <sup>+</sup> ppm					0.2					
Cl <sup>-</sup> ppm					182					
SO <sub>4</sub> <sup>=</sup> ppm					6.9					
HCO <sub>3</sub> <sup>-</sup> ppm					26.8					
SiO <sub>2</sub> ppm					12.6					
FeTOT ppm					0.19					
PO <sub>4</sub> ppm					<0.01					
NO <sub>3</sub> <sup>-</sup> ppm					0.15					
Org. C ppm					1.1					
Calcite Sat.					0.70					
Charge Bal. (Lab Alk.)					+0.9 (+4.3)					
18O ‰ SMOW	-12.6	-12.5						-12.4		-12.4
2H ‰ SMOW		-91.9								
3H T.U.		8±8		0.4±0.2		45±6			0.8±0.3	
13C ‰ PDB			-18.3				-16.9			
14C pmC										

## STRIPA

SAMPLE NO	6-27	6-28	6-29	6-30		7-1		8-1		9
DATE	14.9.77	14.9.77	14.9.77	14.9.77		8.9.77		8.9.77		12.9.77
Temp. °C'		8.2		8.2						13.2
Cond µS		464		464		260		445		152
Field (Lab) pH		9.54		9.54(9.1)				7.3		7.57(7.5)
Field Eh		+72		+72						
Field Alk.		31.5		31.5						
										48.8
LABORATORY	E	IAEA	UW	HYDRO		UW		UW		HYDRO
Ca <sup>++</sup> ppm		36.8		37						26
Mg <sup>++</sup> ppm		0.09		<0.5						5.5
Na <sup>+</sup> ppm		100		100						6.9
K <sup>+</sup> ppm		0.37		0.2						1.9
Cl <sup>-</sup> ppm		192		185						11
SO <sub>4</sub> <sup>=</sup> ppm		8.0		6.2						15
HCO <sub>3</sub> <sup>-</sup> ppm		28		25.6						79.3
SiO <sub>2</sub> ppm		13.1		12.8						6.2
Fe <sub>TOT</sub> ppm				0.03						0.43
PO <sub>4</sub> ppm				0.01						<0.01
NO <sub>3</sub> <sup>-</sup> ppm				0.15						1.66
Org. C ppm				0.4						5.0
Calcite Sat.		.57		0.63						-0.65
Charge Bal.				5.7						+2.9
(Lab Alk.)		(+2.9)		(7.4)						(+7.5)
<sup>18</sup> O ‰ SMOW			-12.4			-11.9		-10.8		
<sup>2</sup> H ‰ SMOW			-91.2							
<sup>3</sup> H T.U.	11±6	0.3±0.2	-0.6±8			-8±8				
<sup>13</sup> C ‰ PDB										
<sup>14</sup> C ‰										

## STRIPA

SAMPLE NO	9-1	10	11	12	13-1	13-2
DATE	12.9.77	12.9.77	12.9.77	13.9.77	13.9.77	15.9.77
Temp. °C		12.9	9.3	10.4	10.4	
Cond $\mu$ S		25	31	219	229	
Field (Lab) pH		6.5(6.0)	6.73(6.55)			
Field Eh						
Field Alk.						
		6.1	8.6			
LABORATORY		HYDRO	HYDRO	UW	UW	UW
Ca <sup>++</sup> ppm		3.5	4.5			
Mg <sup>++</sup> ppm		0.5	1.0			
Na <sup>+</sup> ppm		1.7	1.8			
K <sup>+</sup> ppm		0.4	0.6			
Cl <sup>-</sup> ppm		2.9	3.3			51.0
SO <sub>4</sub> <sup>=</sup> ppm		7.5	9.0			
HCO <sub>3</sub> <sup>-</sup> ppm		1.8	5.5			
SiO <sub>2</sub> ppm		3.8	4.4			
Fe <sub>TOT</sub> ppm		0.23	0.39			
PO <sub>4</sub> ppm		<0.01	<0.01			
NO <sub>3</sub> <sup>-</sup> ppm		0.41	0.48			
Org. C ppm		4.9	4.9			
Calcite Sat.		-4.2	-3.4			
Charge Bal.		-13.4	-6.6			
(Lab Alk.)		(+10.0)	(+6.4)			
<sup>18</sup> O ‰ SMOW						-12.2
<sup>2</sup> H ‰ SMOW				133±11	-87.2	
<sup>3</sup> H T.U.					20±9	
<sup>13</sup> C ‰ PDB	-23.2					
<sup>14</sup> C pmC						

## STRIPA

SAMPLE NO	14-1	15-1	15-2	15-4	15-5	15-6	15-7/23 15/19	15-11	15-24	15-26 A	15-26 B
DATE	13.9.77	14.9.77	15.9.77	15.9.77	15.9.77	15.9.77	9.77	16.9.77	20.9.77	20.9.77	20.9.77
Temp. °C'				8.0						8.0	
Cond µS				463						458	
Field (Lab) pH				9.49(9.0)						9.5	
Field Eh				+7						+112	
Field Alk.				29.0						24.2	
LABORATORY	UW	UW	UW	HYDRO	IAEA	UW	IAEA		UW	IAEA	E
Ca <sup>++</sup> ppm				37						37.2	
Mg <sup>++</sup> ppm				<0.5						0.03	
Na <sup>+</sup> ppm				100						101	
K <sup>+</sup> ppm				0.2						0.3	
Cl <sup>-</sup> ppm				189						192	
SO <sub>4</sub> <sup>=</sup> ppm				7.2						8.6	
HCO <sub>3</sub> <sup>-</sup> ppm				25.6						27.8	
SiO <sub>2</sub> ppm				12.8						13.2	
FeTOT ppm				0.02							
PO <sub>4</sub> ppm				0.01							
NO <sub>3</sub> <sup>-</sup> ppm				0.14							
Org. C ppm				0.4							
Calcite Sat.				0.65						0.63	
Charge Bal. (Lab Alk.)				+4.7 (+5.7)						(3.4)	
18O ‰/‰ SMOW	-11.1	-12.7	-12.6						-12.6		
2H ‰/‰ SMOW	-81.2	-91.7	-91.2						-91.2		
3H T.U.	115±10	19±8	3±9		0.4±0.2				-1±9	0.5±0.2	65±6
13C ‰/‰ PDB							-17.8	-18.6			
14C pmC											

## STRIPA

SAMPLE NO	15-27		16-1	16-2	16-3	16-4	16-5	16-6/36 30.9.70	16-21	16-22
DATE	20.9.77		21.9.77	22.9.77	26.9.77	26.9.77	26.9.77	-15.11.77	20.10.77	19.10.77
Temp. °C'	8.0		11.0	11.3			10.8			
Cond $\mu$ S	458		224	218						
Field (Lab) pH	9.5(8.85)		8.85							
Field Eh	+112						+97			
Field Alk.	24.2						83.0			
LABORATORY	HYDRO		UW	UW	UW	IAEA	HYDRO	IAEA	UW	UW
Ca <sup>++</sup> ppm	37						15			
Mg <sup>++</sup> ppm	<0.05						<0.5			
Na <sup>+</sup> ppm	100						43			
K <sup>+</sup> ppm	0.2						0.3			
Cl <sup>-</sup> ppm	188						52			
SO <sub>4</sub> <sup>=</sup> ppm	8.1						2.1			
HCO <sub>3</sub> <sup>-</sup> ppm	25.6						76.9			
SiO <sub>2</sub> ppm	12.8						11.6			
Fe <sub>TOT</sub> ppm	0.02						0.07			
PO <sub>4</sub> ppm	0.01						<0.01			
NO <sub>3</sub> <sup>-</sup> ppm	0.15						0.24			
Org. C ppm	0.9						0.7			
Calcite Sat.	0.59						0.28			
Charge Bal.	+6.2						-7.6			
(Lab Alk.)	(+5.8)						(-4.0)			
18O ‰/‰ SMOW			-11.8							-11.8
2H ‰/‰ SMOW			-86.9							-87.7
3H T.U.					-2±9	0.7±0.3				
13C ‰/‰ PDB								-15.8	-13.2	
14C pmC								2.46		

STRIPA

SAMPLE NO	16-23 A	16-23 B	16-24	16-37	16-38	16-39	16-41		17-1	17-2
DATE	19.10.77	19.10.77	19.10.77	29.11.77	04.01.78	24.01.78	24.02.78		22.9.77	26.9.77
Temp. °C'										
Cond µS	210		210							
Field (Lab) pH	8.7		8.7(8.45)							
Field Eh	+92		+92							
Field Alk.	78.7		78.7							
LABORATORY	IAEA	E	HYDRO	UW	UW	UW	UW		UW	IAEA
Ca <sup>++</sup> ppm	14.1		16							
Mg <sup>++</sup> ppm	0.3		0.5							
Na <sup>+</sup> ppm	50.8		43							
K <sup>+</sup> ppm	0.2		0.2							
Cl <sup>-</sup> ppm	49.3		52							
SO <sub>4</sub> <sup>=</sup> ppm	1.4		2.7							
HCO <sub>3</sub> <sup>-</sup> ppm	73		76.3							
SiO <sub>2</sub> ppm	12.0		11.0							
FeTOT ppm			0.24							
PO <sub>4</sub> ppm			<0.01							
NO <sub>3</sub> <sup>-</sup> ppm			0.16							
Org. C ppm			0.6							
Calcite Sat.	0.23		0.30							
Charge Bal.			-3.7							
(Lab Alk.)	(+11.8)		(+2.3)							
18O ‰/‰ SMOW				-11.9	-11.9	-11.9	-11.9		-12.1	
2H ‰/‰ SMOW										
3H T.U.	0.5±3	4±6								1±0.2
13C ‰/‰ PDB										
14C ‰‰C										



## STRIPA

SAMPLE NO	17-4	17-5	17-6/29 28.9.77-	17-31	17-32	17-33 A	17-33	17-38		
DATE	26.9.77	26.9.77	3.10.77	3.10.77	3.10.77	3.10.77	3.10.77	20.10.77		
Temp. °C'					8.0	8.0				
Cond µS					262	262				
Field (Lab) pH					8.83(7.95)	8.83(7.95)				
Field Eh					-1	-1				
Field Alk.					53.8	53.8				
LABORATORY	UW	UW	IAEA	UW	HYDRO	IAEA	E	UW		
Ca <sup>++</sup> ppm					18	17.5				
Mg <sup>++</sup> ppm					<0.5	0.3				
Na <sup>+</sup> ppm					56	60.7				
K <sup>+</sup> ppm					0.4	0.25				
Cl <sup>-</sup> ppm					84	84.8				
SO <sub>4</sub> <sup>=</sup> ppm					3.3	2.4				
HCO <sub>3</sub> <sup>-</sup> ppm					51.9	52				
SiO <sub>2</sub> ppm					11.2	12.1				
Fe <sub>TOT</sub> ppm					0.15					
PO <sub>4</sub> ppm					<0.01					
NO <sub>3</sub> <sup>-</sup> ppm					0.20					
Org. C ppm					0.6					
Calcite Sat.					0.22	0.11				
Charge Bal. (Lab Alk.)					+0.4 (+2.3)	+2.8 (+6.7)				
18O ‰/‰ SMOW	-12.2			-12.0				-12.3		
2H ‰/‰ SMOW	-88.8			-89.0						
3H T.U.	9±9			12±9		0.6±3	4±6			
13C ‰/‰ PDB		-16.1	-15.5							
14C ‰/‰			6.0							

## STRIPA

SAMPLE NO	23-15	23-16	23-23	23-24	23-25	23-26	23-27	23-28	23-29	23-30
DATE	24.10.77	24.10.77	24.10.77	25.10.77	25.10.77	25.10.77	25.10.77	27.10.77	27.10.77	27.10.77
Temp. °C'									6.8	
Cond µS									108	
Field (Lab) pH									7.0(7.9)	
Field Eh									+371	
Field Alk.									100.7	
LABORATORY	IAEA	UW	UW	UW	IAEA	UW	IAEA	UW	HYDRO	IAEA
Ca <sup>++</sup> ppm									22	
Mg <sup>++</sup> ppm									2.5	
Na <sup>+</sup> ppm									3.6	
K <sup>+</sup> ppm									1.4	
Cl <sup>-</sup> ppm									6.1	
SO <sub>4</sub> <sup>=</sup> ppm									3.3	
HCO <sub>3</sub> <sup>-</sup> ppm									96.4	
SiO <sub>2</sub> ppm									13	
FeTOT ppm									0.04	
PO <sub>4</sub> ppm									<0.01	
NO <sub>3</sub> <sup>-</sup> ppm									0.75	
Org. C ppm									0.4	
Calcite Sat.									-1.31	
Charge Bal. (Lab Alk.)									-23.8 (-19.9)	
18O ‰/‰ SMOW						-10.8		-11.0		
2H ‰/‰ SMOW								-79.1		
3H T.U.	6.8±1							38±10		6.8±1
13C ‰/‰ PDB			-15.2							
14C pmC										

## STRIPA

SAMPLE NO	24-1	24-2	24-3	24-4	24-6/22	24-16/21	24-8	24-10		
DATE	10.11.77	10.11.77	10.11.77	10.11.77	14.11.77- 18.11.77	17.11.77- 18.11.77	14.11.77	14.11.77		
Temp. °C'		7.6								
Cond $\mu$ S		308								
Field (Lab) pH		9.25(8.5)								
Field Eh		+29								
Field Alk.		45.8								
LABORATORY	UW	HYDRO	IAEA	E	UW	UW	UW	UW		
Ca <sup>++</sup> ppm		23								
Mg <sup>++</sup> ppm		<0.5								
Na <sup>+</sup> ppm		64								
K <sup>+</sup> ppm		5.4								
Cl <sup>-</sup> ppm		114								
SO <sub>4</sub> <sup>=</sup> ppm		3.6								
HCO <sub>3</sub> <sup>-</sup> ppm		45.8								
SiO <sub>2</sub> ppm		11.2								
FeTOT ppm		0.05								
PO <sub>4</sub> ppm		<0.01								
NO <sub>3</sub> <sup>-</sup> ppm		0.15								
Org. C ppm		0.7								
Calcite Sat.		0.56								
Charge Bal.		+1.6								
(Lab Alk.)		(+1.6)								
<sup>18</sup> O ‰ SMOW	-12.5							-12.9		
<sup>2</sup> H ‰ SMOW	-91.8									
<sup>3</sup> H T.U.										
<sup>13</sup> C ‰ PDB					-15.9	-18.5	-16.1			
<sup>14</sup> C pmC					5.4	4.7				

## STRIPA

SAMPLE NO	25-1	25-2	25-3 A	25-3 B	25-4	26-1	26-3	26-4	26-5
DATE	7.11.77	7.11.77	11.11.77	11.11.77	11.11.77	17.11.77	17.11.77	17.11.77	18.11.77
Temp. °C	10.0								
Cond µS									
Field (Lab) pH	8.1(7.85)						8.35(8.1)		
Field Eh									
Field Alk.	118						129		
LABORATORY	HYDRO	UW	IAEA	E	UW	IAEA	HYDRO	UW	UW
Ca <sup>++</sup> ppm	46						52		
Mg <sup>++</sup> ppm	11						3.5		
Na <sup>+</sup> ppm	8.0						38		
K <sup>+</sup> ppm	2.1						0.6		
Cl <sup>-</sup> ppm	18						28		
SO <sub>4</sub> <sup>=</sup> ppm	28						89		
HCO <sub>3</sub> <sup>-</sup> ppm	133						122		
SiO <sub>2</sub> ppm	12						9.6		
Fe <sub>TOT</sub> ppm	0.03						0.05		
PO <sub>4</sub> ppm	<0.01						<0.01		
NO <sub>3</sub> <sup>-</sup> ppm	12.6						1.12		
Org. C ppm	3.0						1.7		
Calcite Sat.	0.23						0.45		
Charge Bal. (Lab Alk.)	+11.5 (+3.9)						-2.5 (-2.4)		
18O ‰ SMOW					-10.9			-10.8	-10.9
2H ‰ SMOW		-81.4						-79.4	
3H T.U.			6.8±1	21±6					
13C ‰ PDB									
14C pmC									

## STRIPA

SAMPLE NO	27-1	27-2	27-3	27-4		28-1	28-2		29-1	29-3
DATE	17.11.77	17.11.77	17.11.77	17.11.77		6.12.77	7.12.77		30.1.78	30.1.78
Temp. °C										7.5
Cond µS										600
Field (Lab) pH				8.1(7.85)						9.75(8.95)
Field Eh										+169
Field Alk.				104						15.4
LABORATORY	IAEA	E	UW	HYDRO		UW	UW		UW	HYDRO
Ca <sup>++</sup> ppm				81						59
Mg <sup>++</sup> ppm				6						0.5
Na <sup>+</sup> ppm				45						125
K <sup>+</sup> ppm				2.9						0.4
Cl <sup>-</sup> ppm				26			43.6			283
SO <sub>4</sub> <sup>=</sup> ppm				147						19
HCO <sub>3</sub> <sup>-</sup> ppm				96.4						12.8
SiO <sub>2</sub> ppm				9.4						11.2
FeTOT ppm				0.04						< 0.02
PO <sub>4</sub> ppm				<0.01						< 0.01
NO <sub>3</sub> <sup>-</sup> ppm				75						0.28
Org. C ppm				2.0						0.8
Calcite Sat.				0.29						0.52
Charge Bal.				-2.4						-2.4
(Lab Alk.)				(-0.3)						(-1.9)
<sup>18</sup> O ‰ SMOW				-10.7			-11.9	-12.1		-13.2
<sup>2</sup> H ‰ SMOW				-79.4				-88.0		-93.7
<sup>3</sup> H T.U.										2±10
<sup>13</sup> C ‰ PDB										
<sup>14</sup> C pmC										

STRIPA

SAMPLE NO	29-4/42	29-34 A	29-39	29-41	29-61	29-65		30-1		31-1
DATE	27.2.78	22.2.78	23.2.78	24.2.78		13.3.78		2.3.78		2.3.78
Temp. °C		7.0	7.0							
Cond µS		600	600							
Field (Lab) pH		9.7(7.9)	9.7(8.4)		(9.15)					
Field Eh		+144	+144							
Field Alk.		12.3	12.3							
LABORATORY	UW	SCAND.	HYDRO	UW	HYDRO	UW		UW		UW
Ca <sup>++</sup> ppm		55	61		63					
Mg <sup>++</sup> ppm		0.1	<0.5		<0.5					
Na <sup>+</sup> ppm		120	120		120					
K <sup>+</sup> ppm		0.4	0.8		0.6					
Cl <sup>-</sup> ppm		290	285		283					59.1
SO <sub>4</sub> <sup>=</sup> ppm		19	18		18					
HCO <sub>3</sub> <sup>-</sup> ppm		12	15.9		7					
SiO <sub>2</sub> ppm		17 NH <sub>4</sub>	12.8		12.0 NH <sub>4</sub>					
Fe <sub>TOT</sub> ppm		0.08 0.01	<0.02		0.63 0.02					
PO <sub>4</sub> ppm		<0.01	<0.01		<0.01 NO <sub>2</sub>					
NO <sub>3</sub> <sup>-</sup> ppm		0.05 NO <sub>2</sub>	0.19		0.12 <0.01					
Org. C ppm		<0.001	0.6		0.5 4.2					
Calcite Sat.		0.40 3.7			<0.02					
Charge Bal. (Lab Alk.)		-9.6 (-9.5)								
18O ‰ SMOW						-12.9		-10.9		-10.8
2H ‰ SMOW						-95.9		-82.1, -83.2		-80.6
								-83.8		
3H T.U.										
13C ‰ PDB										
14C ‰	insuff.									

## STRIPA

SAMPLE NO	32-1	32-2		35		36-1	36-3		37-1	
DATE	2.3.78	?3.78		30.5.78		30.5.78	13.6.78		30.5.78	
Temp. °C'										
Cond $\mu$ S										
Field (Lab) pH										
Field Eh										
Field Alk.						99.2	94.0			
LABORATORY	UW	UW		UW		UW			UW	
Ca <sup>++</sup> ppm										
Mg <sup>++</sup> ppm										
Na <sup>+</sup> ppm										
K <sup>+</sup> ppm										
Cl <sup>-</sup> ppm				63.2		36.1			310.0	
SO <sub>4</sub> <sup>=</sup> ppm										
HCO <sub>3</sub> <sup>-</sup> ppm										
SiO <sub>2</sub> ppm										
Fe <sub>TOT</sub> ppm										
PO <sub>4</sub> ppm										
NO <sub>3</sub> <sup>-</sup> ppm										
Org. C ppm										
Calcite Sat.										
Charge Bal. (Lab Alk.)										
<sup>18</sup> O ‰ SMOW	-11.2,-11.0	-12.4		-12.2		-12.1				
<sup>2</sup> H ‰ SMOW	-80.5			-87.9		-87.9			-93.8	
<sup>3</sup> H T.U.				-86.4						
<sup>13</sup> C ‰ PDB						-1±8				
<sup>14</sup> C pmC										

## STRIPA

SAMPLE NO	38-1	38-2	38-3	38-4	38-5		39-1		40-1	40-2
DATE	31.5.78	1.6.78	2.6.78	7.6.78	14.6.78		31.5.78		31.5.78	1.6.78
Temp. °C			HEATER ON							
Cond µS										
Field (Lab) pH							12.09		(8.02)	8.10
Field Eh										
Field Alk.	78.1	81.1		65.9	34.2		474		81.8	82.4
LABORATORY	UW	UW	UW	UW	UW					UW
Ca <sup>++</sup> ppm										
Mg <sup>++</sup> ppm										
Na <sup>+</sup> ppm										
K <sup>+</sup> ppm										
Cl <sup>-</sup> ppm			56.9							59.3
										55.7
SO <sub>4</sub> <sup>=</sup> ppm										
HCO <sub>3</sub> <sup>-</sup> ppm										
SiO <sub>2</sub> ppm										
FeTOT ppm										
PO <sub>4</sub> ppm										
NO <sub>3</sub> <sup>-</sup> ppm										
Org. C ppm										
Calcite Sat.										
Charge Bal. (Lab Alk.)										
18O ‰ SMOW			-12.4							-11.3
2H ‰ SMOW			-89.4							-82.1
3H T.U.										
13C ‰ PDB										
14C ‰										



STRIPA

SAMPLE NO	40-3	40-4		41-1		42-1	42-2	42-3	42-4	42-5
DATE	2.6.78	7.6.78		31.5.78		31.5.78	7.6.78	14.6.78		
Temp. °C	HEATER ON									
Cond µS										
Field (Lab) pH		7.73		(8.13)						
Field Eh										
Field Alk.		32.9		113				78.7		
						73.2	74.4			
LABORATORY	UW	UW				UW	UW	UW	UW	UW
Ca <sup>++</sup> ppm										
Mg <sup>++</sup> ppm										
Na <sup>+</sup> ppm										
K <sup>+</sup> ppm										
Cl <sup>-</sup> ppm		17.9								
		13.8								
SO <sub>4</sub> <sup>=</sup> ppm										
HCO <sub>3</sub> <sup>-</sup> ppm										
SiO <sub>2</sub> ppm										
Fe <sub>TOT</sub> ppm										
PO <sub>4</sub> ppm										
NO <sub>3</sub> <sup>-</sup> ppm										
Org. C ppm										
Calcite Sat.										
Charge Bal.										
(Lab Alk.)										
18O ‰/‰ SMOW	-11.5	-11.5								
2H ‰/‰ SMOW		-83.1,								
		-83.8								
3H T.U.										
13C ‰/‰ PDB										
14C ‰/‰										

STRIPA

SAMPLE NO	42-6		43-1	43-2	43-3	43-43-A	43.4		45-1	45-2
DATE			6.6.78	6.6.78	6.6.78	8.6.78- 12.6.78	8.6.78		13.6.78	13.6.78
Temp. °C'			LOST		2.5					
Cond µS										
Field (Lab) pH					9.04					
Field Eh					-87					
Field Alk.					57.1					
LABORATORY	UW			UW	UW	UW	UW		UW	UW
Ca <sup>++</sup> ppm										
Mg <sup>++</sup> ppm										
Na <sup>+</sup> ppm										
K <sup>+</sup> ppm										
Cl <sup>-</sup> ppm										
SO <sub>4</sub> <sup>=</sup> ppm										
HCO <sub>3</sub> <sup>-</sup> ppm										
SiO <sub>2</sub> ppm										
FeTOT ppm										
PO <sub>4</sub> ppm										
NO <sub>3</sub> <sup>-</sup> ppm										
Org. C ppm										
Calcite Sat.										
Charge Bal.										
(Lab Alk.)										
18O ‰ SMOW				-12.6						-13.0
2H ‰ SMOW				-90.7						-91.7
3H T.U.										
13C ‰ PDB						-15.7	-16.8		-18.7	
14C pmC						3.4				

STRIPA

SAMPLE NO	45-3	45-1-A		46-1		47-1		48-1	
DATE	13.6.78	16.6.78		16.6.78		16.6.78		16.6.78	
Temp. °C'	8.0								
Cond µS									
Field (Lab) pH	9.40								
Field Eh	+23								
Field Alk.	27.3								
LABORATORY	UW	UW		UW		UW		UW	
Ca <sup>++</sup> ppm									
Mg <sup>++</sup> ppm									
Na <sup>+</sup> ppm									
K <sup>+</sup> ppm									
Cl <sup>-</sup> ppm				44.4		44.9		40.8	
SO <sub>4</sub> <sup>=</sup> ppm									
HCO <sub>3</sub> <sup>-</sup> ppm									
SiO <sub>2</sub> ppm									
FeTOT ppm									
PO <sub>4</sub> ppm									
NO <sub>3</sub> <sup>-</sup> ppm									
Org. C ppm									
Calcite Sat.									
Charge Bal. (Lab Alk.)									
18O ‰ SMOW				-12.3		-12.3		-12.2	
2H ‰ SMOW				-90.6		-88.8		-87.7	
3H T.U.									
13C ‰ PDB		-17.5							
14C pmC		13.5							

U.S.GPO:1979-689-058 (P) 29



This report is part of a cooperative Swedish-American project supported by the U.S. Department of Energy and/or the Swedish Nuclear Fuel Supply Company. Any conclusions or opinions expressed in this report represent solely those of the author(s) and not necessarily those of The Regents of the University of California, the Lawrence Berkeley Laboratory, the Department of Energy, or the Swedish Nuclear Fuel Supply Company.

Reference to a company or product name does not imply approval or recommendation of the product by the University of California or the U.S. Department of Energy to the exclusion of others that may be suitable.



TECHNICAL INFORMATION DIVISION  
LAWRENCE BERKELEY LABORATORY  
UNIVERSITY OF CALIFORNIA  
BERKELEY, CALIFORNIA 94720